10
2-11-92 JSO

SANDIA REPORT

SAND91—0791 • UC—814
Unlimited Release
Printed December 1991

Yucca Mountain Site Characterization Project

Movement of Shaft and Drift Construction Water in Yucca Mountain, Nevada – An Extended Study

Steven R. Sobolik, Merton E. Fewell, Roger R. Eaton

Prepared by
Sandia Naticnal Laboratories
Albuquerque, New Mexico 87185 and Livermore, California 94550
for the United States Department of Energy
under Contract DE-AC04-76DP00789

"Prepared by Yucca Mountain Site Characterization Project (YMSCP) participants as part of the Civilian Radioactive Waste Management Program (CRWM). The YMSCP is managed by the Yucca Mountain Project Office of the U.S. Department of Energy, DOE Field Office, Nevada (DOE/NV). YMSCP work is sponsored by the Office of Geologic Repositories (OGR) of the DOE Office of Civilian Radioactive Waste Management (OCRWM)."

Issued by Sandia National Laboratories, operated for the United States Department of Energy by Sandia Corporation.

Available to DOE and DOE contractors from
Office of Scientific and Technical Information
PO Box 62
Oak Ridge, TN 37831

Prices available from (615) 576-8401, FTS 626-8401

Available to the public from
National Technical Information Service
US Department of Commerce
5285 Port Royal Rd
Springfield, VA 22161

NTIS price codes
Printed copy: A05
Microfiche copy: A01

SAND--91-0791

DE92 006614

SAND91-0791
Unlimited Release
Printed December 1991

Movement of Shaft and Drift Construction Water in Yucca Mountain, Nevada - An Extended Study

Steven R. Sobolik and Merton E. Fewell
Performance Assessment Development Division 6313
Sandia National Laboratories
Albuquerque, New Mexico 87185

Roger R. Eaton
Fluid, Thermal, and Structural Sciences Department
Sandia National Laboratories
Albuquerque, New Mexico 87185

Abstract

The Yucca Mountain Site Characterization Project is studying Yucca Mountain in southwestern Nevada as a potential site for a high-level nuclear waste repository. Site characterization includes surface-based and underground testing. Analyses have been performed to design site characterization activities with minimal impact on the ability of the site to isolate waste, and on tests performed as part of the characterization process. One activity of site characterization is the construction of an Exploratory Studies Facility, for which many design options are being considered, including shafts, drifts, and ramps. The information in this report pertains to: (1) engineering calculations of the potential distribution of residual water from constructing the shafts and drifts; (2) numerical calculations predicting the movement of residual construction water from the shaft and drift walls into the rock; and (3) numerical calculations of the movement of residual water and how the movement is affected by ventilation. This document contains information that has been used in preparing Appendix I of the Exploratory Studies Facility Design Requirements document for the Yucca Mountain Project.

The work reported here was conducted under Work Breakdown Structure (WBS) element 1.2.1.4.7.

TABLE OF CONTENTS

ACKNOWLEDGEMENTS

The authors would like to acknowledge the work of the following people who assisted in creating this report:

Sharon Shannon, who produced many of the graphs in this document from the computer solutions;

Andy Peterson, on whose original work this document is based, for his assistance and advice;

Tom Hinkebein and Franz Lauffer, for reviewing this document and the analyses contained herein.

1.0 INTRODUCTION

The Yucca Mountain Site Characterization Project is studying Yucca Mountain in southwestern Nevada as a potential site for a high-level nuclear waste repository. Site characterization includes surface-based and underground testing. Underground testing is to be facilitated by the construction of an Exploratory Studies Facility (ESF),[1] for which many design options are being considered, including shafts, drifts, and ramps. Water will be used during construction of the exploratory facility to drill holes for emplacing explosives, as well as for dust control during tunnel boring and mining operations. There may be some potential for this water to be retained and distributed in the surrounding rock and affect potential repository performance and experiments. This report describes calculations that evaluate the movement of the water retained in the rock walls and not removed during the mucking operation associated with sinking of shafts and driving of drifts. The results of the calculations will be used to support ESF design, will be incorporated in the Exploratory Studies Facility Design Requirements document (ESF DR), and will be available for guidance in monitoring saturation levels near shafts, drifts, and ramps, and in locating experiments.

These calculations constitute one of eleven ESF analyses performed in support of the ESF DR. The particular analysis described in this report is ESF Analysis Number 2, and it evaluated the movement of water used for the construction of shafts and drifts in the ESF. The calculations and analyses performed for ESF Analysis Number 2 were conducted as Quality-Related in accordance with Sandia National Laboratories' implementation of the Yucca Mountain Project Quality Assurance plan and were controlled by Problem Definition Memo (PDM) 72-30.

The definition of this ESF Analysis supported the ESF Title I Design [YMP, 1989], which included the use of shafts for access from the surface to the ESF and other underground drifts. However, as a result of the recent ESF Alternatives Study, the preferred preliminary designs use access ramps and not shafts. The use of shafts has not been entirely ruled out, but it is no longer the dominant means of access to the underground facility. This analysis makes an initial attempt to determine the effects of drilling water used for underground excavation on experiments and potential repository performance. It is expected that ramp walls will experience similar effects as the drift walls, and that later refinement of these calculations will be necessary based on proposed ramp and drift sizes and new hydrogeologic information from Yucca Mountain.

These calculations are based on available data and on the present conceptual understanding of the processes and mechanisms perceived active at Yucca Mountain. Due to our limited knowledge of Yucca Mountain prior to site characterization, the hydrogeological conceptual model, existing conceptual models of the physical processes, and the mathematical models used in these analyses are not validated. Therefore, considerable uncertainty exists in these results. Recommendations based on the results of these analyses are intended to provide guidance for applying engineering judgment during the

---

1. The Exploratory Shaft Facility was renamed the Exploratory Studies Facility in February 1991.

design, construction, and operation of the ESF, and therefore must provide relevant results to the architects and engineers who design the ESF. Refinement of the results is an ongoing and iterative process, which must complement site characterization. These calculations may be refined as better understanding evolves through site characterization and through additional analyses, which will address uncertainties and the sensitivity of the results to alternate conceptual models.

2.0 PROBLEM DEFINITION

PDM 72-30 describes the analyses as an extension of a previous work [Peterson et al., 1988], a collection of technical letters which describes analyses done in support of a preliminary evaluation of ESF construction on the in-situ experiments and postclosure radionuclide transport. Appendix A from Peterson et al. addresses the distance to which rock could be affected when up to 10% of the expected construction water is retained in the walls of the shafts and drifts. The initial conditions were that the rock is unsaturated, the fractures are essentially dry, and the retained construction water enters the rock at a rate that initially saturates only the fractures. An estimate of the distance that water would travel from the shaft and drift walls was made by a geometric calculation based on the volume of retained water and the capacity of the initially unsaturated fractures (fracture porosity). The results of these calculations indicated that at the Topopah Spring repository horizon, 10% of construction water can be stored in fractures within 24 m of the centerline of the shafts. Appendices B and C from Peterson et al. show analyses of the time-dependent, one-dimensional, radial (for a shaft) or cartesian horizontal (for a drift) flow of the residual construction water in the rock matrix adjacent to the shaft and drift liners. These calculations were performed using NORIA [Bixler, 1985] for saturation levels out to 25 m from the shaft centerline and for times up to 1000 years. The steady-state surface infiltration rate was assumed to be 0.1 mm/yr. In Appendix B, the increase in saturation at radial distances greater than 5 m from the shaft centerline was less than 0.03. In Appendix C, the additional effects of drift ventilation on the movement of water were included. This study indicated that changes in the saturation of the rock near the drift walls is completely dominated by ventilation and that the walls may reach a saturation level less than their original state. All of these calculations were originally performed at Quality Assurance Level III, which is now referred to as "Not Quality Related."

In this extended study, the effects of shaft and drift construction water were studied in two sets of analyses: uniform distribution limiting cases, and time-dependent water flow cases. The first set of calculations estimated the effects of the absorbed water assuming uniform distribution of the water into the rock. Included in this set of calculations are the following: calculations to predict the radial distance that retained water would move if the water initially flowed only in the fractures; the resulting change in saturation if that water were then imbibed into the matrix; and separate calculations to determine the change in saturation due to the uniform distribution of the retained water in the matrix as a function of the radius from shaft centerline (or, for drifts, the distance from the wall surface). The construction water retained in the rock walls will probably be nonuniformly distributed, with more water absorbed near the shaft or drift wall than in the rock. The second set of calculations were for a one-

dimensional, transient flow, and were performed to evaluate the radial horizontal movement of initially nonuniformly distributed water. The results of these analyses include saturation profile plots at selected times during the analysis. The goals of the analyses of shaft and drift construction water movement were the following:

- Using the most current, widely accepted boundary conditions for steady state infiltration rate, volume of water used for drilling and excavation, fraction of the water retained in the disturbed rock, and ventilation, determine the potential effects of shaft and drift construction water on repository performance; and

- Using the same calculations, determine the potential effects on experiments to be conducted in the ESF, and set guidelines for locations of experiments.

3.0 UNIFORM DISTRIBUTION - LIMITING CASES

3.1 Discussion of Calculations

The work described in Appendix A of Peterson et al. was repeated as a Quality-Related activity that extended the range of water-retention factors. In the original work, a set of geometric calculations was written up as a FORTRAN program to allow the calculation for a number of cases. The FORTRAN programs used in the original work were incorporated into an EXCEL 2.2 spreadsheet for this analysis. Combined listings of this spreadsheet for all the cases discussed below are included in Appendix A. The results of the spreadsheet calculations, with all of the original values for the various parameters, were compared with the results of the FORTRAN programs of the original work for verification. These spreadsheets performed calculations for the following limiting cases as described in the above reference:

Case 1. The rate at which water enters the walls during sinking of shafts or driving of drifts is assumed to be so rapid that the water flow is predominantly through the fractures. Afterwards the water is imbibed from the fractures into the surrounding rock matrix.

Case 2. The rate at which water enters the walls during sinking of shafts or driving of drifts is assumed to be so slow that the water flow is predominantly into the host rock matrix with negligible fracture flow.

For these analyses, it was assumed that the fractures had a small initial residual saturation and that the matrix initial saturation was low enough that when the water moved from the fractures into the matrix, the matrix did not become fully saturated. The hydrogeologic units that were included in these analyses are referred to in this report as the following [Ortiz et al., 1985]:

- Tiva Canyon (Tiva Canyon welded unit, TCw),
- Paintbrush Tuff (Upper Paintbrush nonwelded unit, PTn),
- Topopah Litho (Topopah Spring welded unit, lithophysae-rich, TSw1),
- Topopah Rep (Topopah Spring welded unit, lithophysae-poor, TSw2, at the potential repository horizon), and
- Calico Hills (Calico Hills nonwelded unit, CHn), respectively.

Case 1

Calculations were performed for the shaft and drift geometries to determine the distance that water retained from construction could move from the excavated wall surface into the rock if the water is assumed to initially saturate the fractures and not be absorbed into the matrix. The Case 1 analyses apply to the shaft and drift, with slightly different geometries and drilling water requirements for the two situations. For both analyses, the residual drilling water is assumed to enter the rock at a rate such that it initially stays in the fractures, uniformly filling them out to a radius, R, which is determined from the conservation of retained water. The change in the matrix saturation that would occur when the water from the fractures moved into the matrix was also calculated. It is assumed that for longer times, the extremely large capillary forces that are found in tuff rock, pull the water from the fractures into the rock matrix, thus providing a means to approximate the expected increase in saturation in the host rock between the walls at radius R_o, and the fracture fill radius, R (see Figure 1 in Appendix C).

For the evaluation of Case 1, it is first assumed that the flow is entirely through the fractures. The fill radius R is the radius to which the fractures would fill for a given percentage of drilling water left in the shaft or drift after drilling. This fill radius is also dependent on the fracture porosity of each material. The only assumptions made about fracture characteristics are that they are sufficiently connected to allow continuous flow, and that their volume within the host rock is described by the fracture porosity. Equation 1, based on the conservation of mass, where the available volume in the fractures equals the volume of water retained for this scenario, is

$$R = \sqrt{\frac{nV}{\pi\phi_f\,(1 - s_{rf})} + R_o^2} \quad , \qquad (1)$$

where R = the fill radius to which the fractures are saturated (m); n = the fraction of the construction water left in the rock (non-dimensional); V = the total volume of construction water used per meter of drilling (m^3/m); ϕ_f = fracture porosity (non-dimensional); s_{rf} = residual saturation of the fractures (non-dimensional); and R_o = outside radius of the concrete shaft liner (m).

In these calculations, the radius of the outside of the shaft concrete liner was assumed to be 2.21 m (see Figure 1 in Appendix C). For the drift case, the drift geometry shown in Figure 2 in Appendix C was used as the basis for the calculations. The drift was analyzed as a right circular cylinder having the same circular area as the drift shown in Figure 2. This resulted in the drift being analyzed as a circle with a radius of 3.38 m. Equation 1 was also used for this case with the inside radius of the drift wall, R_o, equaling 3.38 m. Both of these geometries were obtained from the Title I Design of the ESF.

The expected amount of water to be used in the shaft sinking operation for the Title I design is 230 gal/ft (2.856 m^3/m), and the expected amount of water to be used in the drift excavating operation is 235 gal/ft (2.918 m^3/m). These

values were obtained during a personal communication with Ralph Musick of Raytheon Services Nevada.

The calculations for Equation 1 are shown in Appendix A for the shaft and the drift. The fill radius is calculated as a function of the percentage of drilling water not removed during mucking operations. Figure 3 in Appendix C illustrates the fracture fill radius for a shaft for water retention rates up to 10%; it can be seen from Appendix A that results for the drift are similar. Note that the fill radius for a material is inversely proportional to its fracture porosity.

After the fractures are filled, the water is imbibed into the surrounding matrix material through capillary suction, in a volume based on the same total radius, R. The resulting change in saturation is calculated as a function of matrix porosity. The equation for the saturation increase based on conservation of water volume is

$$(s_f - s_i)_m = \frac{\phi_f (1 - s_{rf})}{\phi_m} \quad , \qquad (2)$$

where $(s_f - s_i)_m$ = matrix saturation increase (non-dimensional); $(1 - s_{rf})$ = fracture saturation decrease (non-dimensional); ϕ_f = fracture porosity (non-dimensional); and ϕ_m = matrix porosity (non-dimensional). As shown by Equation 2, the increase in saturation does not depend on the radius to which the fractures are saturated. The increase is dependent on the fracture porosity and residual saturation, and the matrix porosity. To investigate the effect of matrix porosity on the change in saturation for each hydrogeologic unit, calculations were performed using the fracture characteristics for each unit for varying matrix porosities ranging from 0.05 to 0.5. The results of these calculations are shown in Appendix A.

Case 2

In this case, it is assumed that the primary driving force for the transport of water into the rock is capillarity. Additionally, it is assumed that the water distributed between R and R_o is at uniform saturation. **Equation 3** is an expression for the conservation of water under these assumptions.

$$(s_f - s_i)_m = \frac{nV}{\phi_m \pi (R^2 - R_o^2)} \quad . \qquad (3)$$

The change in saturation is calculated as a function of the percentage of water remaining in the shaft or drift after drilling (the retention rate n), and as a function of the fill radius. The calculations of saturation increase as a function of fill radius were done for retention rates of 10%, 15%, and 20%, and are shown in Appendix A. Figure 4 in Appendix C shows the increase in matrix saturation for varying fill radii resulting from 15% of the drilling water remaining in the rock wall of the shaft.

3.2 Results

These analyses assumed the distribution of the retained water was uniform; however, this is probably not true. Therefore, to investigate the potential effects of the initial distribution of the retained water, time-dependent, one-dimensional calculations were performed using the NORIA-SP finite element code.

4.0 TIME-DEPENDENT WATER FLOW IN SHAFT

4.1 Discussion of Calculations

In these calculations, time-dependent, one-dimensional radial flow of the residual drilling water in the rock matrix adjacent to the shaft liner is modelled. The water is assumed to be in isothermal matrix/fracture equilibrium at all times. The water is transported as a result of pressure gradients. As designated in PDM 72-30, the computer program NORIA-SP [Hopkins et al., 1991] was used to perform the time-dependent calculations. NORIA-SP numerically solves the two-dimensional Richards' equation for single-phase flow (liquid water) in porous media using the composite fracture/matrix porosity model. When using NORIA-SP, it is necessary to describe the material characteristics, such as saturation and permeability, as a function of pressure head. This is done in two user-written subroutines, PERM and FLUIDC. An additional condition of ventilation through the shaft is also considered in the calculations (through the use of Equation 4, which is discussed later).

The following assumptions were used for the time-dependent analyses.

- The stratigraphy used was that for well USW G-4, obtained from the Reference Information Base (RIB).

- The hydrologic properties used were the current best available data from USW G-4 and USW GU-3 [Peters et al., 1984]. These hydrologic properties were used to maintain consistency with other calculations performed for ESF Analyses. Appendix B contains a list of all hydrologic properties used for this analysis. The hydrologic properties in each layer were assumed to be homogeneous and isotropic throughout that layer.

- A steady-state infiltration of 0.01 mm/year was specified as the initial condition. This infiltration rate was chosen, rather than the rate of 0.1 mm/year used by Peterson et al., because of various recent works. Weeks and Wilson (1984) report a vertical flux of between 0.003 and 0.2 mm/yr in the Topopah Spring member at USW-H1. Montazer and Wilson (1984) report a vertical flux of between 10^{-4} and 10^{-7} mm/yr in the Topopah Spring member at USW-G1.

- The steady-state conditions used for initial saturation in these analyses were those from the NORIA-SP calculations performed under PDM 72-29, which determined the steady-state saturation levels throughout the stratigraphy. A steady-state infiltration rate of 0.01 mm/yr was specified in PDM 72-29. These steady-state conditions served as the initial state ("time zero") for the time-dependent flow calculations. The calculated steady-state saturation levels were

within the range of values recorded in the RIB for all the hydrogeologic members except the PTn member.

- The shaft problem was set up as a two-dimensional, axisymmetric computational grid. A grid of 1 m height and 25 m radius, with the radius of the shaft concrete wall equal to 2.21 m, was used for each of the four selected materials (Tiva Canyon, Paintbrush, Topopah Springs, and Calico Hills). The small height of the grid, and the fact that the major source of pressure head is from the shaft wall and not from above, combine to make the effects of gravity negligible to this problem; although gravity is still in the equation, the NORIA-SP calculations are, in effect, "one-dimensional."

- The portion of the grid within the modified permeability zone (MPZ) is defined for the shaft as one shaft radius from the shaft wall [Case and Kelsall, 1987]. All hydrologic properties in the MPZ are the same as in the unmodified zone, except for the bulk-rock permeability, which is 80 times higher than the bulk-rock permeability in the unmodified zone.[2] The drilling water will most likely be nearly evenly distributed in this region before being transported into the unmodified zone through capillary action. Therefore, the initial distribution of drilling water in the MPZ should have little effect on the time-dependent results, and is thus set to a uniform saturation equal to the amount determined from the limiting-case analysis for a fill radius of 4.42 m.

- The following parameters for the expected amount of water used in the sinking operation, and the percentage of water retained, or not pumped out of the drill hole, were obtained during a personal communication with Ralph Musick of Raytheon Services Nevada, and are based on the Title I Design of the shafts in the ESF:

  Water used for shaft sinking = 230 gallons/ft (2.856 m^3/m)
  Percent of construction water not removed (expected retention factor) = 15%

- Appendix B from Peterson et al. was used as a reference for the setup of these calculations. Appendix C from Peterson et al. and SAND86-1571 [Hopkins, Eaton, Sinnock, 1987] were used as references for the ventilation boundary condition. For the case of no ventilation, the shaft wall boundary had a no-flow boundary condition. For the case with ventilation, the shaft wall had a pressure head boundary condition described by the equation

---

2. See Section 6.0 for a discussion on the interpretation of the results of Case and Kelsall as used in this analysis.

$$W = \frac{RT}{Mg} \ln \frac{u}{100} \qquad (4),$$

where W = pressure head (m),
R = universal gas constant = $8.314 \times 10^3 \frac{J}{(kg\text{-}mol)(K)}$,
T = ventilation temperature = 299.15 K,
M = molecular weight of water = 18.0 kg/kg-mol,
g = gravitational constant = 9.8 m/s^2, and
u = relative humidity = 10.0 %.

The boundary condition subroutine changed the shaft wall boundary values from ambient to the above condition gradually over a period of one day. For these calculations, the ventilation boundary condition was maintained over the entire calculational period (1000 years); in reality, the shafts will be backfilled after the 100-year active life of the repository.

- The other vertical boundary of the computational grid had a no-flow boundary condition. The top and bottom boundaries also had no-flow boundary conditions.

The following time-dependent flow calculations were performed for each of the four materials (CHnz, TSw2, PTn, TCw) with the expected amount of water:

- One calculation at the expected retention factor, with no ventilation, and
- Three calculations, with ventilation, at retention factors 10%, 15%, and 20%.

4.2 Results

The results of the shaft construction water calculations are presented in Figures 5 through 33 in Appendix C. The figures are grouped in this manner:

Tiva Canyon - Figures 5-12
Paintbrush - Figures 13-19
Topopah Springs - Figures 20-27
Calico Hills - Figures 28-33

The first figure in each group plots saturation as a function of the radial distance from the shaft centerline, with the shaft wall at radius = 2.21 m and the end of the MPZ at radius = 4.42 m, with the expected amount of drilling water, retention rate, and no ventilation, and at various times up to 1000 years. The next few figures in each group (the number varies between groups) plot the radial extent of a specified absolute change in saturation as a function of time. For example, the plot for a change in saturation of 0.001 from in-situ saturation in Tiva Canyon means a change from the in-situ saturation of 0.732 (73.2%) to a saturation of at least 0.733 (73.3%). The last three figures in each group show the effects of ventilation on the saturation of each stratigraphic member, by plotting saturation as a function of the radial distance from the shaft centerline.

For the purposes of this discussion, it is assumed that a significant (i.e., measurable) change in saturation, Δsat, is a deviation from the in-situ saturation level of at least 0.005; that is, $\Delta sat \geq |\pm 0.005|$. The standard deviation of previous measurements of in-situ saturation are much larger than this (as indicated in the RIB), so this is a conservative, yet reasonable statement. The following conclusions about the effects of shaft construction water on each of the stratigraphic members can be drawn from Figures 5-33:

Tiva Canyon (TCw) - Significant change in saturation is confined to within 10 m of the shaft centerline during the active life (the first 100 years) of the repository facility, for the case with no ventilation (Figure 5). Figures 6-9 in Appendix C illustrate the extent of dispersion by the radial extent of the change in in-situ saturation. As the change in in-situ saturation increase, the radial extent of the change in saturation decreases. The effects of ventilation are much greater, with significant effects to in-situ saturation seen out to 15 meters during the active life of the facility (Figures 10-12).

Paintbrush (PTn) - Significant change in saturation is confined to within roughly 6 m of the shaft centerline during the active life of the repository facility, for the case with no ventilation (Figure 13). Figures 14-16 in Appendix C illustrate the extent of dispersion by the radial extent of the change in in-situ saturation. Figures 15 and 16 indicate that the saturation in the MPZ reverts back to approximately the original in-situ level. The effects of ventilation are insignificant outside the MPZ (Figures 17-19).

Topopah Springs (TSw2) - Significant change in saturation is confined to within 10 m of the shaft centerline during the active life of the repository facility, for the case with no ventilation (Figure 20). Figures 21-24 in Appendix C illustrate the extent of dispersion by the radial extent of the change in in-situ saturation. As the change in in-situ saturation increase, the radial extent of the change in saturation decreases. The effects of ventilation are much greater, with significant effects to in-situ saturation seen out to 20 m during the active life of the facility (Figures 25-27).

Calico Hills (CHn) - Significant change in saturation is confined to within 6 m of the shaft centerline during the active life (the first 100 years) of the repository facility for the case with no ventilation (Figure 28). Figures 29 and 30 in Appendix C indicate that the saturation in the MPZ reverts back to approximately the original in-situ level. The effects of ventilation are much more dramatic, with significant effects to in-situ saturation seen out to 25 m (the boundary of the computational grid) during the active life of the facility, and out to nearly 20 m during the first ten years of the facility (Figures 31-33).

5.0 TIME-DEPENDENT WATER FLOW IN DRIFT

5.1 Discussion of Calculations

In these calculations, time-dependent, one-dimensional flow of the residual drilling water and in-situ pore water in the rock matrix adjacent to the drift walls is modelled. The water is assumed to be in isothermal matrix/fracture equilibrium at all times. The water is transported as a result of pressure gradients. As designated in PDM 72-30, the computer program NORIA-SP [Hopkins et al., 1991] was used to perform the time-dependent calculations. NORIA-SP numerically solves the two-dimensional Richards' equation for single-phase flow (liquid water) in porous media using the composite fracture/matrix porosity model. When using NORIA-SP, it is necessary to describe the material characteristics, such as saturation and permeability, as a function of pressure head. This is done in two user-written subroutines, PERM and FLUIDC. An additional condition, of ventilation through the drift, is also considered in the calculations.

The following assumptions and decisions were used for the time-dependent analyses (most of these are similar to those for the shaft calculations):

- The stratigraphy used was that for well USW G-4, obtained from the RIB.

- The hydrologic properties used were the current best available data from USW G-4 and USW GU-3 [Peters et al., 1984] (see Appendix B). The hydrologic properties in each layer were assumed to be homogeneous and isotropic throughout that layer.

- A steady-state infiltration of 0.01 mm/year was specified as the initial condition.

- The steady-state conditions used for initial saturation were those from the NORIA-SP calculations performed under PDM 72-29, which determined the steady-state saturation levels throughout the stratigraphy. A steady-state infiltration rate of 0.01 mm/yr was specified in PDM 72-29. These steady-state conditions served as the initial state ("time zero") for the time-dependent flow calculations. The calculated steady-state saturation levels were within the range of values recorded in the RIB for all the hydrogeological members except the PTn member.

- The drift problem was set up as a two-dimensional, cartesian region. A grid of 1 m height and 25 m width was used for each of the two selected materials for drift construction (Topopah Springs and Calico Hills). The elements start at X=0 m at the drift wall, and extend to 25 m. The small height of the grid, and the fact that the major source of pressure head is from the drift wall and not from above, combine to make the effects of gravity negligible to this problem; although gravity is still in the equation, the NORIA-SP calculations are, in effect, "one-dimensional."

- The portion of the grid within the MPZ is defined for the drift as 2.76 m from the drift wall [Case and Kelsall, 1987]. All hydrologic

properties in the MPZ are the same as in the unmodified zone, except for the bulk-rock permeability, which is 80 times higher than the bulk-rock permeability in the unmodified zone. Therefore, the initial distribution of drilling water in the MPZ was set to a uniform level equal to the amount determined from the limiting-case analysis for a fill radius of 2.76 m.

- The following parameters for the expected amount of water used in the drift excavating operation, and the percentage of water retained, or not pumped out of the drift, were obtained during a personal communication with Ralph Musick of Raytheon Services Nevada, and are based on the Title I Design of the drifts in the ESF:

  Water used for drift driving = 235 gal/ft (2.918 m^3/m)
  Percent of construction water not removed (expected retention factor) = 15%

- Appendix C from Peterson et al. was used as a reference for the setup of these calculations, and SAND86-1571 [Hopkins, Eaton, Sinnock, 1987] was used as the reference for the ventilation boundary condition. For the case of no ventilation, the drift wall boundary had a no-flow boundary condition. For the case with ventilation, the drift wall had a pressure head boundary condition described by Equation 4. The boundary condition subroutine changed the drift wall boundary values from ambient to the above condition gradually over a period of one day. For these calculations, the ventilation boundary condition was maintained over the entire calculational period (1000 years); in reality, the shafts will be backfilled after the 100-year active life of the repository.

- The other vertical boundary of the computational grid had a no-flow boundary condition. The top and bottom boundaries also had no-flow boundary conditions.

The following time-dependent flow calculations were performed for each of the two materials (CHnz, TSw2) with the expected amount of water:

- One calculation at the expected retention factor, with no ventilation, and
- Three calculations, with ventilation, at retention factors 10%, 15%, and 20%.

5.2 Results

The results of the drift construction water calculations are presented in Figures 34 through 47 in Appendix C. The figures are grouped in this manner:

Topopah Springs - Figures 34-41
Calico Hills - Figures 42-47

The first figure in each group plots saturation as a function of the horizontal distance from the drift wall, with the end of the MPZ 2.76 m from the wall, with the expected amount of drilling water, expected retention rate, and no ventilation, and at various times up to 1000 years. The next few

figures in each group (the number varies between groups) plot the horizontal extent of a specified absolute change in saturation as a function of time. For example, the plot for a change in saturation of 0.001 from in-situ saturation in Tiva Canyon means a change from the in-situ saturation of 0.732 (73.2%) to a saturation of at least 0.733 (73.3%). The last three figures in each group show the effects of ventilation on the saturation of each stratigraphic member by plotting saturation as a function of the distance from the drift wall.

For the purposes of this discussion, it is assumed that a significant (i.e., measurable) change in saturation, Δsat, is a deviation from the in-situ saturation level of at least 0.005; that is, $\Delta sat \geq |\pm 0.005|$. The standard deviation of previous measurements of in-situ saturation are much larger than this (as indicated in the RIB), so this is a conservative, yet reasonable statement. The following conclusions about the effects of drift construction water on each of the stratigraphic members can be drawn from Figures 34-47:

Topopah Springs - Significant change in saturation is confined to approximately 10 m of the drift wall during the active life of the repository facility, for the case with no ventilation (Figure 34). Figures 35-38 in Appendix C illustrate the extent of dispersion by the radial extent of the change in in-situ saturation. As the change in in-situ saturation increase, the radial extent of the change in saturation decreases. The effects of ventilation are much greater, with significant effects to in-situ saturation seen out to 20 m during the active life of the facility (Figures 39-41).

Calico Hills - Significant change in saturation is confined to within 4 m of the drift wall during the active life (the first 100 years) of the repository facility, for the case with no ventilation (Figure 42). Figures 43 and 44 in Appendix C indicate that the saturation throughout the rock in the drift wall reverts back to approximately the original in-situ level. The effects of ventilation are much more dramatic, with significant effects to in-situ saturation seen out to 25 m (the boundary of the computational grid) during the active life of the facility, and out to nearly 20 m during the first ten years of the facility (Figures 45-47).

6.0 DISCUSSION OF THE MODIFIED PERMEABILITY ZONE MODEL

The modified permeability zone model described by Case and Kelsall (1987) is used in this report to describe the characteristics of rock disturbed by shaft/drift excavation processes. Using both experimental results and analysis, Case and Kelsall evaluated the change in bulk-rock permeability based on stress redistribution due to excavation. They evaluated the effects of tunnel-boring methods separately and in combination with blasting, and calculated an equivalent permeability for expected, lower-bound, and upper-bound cases. The equivalent permeability was defined as the bulk-rock permeability of the MPZ (averaged over an annulus one radius wide around the shaft), normalized by the in-situ bulk-rock permeability of the undisturbed rock. The results of their analyses indicate that the worst case is described by a combination of boring and blasting excavation methods and the upper-bound case of elastoplastic deformations; an equivalent bulk-rock permeability of 80 was calculated for this scenario.

There are two possible interpretations for this 80-fold increase in bulk-rock permeability. In the predecessor to this work by Peterson et al., this increase was simulated as an 80-fold increase of the matrix permeability. This interpretation is implemented in the PERM subroutine to NORIA-SP, where the matrix permeability of the MPZ is defined as the matrix permeability of the unaffected rock layer multiplied by 80. The reason for this interpretation was due to the experimental results described by Case and Kelsall. Water flow was induced in modified rock, and the resulting permeability was compared to that for unmodified rock. It is unclear from the Case and Kelsall report if the rock is saturated during the experiment. According to the widely used conceptual model implemented in this work, matrix flow is the dominant flow mechanism except where the rock is very nearly or completely saturated, where fracture flow dominates. The results of the work of Peterson et al. showed the water imbibed into the MPZ does not raise the saturation level high enough to instigate fracture flow in any of the hydrogeological layers (with the possible exception of the Calico Hills layer). Thus, allowing the increase in bulk-rock permeability to be contained entirely in the matrix is a conservative assumption. For reasons of consistency and conservatism, this assumption is also used for the analyses described in this report.

A second interpretation of the results of Case and Kelsall, which is probably more correct, is that the increase in permeability in the MPZ is contained entirely in the fracture system. According to the analysis, a redistribution of stress will occur in the vicinity of the excavation after boring and/or blasting. This stress redistribution results from two sources: the creation of new fractures in the MPZ, and the opening of the apertures in the existing fracture system due to stress relaxation. As a result, the relative fracture volume increases. There is expected to be no change in the number and size of pores in the matrix of the damaged rock (and, therefore, no change to the matrix permeability). In the particular case described in the preceding paragraph, the fracture volume, and hence the fracture permeability, are increased by a factor of 80. According to the cubic law, the fracture permeability is proportional to the cube of the aperture size; therefore, the fracture aperture (and, accordingly, the fracture porosity) is increased by a factor of approximately 4.3. Application of this interpretation of the Case and Kelsall results into the model used for the problems in this analysis would increase the amount of water initially stored in the MPZ by a negligible amount. Consequently, the saturation in the MPZ would be below the threshold for instigating fracture flow, according to the composite fracture/ matrix model. Increasing the fracture permeability would have insignificant effects on the water movement in the MPZ. Therefore, the use of the assumption of the increase in matrix permeability is more conservative than the fracture-based assumption, albeit less consistent with the physical processes.

Another limitation of the Case and Kelsall study is that the analysis applies primarily to welded tuffs, specifically the Tiva Canyon and Topopah Spring hydrogeologic layers. These layers are densely welded, highly fractured units, with low saturated-matrix conductivities and high saturated-fracture-system conductivities. Nonwelded tuffs, such as PTn and CHn, have low saturated-fracture-system conductivities, and tend not to fracture as much as the welded tuffs when damaged. Therefore, the results presented for the nonwelded tuffs have little application beyond this report.

In determining the value of equivalent permeability for the worst case scenario, it was assumed that blasting methods would be used in the excavation process. However, the recently published findings of the ESF Alternative Study [Stevens and Costin, 1991] suggest that if shafts are used in the ESF design, a mechanical excavation method such as tunnel-boring would be a better way than blasting to sink a shaft with minimal disturbance to the surrounding rock. According to Case and Kelsall, the worst case scenario without blasting would result in an increase in the bulk-rock permeability by a factor of 40. Therefore, the value of 80 used for the equivalent permeability in this report is a conservative value.

7.0 CONCLUSIONS

The analyses described in this report indicate that retained drilling water will introduce no significant changes in saturation outside a zone of 10 m around any shaft or drift construction. A more significant effect is that produced by ventilation, which may dry at least 25 m of rock enough to affect experiments. Designers may use the graphical results of these analyses to locate experiments in relation to excavated areas.[3] Because of the small localized regions of disturbance due to drilling water, and the small magnitudes of those effects, no significant effects of drilling water on repository performance are expected.

8.0 SUGGESTED ADDITIONAL ANALYSES

These calculations are based on available data and on the present conceptual understanding of the processes and mechanisms perceived active at Yucca Mountain. Due to our limited knowledge of Yucca Mountain prior to site characterization, the hydrogeological conceptual model, existing conceptual models of the physical processes, and the mathematical models used in these analyses are not validated. These calculations may be refined as better understanding evolves through site characterization and through additional analyses. The following are suggested additional analyses that may be performed before and during construction of the ESF, and in conjunction with testing performed in the ESF.

- Redo the calculations using the assumption that the increase in bulk-rock permeability is contained entirely within the fracture system (especially for those cases where the MPZ is nearly or completely saturated).

- Perform a similar analysis to determine the possible effects of an underground ramp. The results of the drift calculations can serve as a first approximation.

- Perform the calculations for varying sizes of shafts, drifts, and ramps, and the resulting changes in required drilling water.

---

3. One important consideration not covered in this analysis, but which is covered by another of the ESF Analyses, is the effect of surface construction water on experiments, especially in the TCw and PTn layers.

- It is possible that natural fracture orientations are largely vertical. Perform the calculations with a larger problem domain (e.g., larger height) to include the effects of gravity, and perhaps structure a new grid with elements that model vertical fractures.

- Perform the previous calculations with non-homogeneous, non-isotropic hydrologic parameters.

9.0 REFERENCES

Bixler, N. E., 1985. NORIA-- A Finite Element Computer Program for Analyzing Water, Vapor, Air, and Energy Transport in Porous Media, SAND84-2057, Sandia National Laboratories, Albuquerque, New Mexico. (NNA.870721.0002)

Case, J. B., and P. C. Kelsall, 1987. Modification of Rock Mass Permeability in the Zone Surrounding a Shaft in Fractured, Welded Tuff, SAND86-7001, Sandia National Laboratories, Albuquerque, New Mexico. (HQS.880517.2264)

Hopkins, P. L., N. E. Bixler, and R. R. Eaton, 1991. NORIA-SP - A Finite Element Computer Program for Analyzing Liquid Water Transport in Porous Media, SAND90-2542, Sandia National Laboratories, Albuquerque, New Mexico. (NNA.911202.0031)

Hopkins, Polly L., Roger R. Eaton, and Scott Sinnock, 1987. Effect of Drift Ventilation on Repository Hydrology and Resulting Solute Transport Implications, SAND86-1571, Sandia National Laboratories, Albuquerque, New Mexico. (HQS.880517.2712)

Montazer, P., and W. E. Wilson, 1984. Conceptual Hydrologic Model of Flow in the Unsaturated Zone, Yucca Mountain, Nevada, WRIR 84-4345, U.S. Geologic Survey, Lakewood, Colorado. (HQS.880517.1675)

Ortiz, Terri S., Robert L. Williams, Francis B. Nimick, Bruce C. Whittet, and Don L. South, 1985. A Three-Dimensional Model of Reference Thermal/Mechanical and Hydrological Stratigraphy at Yucca Mountain, Southern Nevada, SAND84-1076, Sandia National Laboratories, Albuquerque, New Mexico. (NNA.890315.0013)

Peters, R. R., E. A. Klavetter, I. J. Hall, S. C. Blair, P. R. Heller, and G. W. Gee, 1984. Fracture and Matrix Hydrologic Characteristics of Tuffaceous Materials from Yucca Mountain, Nye County, Nevada, SAND84-1471, Sandia National Laboratories, Albuquerque, New Mexico. (NNA.870407.0036)

Peterson, Andrew C., Roger R. Eaton, Anthony J. Russo, and John A. Lewin, 1988. Technical Correspondence in Support of an Evaluation of the Hydrologic Effects of Exploratory Shaft Facility Construction at Yucca Mountain, SAND88-2936, Sandia National Laboratories, Albuquerque, New Mexico. (NNA.881202.0206)

Problem Definition Memo, "ESF SDRD Analysis #1 - Effects of Surface Water on Experiments in the ESF," PDM No. 72-29, Sandia National Laboratories, Albuquerque, New Mexico, December 1990. (NNA.910301.0075)

Problem Definition Memo, "ESF SDRD Analysis #2 - Effects of Shaft Construction Water on Experiments in the ESF," PDM No. 72-30, Sandia National Laboratories, Albuquerque, New Mexico, December 1990. (NNA.910301.0076)

Stevens, A. L., and L. S. Costin, 1991. Findings of the ESF Alternatives Study, SAND90-3232, Sandia National Laboratories, Albuquerque, New Mexico. (NNA.910219.0003)

Weeks, E. P., and W. E. Wilson, 1984. Preliminary Evaluation of Hydrologic Properties of Cores of Unsaturated Tuff, Test Well USW H-1, Yucca Mountain,

Nevada, WRIR 84-4193, U.S. Geologic Survey, Lakewood, Colorado. (HQS.880517.2570)

YMP (Yucca Mountain Project), 1989. Exploratory Shaft Facility (ESF) Title I Design Acceptability Analysis and Comparative Evaluation of Alternative ESF Locations, YMP/89-3, issued February 3, 1989, Las Vegas, Nevada. (NNA.890522.0003-.0006)

Appendix A

Uniform Distribution - Limiting Cases

SHAFTH2O.XLS

Microsoft EXCEL version of RAD.FOR, used to calculate the radius of fracture fill and change in saturation in the matrix due to the retention of water from ESF shaft drilling activities

W, Total Water, m^3/m	2.85591	X, Expected retention of drill water, fract.	(0.10,0.15,0.20)
gal/ft	230.		
Ro, radius of drill shaft, m	2.21		
SRF, res. sat. in fractures	0.039		

	TCw	PTn	TSw1	TSw2	CHn
Vf, Fracture Porosity	1.40E-04	2.75E-05	4.10E-05	1.80E-04	4.60E-05
PORM, Matrix Porosity	0.08	0.4	0.11	0.11	0.46

Case 1

Fill Radius (m)

% Drill Water	TCw	PTn	TSw1	TSw2	CHn
0	2.21	2.21	2.21	2.21	2.21
1	8.51189965	18.6780179	15.349438	7.5787367	14.5095438
2	11.8330373	26.3220935	21.5945917	10.4876308	20.4002358
3	14.4079529	32.1999513	26.4016579	12.7492568	24.9361661
4	16.5878703	37.1594014	30.4592955	14.6661754	28.76552
5	18.5128544	41.5307762	34.0365954	16.3600076	32.1418404
6	20.255718	45.4839491	37.2721206	17.8942169	35.1957478
7	21.8600652	49.1199947	40.2483804	19.3068938	38.0050447
8	23.3544596	52.5048391	43.0192197	20.6230284	40.6205143
9	24.758819	55.68431	45.6220825	21.8600652	43.0774761
10	26.0876878	58.6917936	48.0842548	23.0307533	45.4016707

Change in Saturation

Porosity	TCw	PTn	TSw1	TSw2	CHn
0.05	2.691E-03	5.285E-04	7.880E-04	3.460E-03	8.841E-04
0.1	1.345E-03	2.643E-04	3.940E-04	1.730E-03	4.421E-04
0.15	8.969E-04	1.762E-04	2.627E-04	1.153E-03	2.947E-04
0.2	6.727E-04	1.321E-04	1.970E-04	8.649E-04	2.210E-04
0.25	5.382E-04	1.057E-04	1.576E-04	6.919E-04	1.768E-04
0.3	4.485E-04	8.809E-05	1.313E-04	5.766E-04	1.474E-04
0.35	3.844E-04	7.551E-05	1.126E-04	4.942E-04	1.263E-04
0.4	3.364E-04	6.607E-05	9.850E-05	4.325E-04	1.105E-04
0.45	2.990E-04	5.873E-05	8.756E-05	3.844E-04	9.824E-05
0.5	2.691E-04	5.286E-05	7.880E-05	3.460E-04	8.841E-05

Case 2

Saturation Increase, Retention rate=0.1

Fill Radius, m	TCw	PTn	TSw1	TSw2	CHn
4.42	7.755E-02	1.551E-02	5.640E-02	5.640E-02	1.349E-02
10	1.195E-02	2.389E-03	8.689E-03	8.689E-03	2.078E-03
20	2.876E-03	5.752E-04	2.092E-03	2.092E-03	5.002E-04
30	1.269E-03	2.539E-04	9.233E-04	9.233E-04	2.208E-04
40	7.124E-04	1.425E-04	5.181E-04	5.181E-04	1.239E-04
50	4.554E-04	9.108E-05	3.312E-04	3.312E-04	7.920E-05
60	3.161E-04	6.322E-05	2.299E-04	2.299E-04	5.497E-05
70	2.321E-04	4.643E-05	1.688E-04	1.688E-04	4.037E-05
80	1.777E-04	3.554E-05	1.292E-04	1.292E-04	3.090E-05
90	1.404E-04	2.807E-05	1.021E-04	1.021E-04	2.441E-05
100	1.137E-04	2.274E-05	8.268E-05	8.268E-05	1.977E-05
110	9.395E-05	1.879E-05	6.833E-05	6.833E-05	1.634E-05

Variable	TCw	PTn	TSw1	TSw2	CHn
Z, height, m	1242.784	1215.752	1116.35	947.782	792.28
NORIA cell no.	761	701	561	421	101
Pressure, from NORIA-SP sol'n ROAD.T1	10712019	10407170	8387019.47	7426215.33	7206548.93
(put in material property card for each material)					
PSI, pressure head(ROAD.T1)	-149.72084	-153.79588	-260.53169	-190.00493	-56.917864
Alpha	0.00821	0.015	0.00567	0.00567	0.00308
Beta	1.558	6.872	1.798	1.798	1.602
Lambda	0.35815148	0.85448196	0.44382647	0.44382647	0.37578027
Mat. Res. Sat.	0.002	0.1	0.08	0.08	0.11
Saturation in ROAD.T1	0.73366005	0.10662689	0.64357711	0.7359098	0.98027498
MPZ saturation-SS+4.42 m fill	0.8112131	0.1221375	0.69997932	0.79231202	0.99376247
PSI, MPZ	-105.19795	-125.05696	-215.46756	-153.57834	-27.256665
Tot. Pressure, MPZ mater. card	11148343.3	10688811.4	8828647.91	7783195.87	7497228.68

Case 2

Fill Radius, m	Saturation Increase, Retention rate=0.15 TCw	PTn	TSw1	TSw2	CHn
4.42	1.163E-01	2.327E-02	8.460E-02	8.460E-02	2.023E-02
10	1.792E-02	3.584E-03	1.303E-02	1.303E-02	3.117E-03
20	4.314E-03	8.628E-04	3.137E-03	3.137E-03	7.502E-04
30	1.904E-03	3.808E-04	1.385E-03	1.385E-03	3.312E-04
40	1.069E-03	2.137E-04	7.771E-04	7.771E-04	1.858E-04
50	6.831E-04	1.366E-04	4.968E-04	4.968E-04	1.188E-04
60	4.741E-04	9.482E-05	3.448E-04	3.448E-04	8.245E-05
70	3.482E-04	6.964E-05	2.532E-04	2.532E-04	6.056E-05
80	2.665E-04	5.331E-05	1.938E-04	1.938E-04	4.635E-05
90	2.106E-04	4.211E-05	1.531E-04	1.531E-04	3.662E-05
100	1.705E-04	3.411E-05	1.240E-04	1.240E-04	2.966E-05
110	1.409E-04	2.818E-05	1.025E-04	1.025E-04	2.451E-05

Variable	TCw	PTn	TSw1	TSw2	CHn
Z, height, m	1242.784	1215.752	1116.35	947.782	792.28
NORIA cell no.	761	701	561	421	101
Pressure, from NORIA-SP sol'n ROAD.T1	10712019	10407170	8387019.47	7426215.33	7206548.93
(put in material property card for each material)					
PSI, pressure head(ROAD.T1)	-149.72084	-153.79588	-260.53169	-190.00493	-56.917864
Alpha	0.00821	0.015	0.00567	0.00567	0.00308
Beta	1.558	6.872	1.798	1.798	1.602
Lambda	0.35815148	0.85448196	0.44382647	0.44382647	0.37578027
Mat. Res. Sat.	0.002	0.1	0.08	0.08	0.11
Saturation in ROAD.T1	0.73366005	0.10662689	0.64357711	0.7359098	0.98027498
MPZ saturation-SS+4.42 m fill	0.84998962	0.1298928	0.72818043	0.82051313	1
PSI, MPZ	-85.469387	-118.72449	-195.30849	-136.48241	0
Tot. Pressure, MPZ mater. card	11341683.2	10750869.6	9026206.84	7950736.02	7764344

SHAFTH2O.XLS (cont.)

Case 2

Saturation Increase, Retention rate=0.2

Fill Radius, m	TCw	PTn	TSw1	TSw2	CHn
4.42	1.551E-01	3.102E-02	1.128E-01	1.128E-01	2.697E-02
10	2.389E-02	4.779E-03	1.738E-02	1.738E-02	4.155E-03
20	5.752E-03	1.150E-03	4.183E-03	4.183E-03	1.000E-03
30	2.539E-03	5.078E-04	1.847E-03	1.847E-03	4.416E-04
40	1.425E-03	2.850E-04	1.036E-03	1.036E-03	2.478E-04
50	9.108E-04	1.822E-04	6.624E-04	6.624E-04	1.584E-04
60	6.322E-04	1.264E-04	4.597E-04	4.597E-04	1.099E-04
70	4.643E-04	9.285E-05	3.377E-04	3.377E-04	8.074E-05
80	3.554E-04	7.107E-05	2.585E-04	2.585E-04	6.180E-05
90	2.807E-04	5.615E-05	2.042E-04	2.042E-04	4.883E-05
100	2.274E-04	4.548E-05	1.654E-04	1.654E-04	3.954E-05
110	1.879E-04	3.758E-05	1.367E-04	1.367E-04	3.268E-05

Variable	TCw	PTn	TSw1	TSw2	CHn
Z, height, m	1242.784	1215.752	1116.35	947.782	792.28
NORIA cell no.	761	701	561	421	101
Pressure, from NORIA-SP sol'n ROAD.T1	10712019	10407170	8387019.47	7426215.33	7206548.93
(put in material property card for each material)					
PSI, pressure head(ROAD.T1)	-149.72084	-153.79588	-260.53169	-190.00493	-56.917864
Alpha	0.00821	0.015	0.00567	0.00567	0.00308
Beta	1.558	6.872	1.798	1.798	1.602
Lambda	0.35815148	0.85448196	0.44382647	0.44382647	0.37578027
Mat. Res. Sat.	0.002	0.1	0.08	0.08	0.11
Saturation in ROAD.T1	0.73366005	0.10662689	0.64357711	0.7359098	0.98027498
MPZ saturation-SS+4.42 m fill	0.88876614	0.13764811	0.75638154	0.84871423	1
PSI, MPZ	-66.653583	-114.05334	-176.35769	-119.81163	0
Tot. Pressure, MPZ mater. card	11526078.1	10796646.8	9211924.68	8114109.58	7764344

DRIFTH2O.XLS

Microsoft EXCEL version of DRIFT.FOR, used to calculate the radius of fracture fill and change in saturation in the matrix due to the retention of water from ESF drift drilling activities

W, Total Water, m^3/m 2.917995
gal/ft 235.

X, Expected retention of drill water, fract. (0.10,0.15,0.20)

Ro, radius of drift ceiling, m 3.38

SRF, res. sat. in fractures 0.039

	TCw	PTn	TSw1	TSw2	CHn
Vf, Fracture Porosity	1.40E-04	2.75E-05	4.10E-05	1.80E-04	4.60E-05
PORM, Matrix Porosity	0.08	0.4	0.11	0.11	0.46

Case 1

Fill Radius (m)

% Drill Water	TCw	PTn	TSw1	TSw2	CHn
0	3.38	3.38	3.38	3.38	3.38
1	8.97003971	19.049582	15.721362	8.069697	14.8841411
2	12.2269712	26.7273034	21.9749413	10.9002578	20.7762102
3	14.7829644	32.6467597	26.8073659	13.134353	25.3330647
4	16.9579848	37.6466876	30.8929068	15.0401742	29.1869392
5	18.8841326	42.0563344	34.4979494	16.7302854	32.5881984
6	20.6312306	46.0456017	37.7603673	18.2646669	35.666566
7	22.2415127	49.7157883	40.7625093	19.6797781	38.4995739
8	23.7428326	53.1330573	43.5582252	20.9997447	41.1379441
9	25.1547076	56.3434464	46.1850171	22.2415127	43.6170116
10	26.4914425	59.3805197	48.6702438	23.4175254	45.9625603

Change in Saturation

Porosity	TCw	PTn	TSw1	TSw2	CHn
0.05	2.691E-03	5.285E-04	7.880E-04	3.460E-03	8.841E-04
0.1	1.345E-03	2.643E-04	3.940E-04	1.730E-03	4.421E-04
0.15	8.969E-04	1.762E-04	2.627E-04	1.153E-03	2.947E-04
0.2	6.727E-04	1.321E-04	1.970E-04	8.649E-04	2.210E-04
0.25	5.382E-04	1.057E-04	1.576E-04	6.919E-04	1.768E-04
0.3	4.485E-04	8.809E-05	1.313E-04	5.766E-04	1.474E-04
0.35	3.844E-04	7.551E-05	1.126E-04	4.942E-04	1.263E-04
0.4	3.364E-04	6.607E-05	9.850E-05	4.325E-04	1.105E-04
0.45	2.990E-04	5.873E-05	8.756E-05	3.844E-04	9.824E-05
0.5	2.691E-04	5.286E-05	7.880E-05	3.460E-04	8.841E-05

Case 2

Saturation Increase, Retention rate=0.1

Fill Radius, m	TCw	PTn	TSw1	TSw2	CHn
6.14	4.419E-02	8.837E-03	3.214E-02	3.214E-02	7.685E-03
10	1.311E-02	2.622E-03	9.533E-03	9.533E-03	2.280E-03
20	2.988E-03	5.976E-04	2.173E-03	2.173E-03	5.196E-04
30	1.307E-03	2.613E-04	9.503E-04	9.503E-04	2.272E-04
40	7.309E-04	1.462E-04	5.315E-04	5.315E-04	1.271E-04
50	4.665E-04	9.331E-05	3.393E-04	3.393E-04	8.114E-05
60	3.235E-04	6.471E-05	2.353E-04	2.353E-04	5.627E-05
70	2.375E-04	4.750E-05	1.727E-04	1.727E-04	4.130E-05
80	1.817E-04	3.635E-05	1.322E-04	1.322E-04	3.161E-05
90	1.435E-04	2.871E-05	1.044E-04	1.044E-04	2.496E-05
100	1.162E-04	2.325E-05	8.454E-05	8.454E-05	2.021E-05
110	9.604E-05	1.921E-05	6.985E-05	6.985E-05	1.670E-05

Variable	TCw	PTn	TSw1	TSw2	CHn
Z, height, m	1242.784	1215.752	1116.35	947.782	792.28
NORIA cell no.	761	701	561	421	101
Pressure, from NORIA-SP sol'n ROAD.T1	10712019	10407170	8387019.47	7426215.33	7206548.93
(put in material property card for each material)					
PSI, pressure head(ROAD.T1)	-149.72084	-153.79588	-260.53169	-190.00493	-56.917864
Alpha	0.00821	0.015	0.00567	0.00567	0.00308
Beta	1.558	6.872	1.798	1.798	1.602
Lambda	0.35815148	0.85448196	0.44382647	0.44382647	0.37578027
Mat. Res. Sat.	0.002	0.1	0.08	0.08	0.11
Saturation in ROAD.T1	0.73366005	0.10662689	0.64357711	0.7359098	0.98027498
MPZ saturation-SS+2.76 m fill	0.77784747	0.11546437	0.67571341	0.76804611	0.98795975
PSI, MPZ	-123.35279	-133.02295	-233.98608	-168.81441	-41.404023
Tot. Pressure, MPZ mater. card	10970425.9	10610744.7	8647166.45	7633882.34	7358584.58

Case 2

Saturation Increase, Retention rate=0.15

Fill Radius, m	TCw	PTn	TSw1	TSw2	CHn
6.14	6.628E-02	1.326E-02	4.820E-02	4.820E-02	1.153E-02
10	1.966E-02	3.932E-03	1.430E-02	1.430E-02	3.419E-03
20	4.482E-03	8.964E-04	3.260E-03	3.260E-03	7.795E-04
30	1.960E-03	3.920E-04	1.425E-03	1.425E-03	3.409E-04
40	1.096E-03	2.193E-04	7.973E-04	7.973E-04	1.907E-04
50	6.998E-04	1.400E-04	5.090E-04	5.090E-04	1.217E-04
60	4.853E-04	9.706E-05	3.529E-04	3.529E-04	8.440E-05
70	3.562E-04	7.125E-05	2.591E-04	2.591E-04	6.196E-05
80	2.726E-04	5.452E-05	1.983E-04	1.983E-04	4.741E-05
90	2.153E-04	4.306E-05	1.566E-04	1.566E-04	3.745E-05
100	1.744E-04	3.487E-05	1.268E-04	1.268E-04	3.032E-05
110	1.441E-04	2.881E-05	1.048E-04	1.048E-04	2.505E-05

Variable	TCw	PTn	TSw1	TSw2	CHn
Z, height, m	1242.784	1215.752	1116.35	947.782	792.28
NORIA cell no.	761	701	561	421	101
Pressure, from NORIA-SP sol'n ROAD.T1	10712019	10407170	8387019.47	7426215.33	7206548.93
(put in material property card for each material)					
PSI, pressure head(ROAD.T1)	-149.72084	-153.79588	-260.53169	-190.00493	-56.917864
Alpha	0.00821	0.015	0.00567	0.00567	0.00308
Beta	1.558	6.872	1.798	1.798	1.602
Lambda	0.35815148	0.85448196	0.44382647	0.44382647	0.37578027
Mat. Res. Sat.	0.002	0.1	0.08	0.08	0.11
Saturation in ROAD.T1	0.73366005	0.10662689	0.64357711	0.7359098	0.98027498
MPZ saturation-SS+2.76 m fill	0.79994119	0.11988311	0.69178157	0.78411426	0.99180214
PSI, MPZ	-111.18937	-127.39437	-221.59208	-158.66287	-32.408923
Tot. Pressure, MPZ mater. card	11089627.4	10665904.7	8768627.6	7733367.49	7446736.56

Case 2

Saturation Increase, Retention rate=0.2

Fill Radius, m	TCw	PTn	TSw1	TSw2	CHn
6.14	8.837E-02	1.767E-02	6.427E-02	6.427E-02	1.537E-02
10	2.622E-02	5.243E-03	1.907E-02	1.907E-02	4.559E-03
20	5.976E-03	1.195E-03	4.346E-03	4.346E-03	1.039E-03
30	2.613E-03	5.226E-04	1.901E-03	1.901E-03	4.545E-04
40	1.462E-03	2.923E-04	1.063E-03	1.063E-03	2.542E-04
50	9.331E-04	1.866E-04	6.786E-04	6.786E-04	1.623E-04
60	6.471E-04	1.294E-04	4.706E-04	4.706E-04	1.125E-04
70	4.750E-04	9.500E-05	3.455E-04	3.455E-04	8.261E-05
80	3.635E-04	7.269E-05	2.643E-04	2.643E-04	6.321E-05
90	2.871E-04	5.742E-05	2.088E-04	2.088E-04	4.993E-05
100	2.325E-04	4.649E-05	1.691E-04	1.691E-04	4.043E-05
110	1.921E-04	3.842E-05	1.397E-04	1.397E-04	3.341E-05

Variable	TCw	PTn	TSw1	TSw2	CHn
Z, height, m	1242.784	1215.752	1116.35	947.782	792.28
NORIA cell no.	761	701	561	421	101
Pressure, from NORIA-SP sol'n ROAD.T1	10712019	10407170	8387019.47	7426215.33	7206548.93
(put in material property card for each material)					
PSI, pressure head(ROAD.T1)	-149.72084	-153.79588	-260.53169	-190.00493	-56.917864
Alpha	0.00821	0.015	0.00567	0.00567	0.00308
Beta	1.558	6.872	1.798	1.798	1.602
Lambda	0.35815148	0.85448196	0.44382647	0.44382647	0.37578027
Mat. Res. Sat.	0.002	0.1	0.08	0.08	0.11
Saturation in ROAD.T1	0.73366005	0.10662689	0.64357711	0.7359098	0.98027498
MPZ saturation-SS+2.76 m fill	0.8220349	0.12430186	0.70784972	0.80018242	0.99564452
PSI, MPZ	-99.56522	-123.05864	-209.70501	-148.75005	-21.729589
Tot. Pressure, MPZ mater. card	11203544	10708394.9	8885120.91	7830513.08	7551394.03

Appendix B

Parameters Used for the Time-Dependent Analyses

Water Properties

Density of water, kg/m^3	1000	Standard
Compressibility of water, 1/m	4.30E-06	Standard
Dyn. Viscosity of water, kg/(m*sec)	0.001	Standard @ 68°F
Acceleration of gravity, m/sec^2	9.8	Standard
Steady-st. infil. rate (q), mm/yr	0.01	
m/sec	3.17E-13	Given: Boundary condition on surface

USW G-4 Stratigraphy and Rock Characteristics

Description of variable, units	Value	Reference
CHnz, Calico Hills		
Min. elevation, m	752	RIB
Max. elevation, m	856	RIB
Matrix effective porosity, none	0.28	CHnz/G4-11 SAND84-1471
Matrix sat. hyd. conductivity, m/s	2.00E-11	CHnz/G4-11 SAND84-1471
Matrix van Genuchten parameters		
Saturation value, none	1	CHnz/G4-11 SAND84-1471
Residual saturation, none	0.11	CHnz/G4-11 SAND84-1471
ALPHA coefficient, 1/m	0.00308	CHnz/G4-11 SAND84-1471
BETA coefficient, none	1.602	CHnz/G4-11 SAND84-1471
Fracture effective porosity, none	1	CHnz/G4-4F SAND84-1471
Fract. sat. hyd. conductivity, m/s	2.00E-04	CHnz/G4-4F SAND84-1471
Fracture van Genuchten parameters		
Saturation value, none	1	CHnz/G4-4F SAND84-1471
Residual saturation, none	0.0395	CHnz/G4-4F SAND84-1471
ALPHA coefficient, 1/m	1.2851	CHnz/G4-4F SAND84-1471
BETA coefficient, none	4.23	CHnz/G4-4F SAND84-1471
Fracture porosity, none	4.60E-05	SAND84-1471
Bulk-rock compressibility, 1/m	2.60E-06	SAND84-1471
Fracture compressibility, 1/m	2.80E-08	SAND84-1471
TSw2, Topopah Springs (repository horizon)		
Min. elevation, m	877	RIB
Max. elevation, m	1066	RIB
Matrix effective porosity, none	0.11	TSw2/G4-6 SAND84-1471
Matrix sat. hyd. conductivity, m/s	1.90E-11	TSw2/G4-6 SAND84-1471
Matrix van Genuchten parameters		
Saturation value, none	1	TSw2/G4-6 SAND84-1471
Residual saturation, none	0.08	TSw2/G4-6 SAND84-1471
ALPHA coefficient, 1/m	0.00567	TSw2/G4-6 SAND84-1471
BETA coefficient, none	1.798	TSw2/G4-6 SAND84-1471
Fracture effective porosity, none	1	TSw2/G4-2F SAND84-1471
Fract. sat. hyd. conductivity, m/s	1.75E-05	TSw2/G4-2F SAND84-1471
Fracture van Genuchten parameters		
Saturation value, none	1	TSw2/G4-2F SAND84-1471
Residual saturation, none	0.0395	TSw2/G4-2F SAND84-1471
ALPHA coefficient, 1/m	1.2851	TSw2/G4-2F SAND84-1471
BETA coefficient, none	4.23	TSw2/G4-2F SAND84-1471
Fracture porosity, none	1.80E-04	SAND84-1471
Bulk-rock compressibility, 1/m	5.80E-07	SAND84-1471
Fracture compressibility, 1/m	1.20E-07	SAND84-1471

USW G-4 Stratigraphy and Rock Characteristics

Description of variable, units	Value	Reference
PTn, Paintbrush Tuff		
Min. elevation, m	1196	RIB
Max. elevation, m	1234	RIB
Matrix effective porosity, none	0.4	PTn/GU3-7 SAND84-1471
Matrix sat. hyd. conductivity, m/s	3.90E-07	PTn/GU3-7 SAND84-1471
Matrix van Genuchten parameters		
Saturation value, none	1	PTn/GU3-7 SAND84-1471
Residual saturation, none	0.1	PTn/GU3-7 SAND84-1471
ALPHA coefficient, 1/m	0.015	PTn/GU3-7 SAND84-1471
BETA coefficient, none	6.872	PTn/GU3-7 SAND84-1471
Fracture effective porosity, none	1	PTn/G4-3F SAND84-1471
Fract. sat. hyd. conductivity, m/s	6.10E-04	PTn/G4-3F SAND84-1471
Fracture van Genuchten parameters		
Saturation value, none	1	PTn/G4-3F SAND84-1471
Residual saturation, none	0.0395	PTn/G4-3F SAND84-1471
ALPHA coefficient, 1/m	1.2851	PTn/G4-3F SAND84-1471
BETA coefficient, none	4.23	PTn/G4-3F SAND84-1471
Fracture porosity, none	2.70E-05	SAND84-1471
Bulk-rock compressibility, 1/m	8.20E-06	SAND84-1471
Fracture compressibility, 1/m	1.90E-07	SAND84-1471
TCw, Tiva Canyon		
Min. elevation, m	1234	RIB
Max. elevation, m	1261	RIB
Matrix effective porosity, none	0.08	TCw/G4-1 SAND84-1471
Matrix sat. hyd. conductivity, m/s	9.70E-12	TCw/G4-1 SAND84-1471
Matrix van Genuchten parameters		
Saturation value, none	1	TCw/G4-1 SAND84-1471
Residual saturation, none	0.002	TCw/G4-1 SAND84-1471
ALPHA coefficient, 1/m	0.00821	TCw/G4-1 SAND84-1471
BETA coefficient, none	1.558	TCw/G4-1 SAND84-1471
Fracture effective porosity, none	1	TCw/G4-2F SAND84-1471
Fract. sat. hyd. conductivity, m/s	3.80E-05	TCw/G4-2F SAND84-1471
Fracture van Genuchten parameters		
Saturation value, none	1	TCw/G4-2F SAND84-1471
Residual saturation, none	0.0395	TCw/G4-2F SAND84-1471
ALPHA coefficient, 1/m	1.2851	TCw/G4-2F SAND84-1471
BETA coefficient, none	4.23	TCw/G4-2F SAND84-1471
Fracture porosity, none	1.40E-04	SAND84-1471
Bulk-rock compressibility, 1/m	6.20E-07	SAND84-1471
Fracture compressibility, 1/m	1.32E-06	SAND84-1471

Appendix C

Figures

PROBLEM GEOMETRY

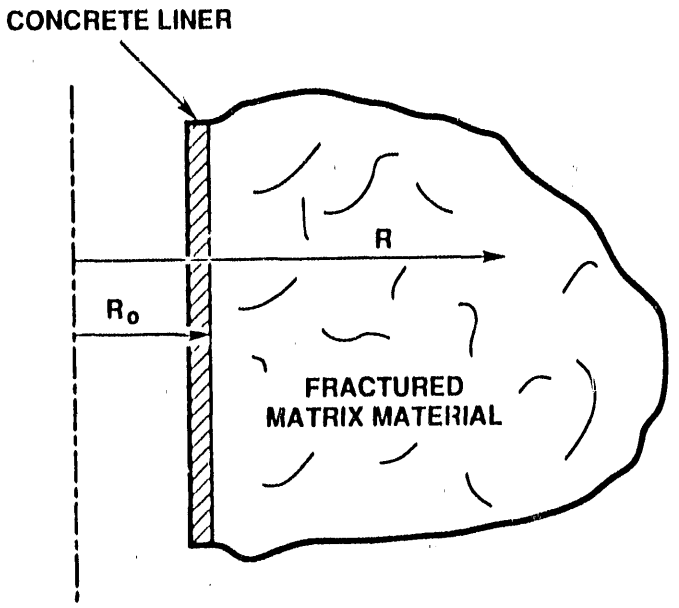

Figure 1: Outline of Shaft Problem Geometry

DRIFT GEOMETRY USED IN ANALYSIS

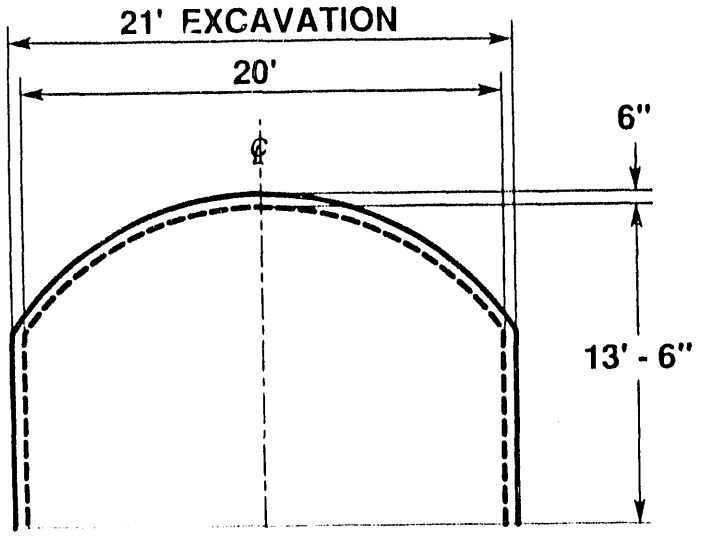

Figure 2: Drift Geometry Used in Analysis

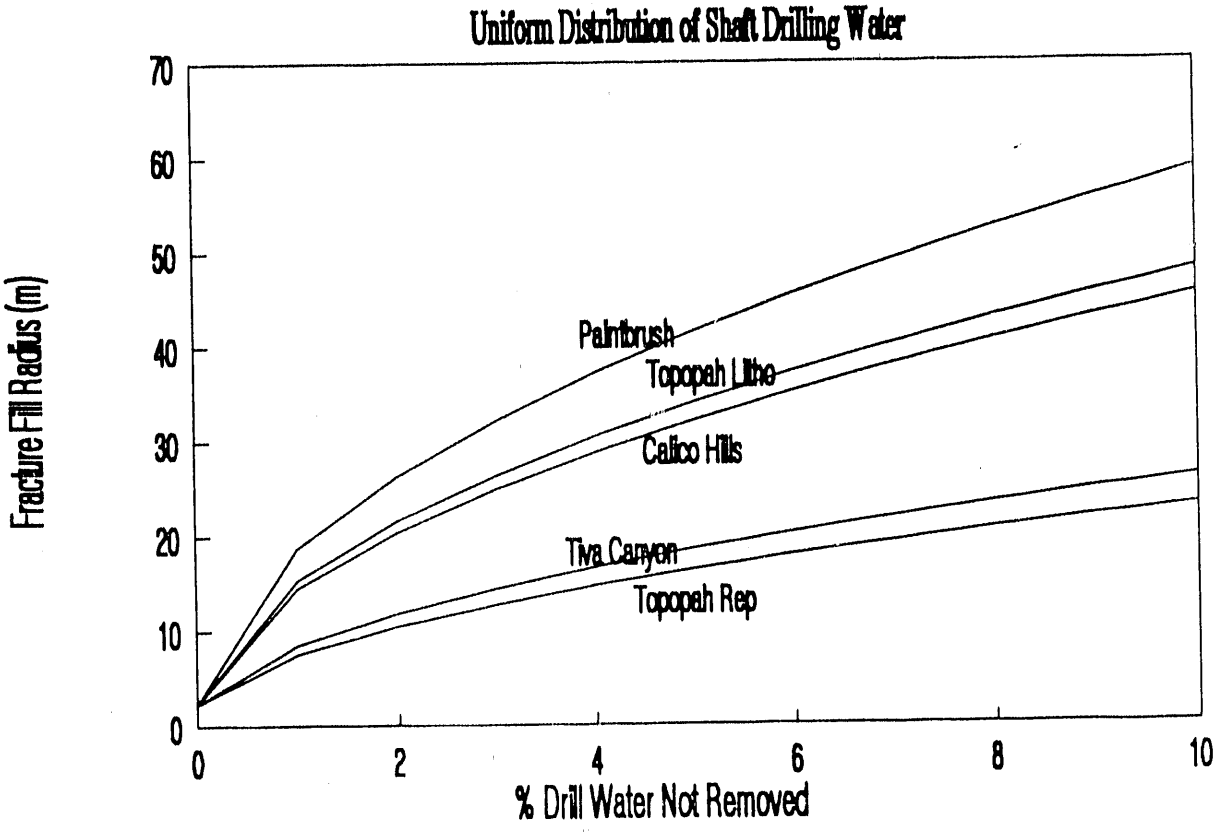

Figure 3: Uniform Distribution of Shaft Drilling Water Through Fracture System

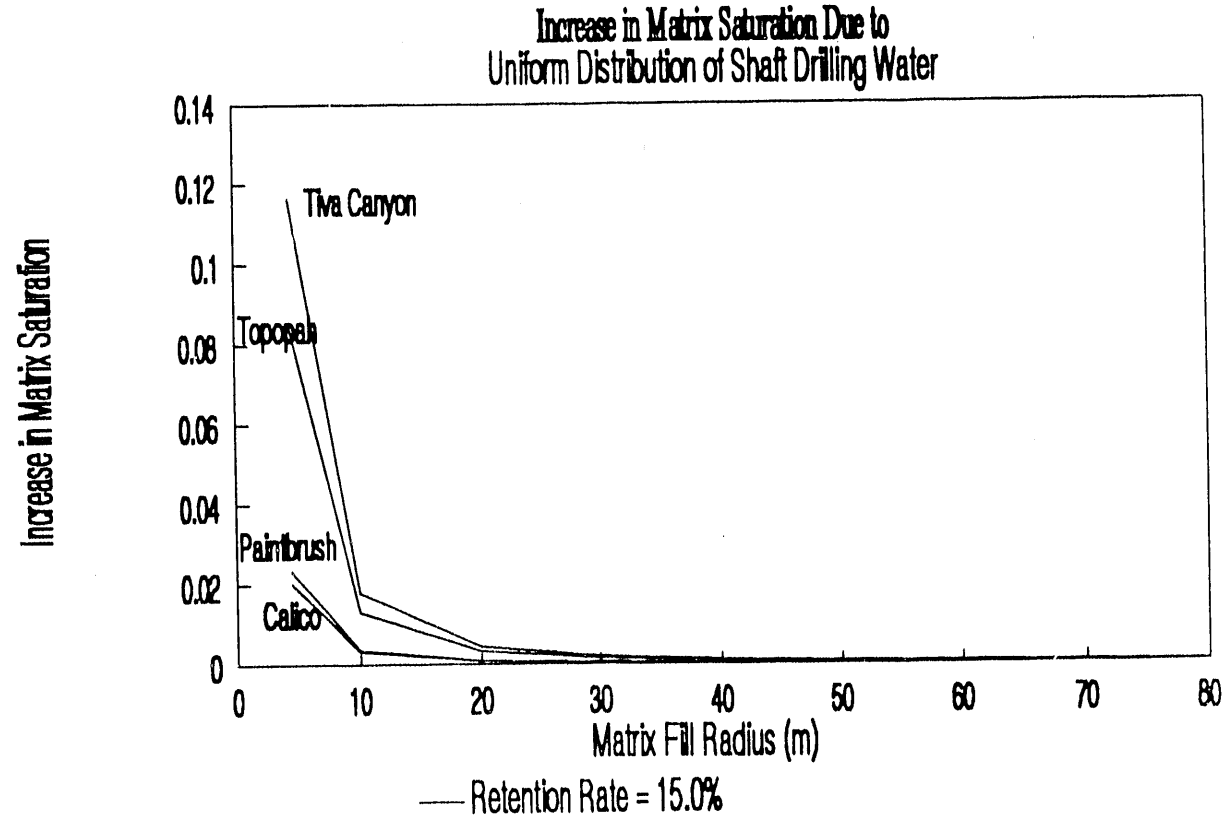

Figure 4: Increase in Matrix Saturation from Shaft Drilling Water

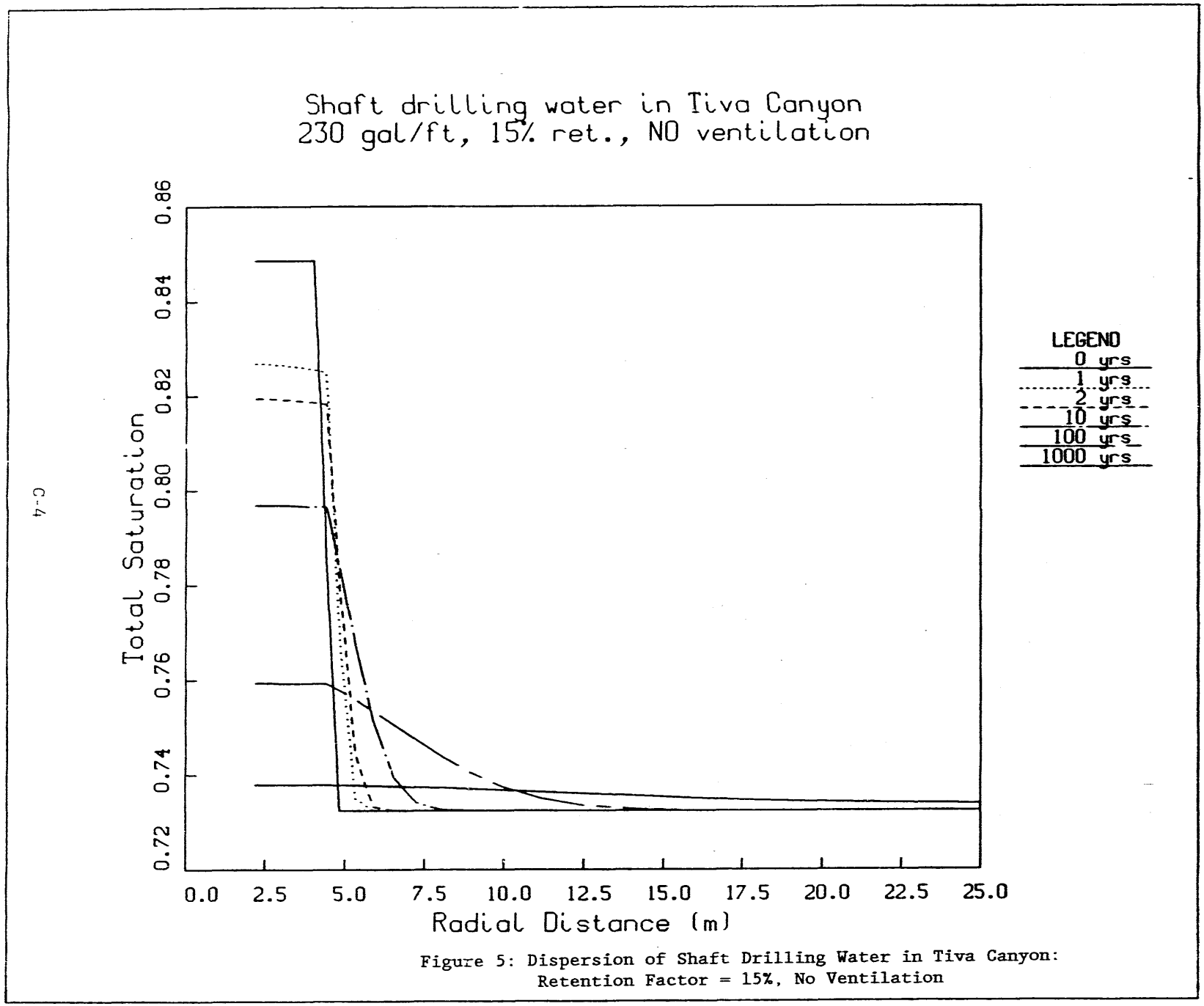

Figure 5: Dispersion of Shaft Drilling Water in Tiva Canyon: Retention Factor = 15%, No Ventilation

Figures 6-9: Dispersion History of Shaft Water in Tiva Canyon: Retention Factor = 15%, No Ventilation

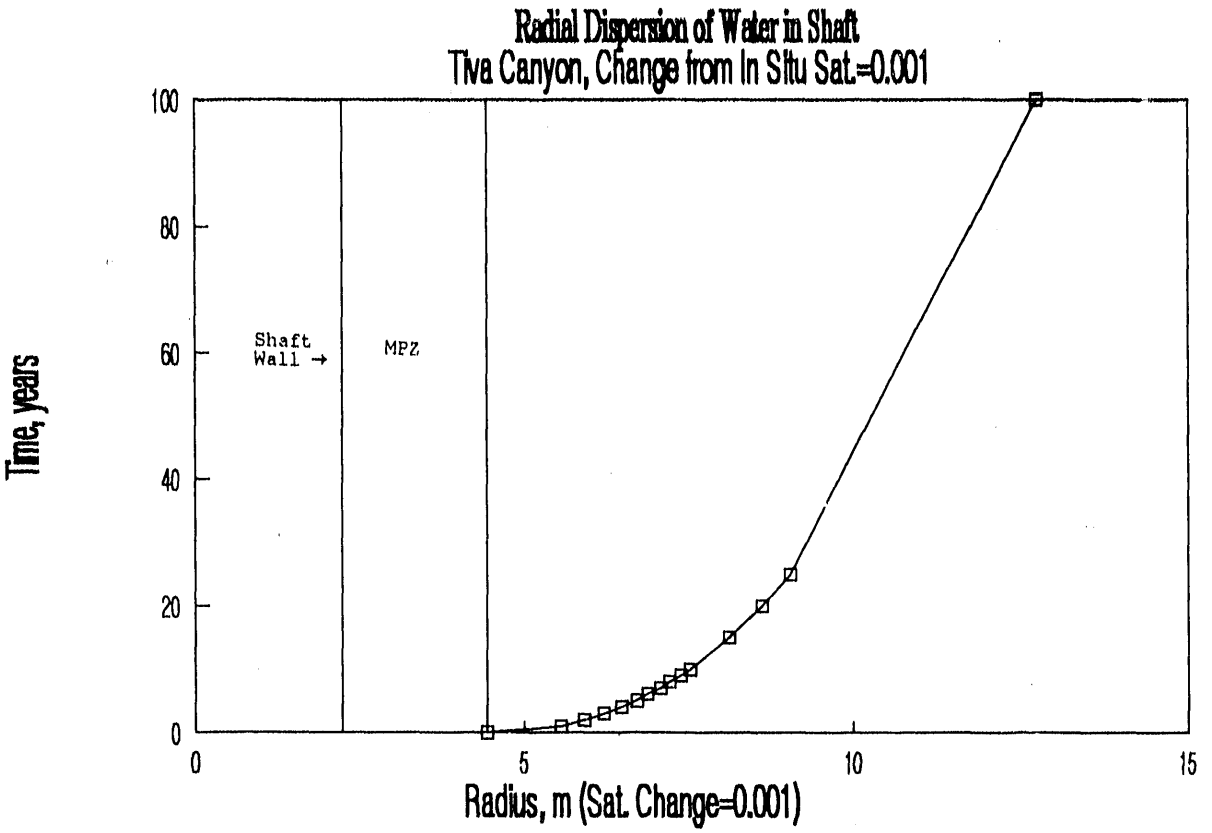

Figure 6: Tiva Canyon, Change from In Situ Saturation=0.001

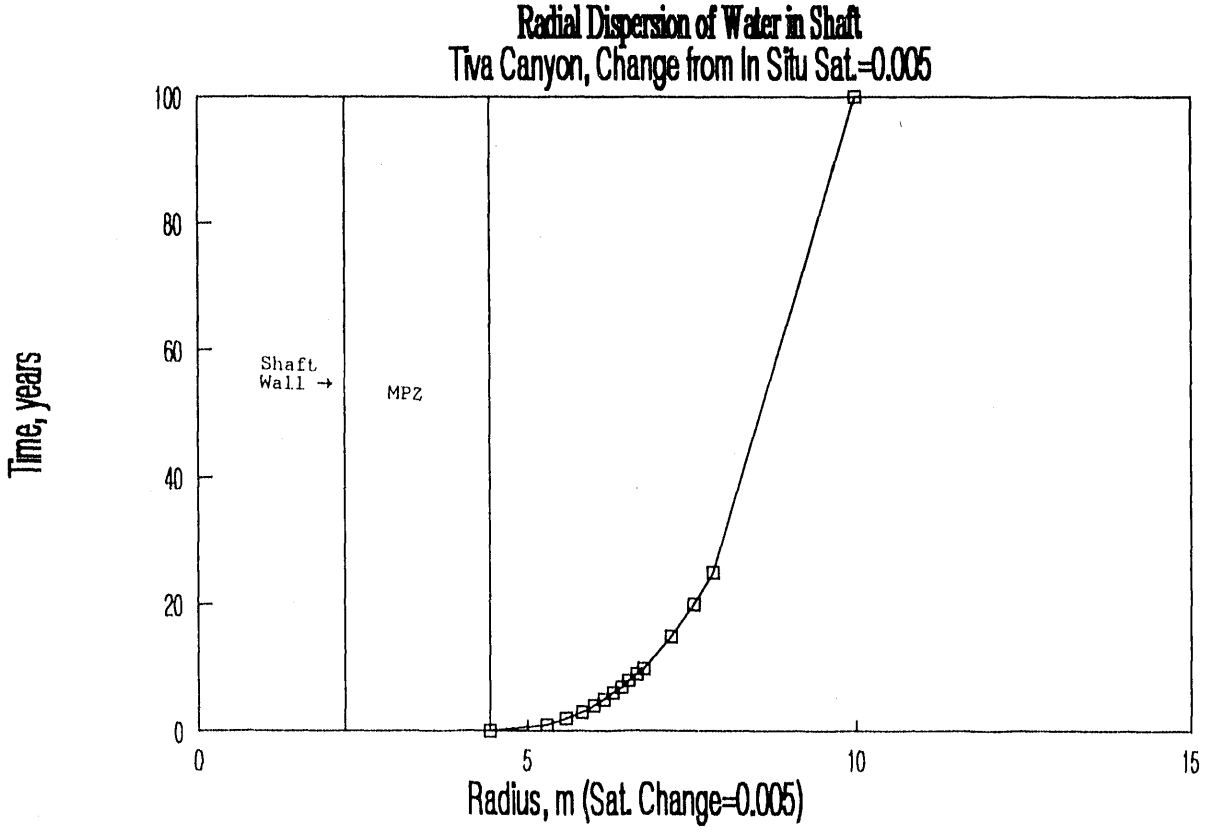

Figure 7: Tiva Canyon, Change from In Situ Saturation=0.005

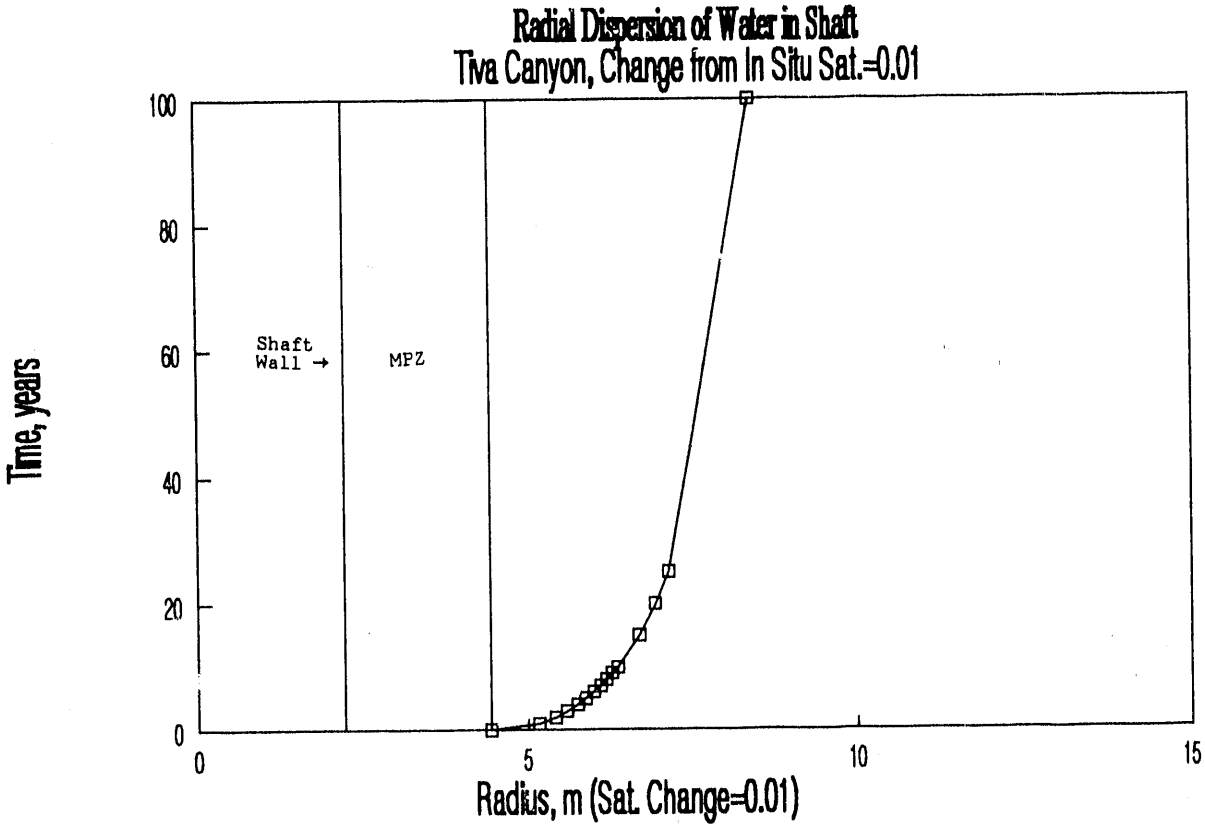

Figure 8: Tiva Canyon, Change from In Situ Saturation=0.01

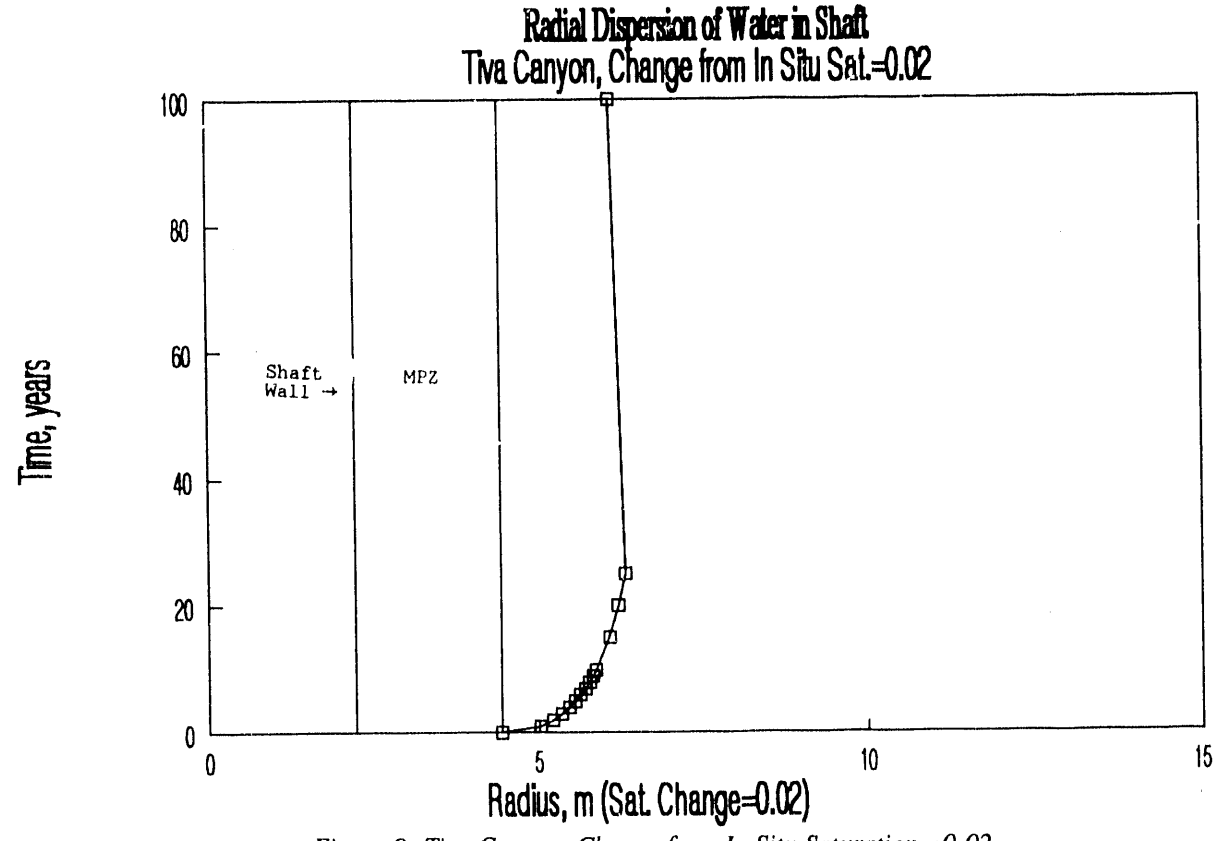

Figure 9: Tiva Canyon, Change from In Situ Saturation=0.02

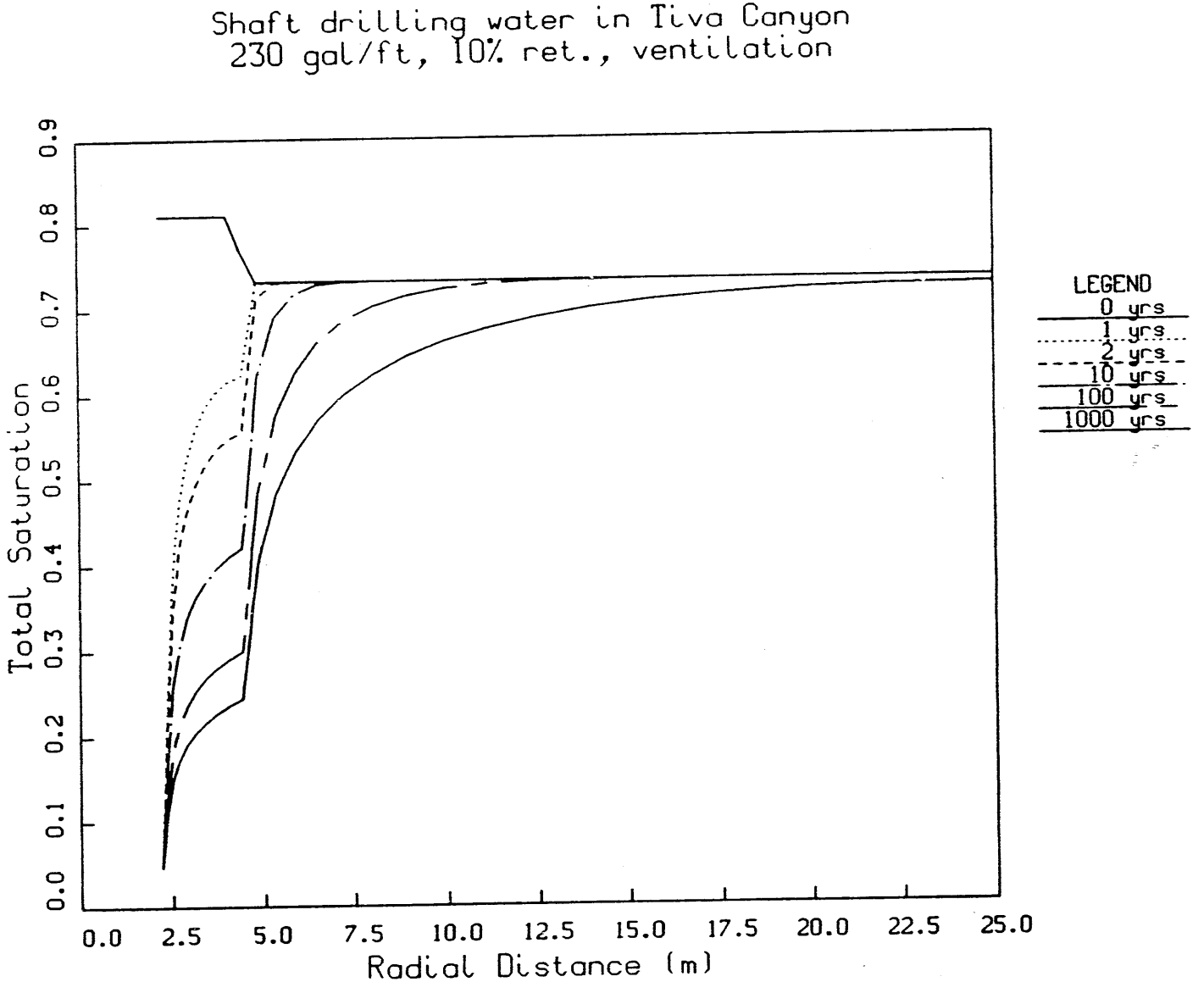

Figure 10: Dispersion of Shaft Drilling Water in Tiva Canyon: Retention Factor = 10%, With Ventilation

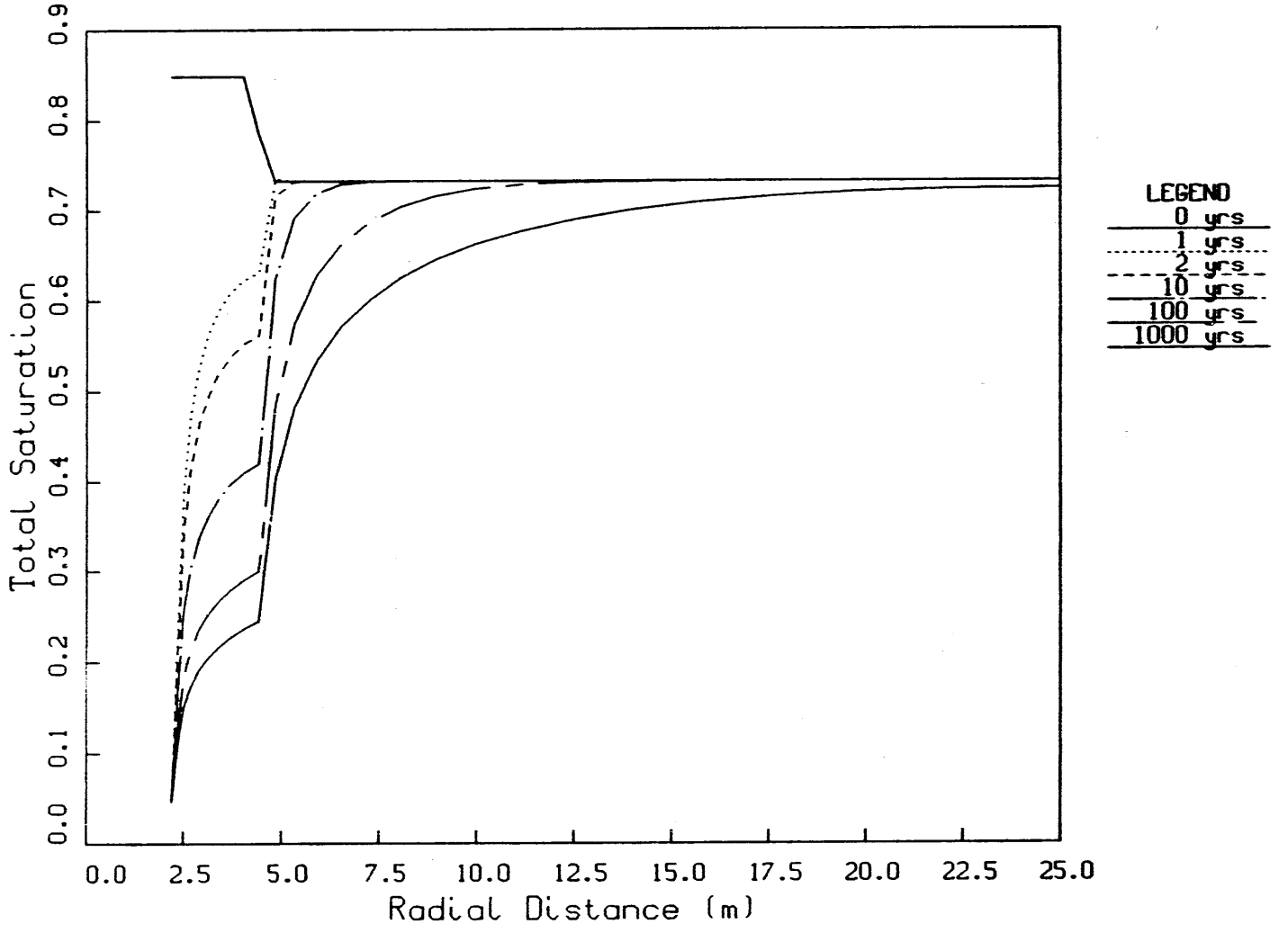

Figure 11: Dispersion of Shaft Drilling Water in Tiva Canyon: Retention Factor = 15%, With Ventilation

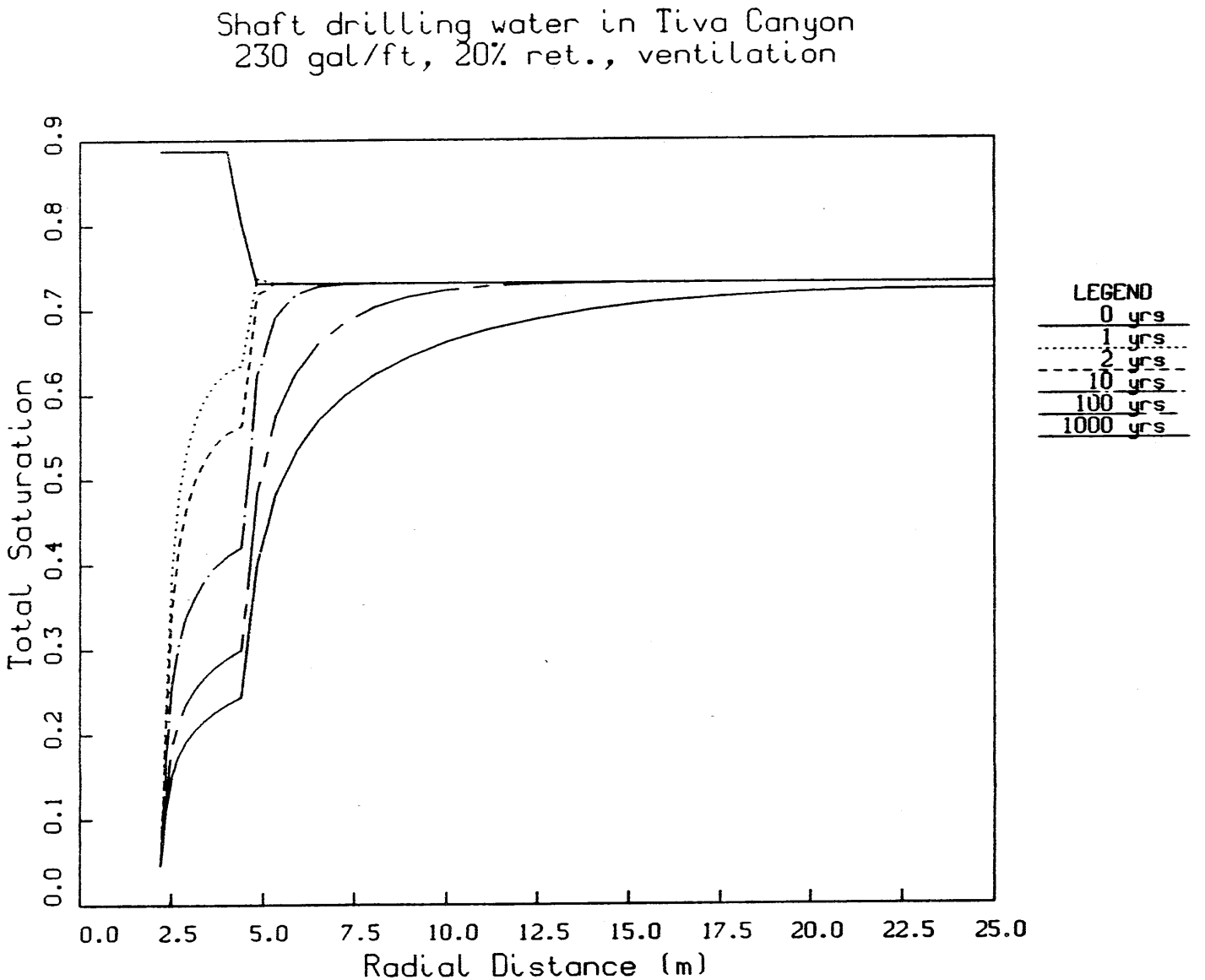

Figure 12: Dispersion of Shaft Drilling Water in Tiva Canyon: Retention Factor = 20%, With Ventilation

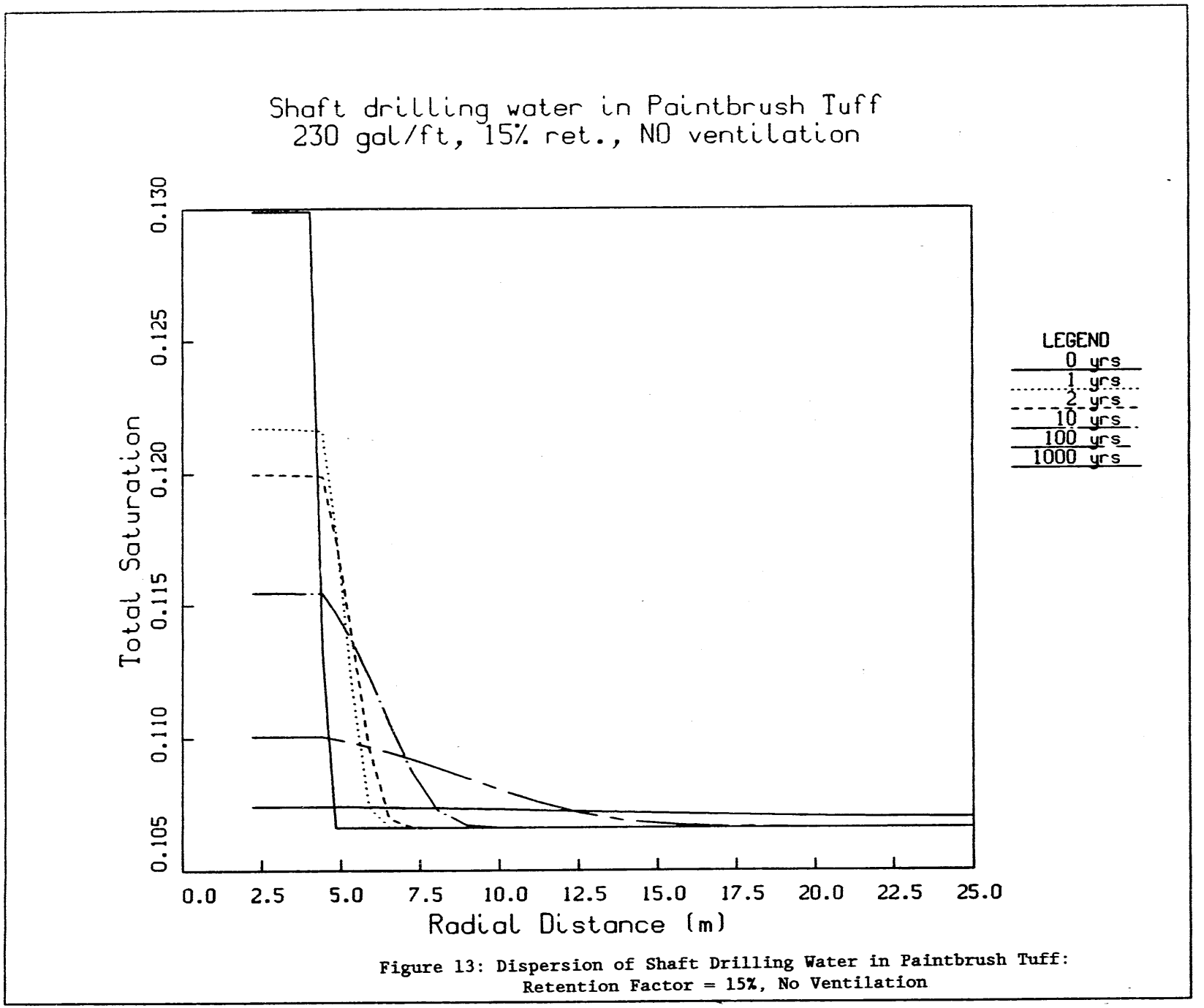

Figure 13: Dispersion of Shaft Drilling Water in Paintbrush Tuff: Retention Factor = 15%, No Ventilation

Figures 14-16: Dispersion History of Shaft Water in Paintbrush Tuff: Retention Factor = 15%, No Ventilation

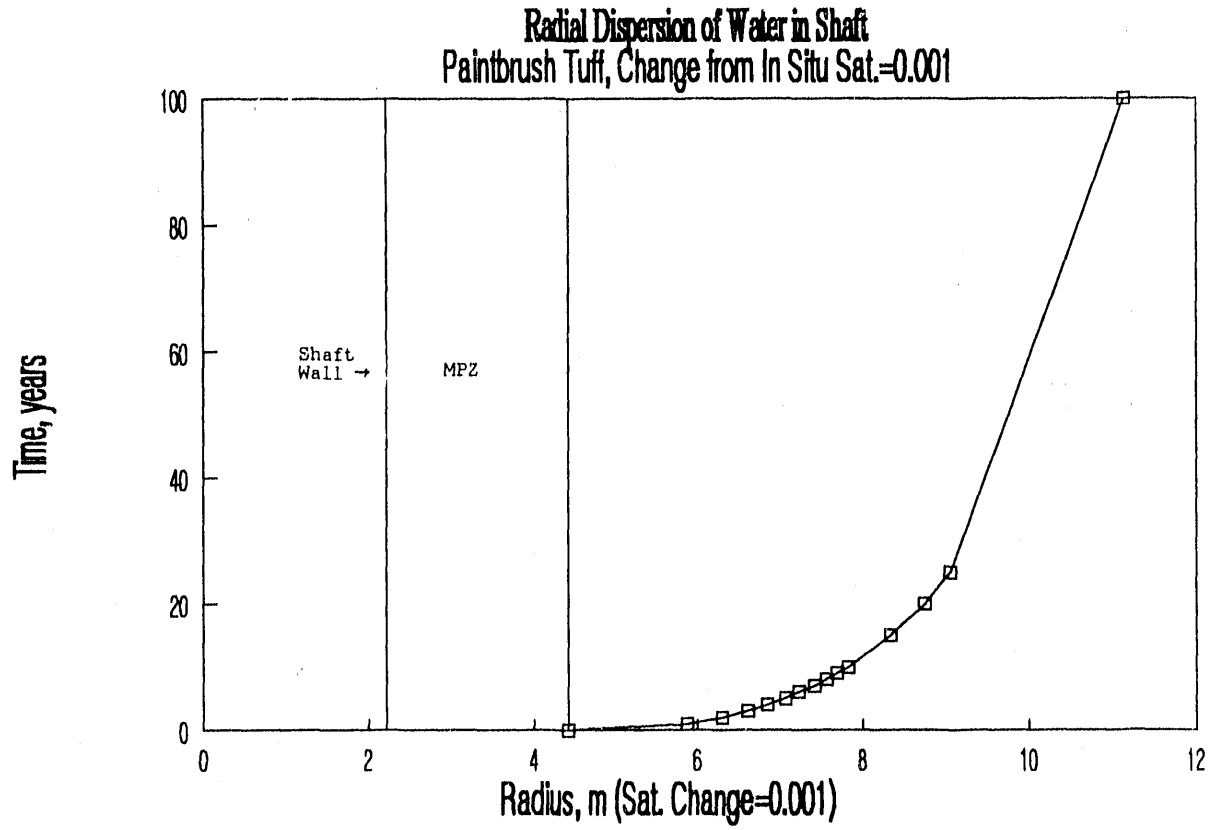

Figure 14: Paintbrush Tuff, Change from In Situ Saturation=0.001

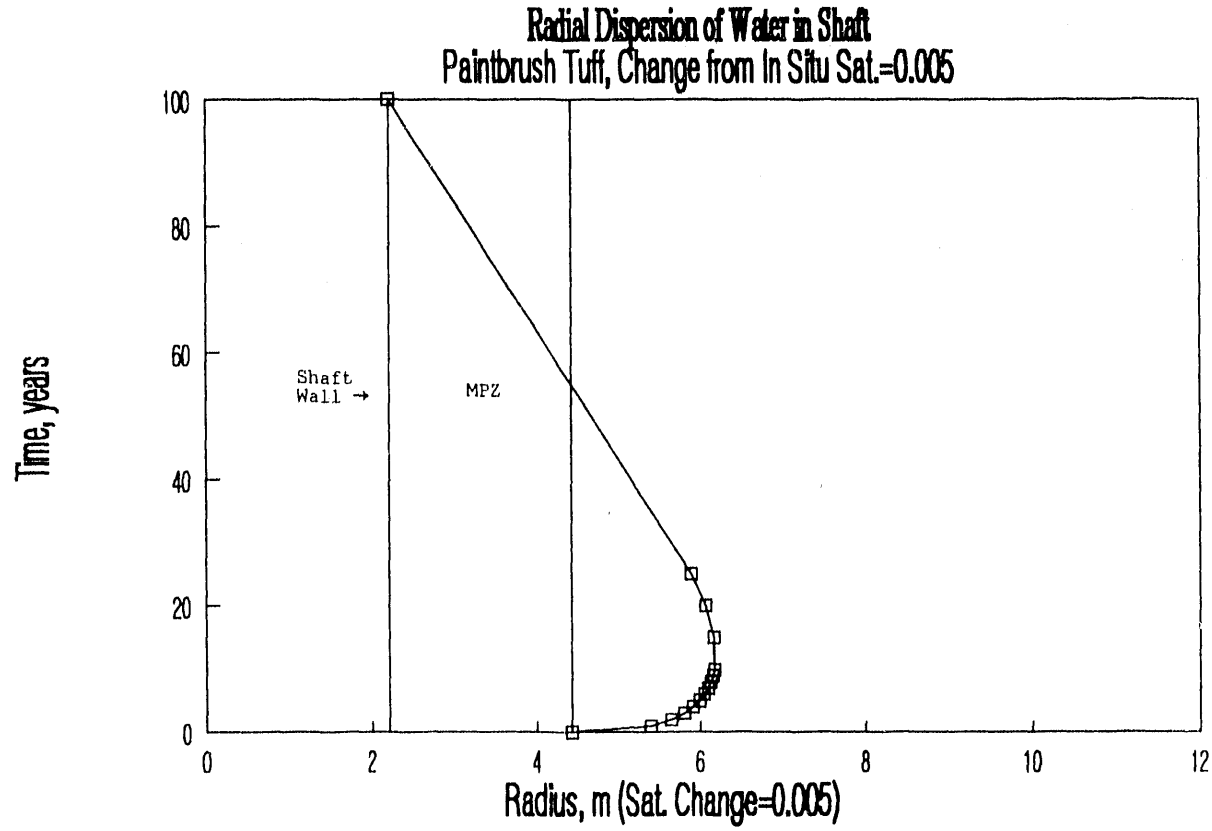

Figure 15: Paintbrush Tuff, Change from In Situ Saturation=0.005

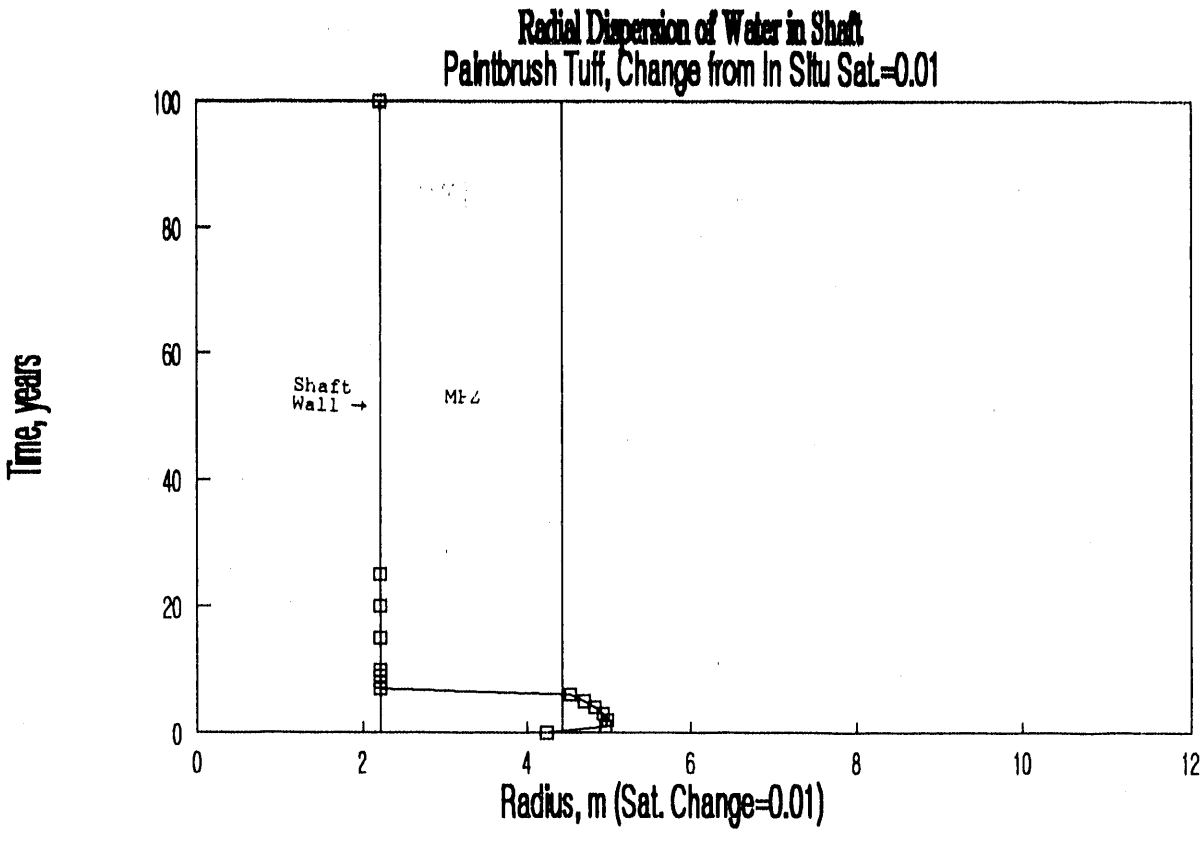

Figure 16: Paintbrush Tuff, Change from In Situ Saturation=0.01

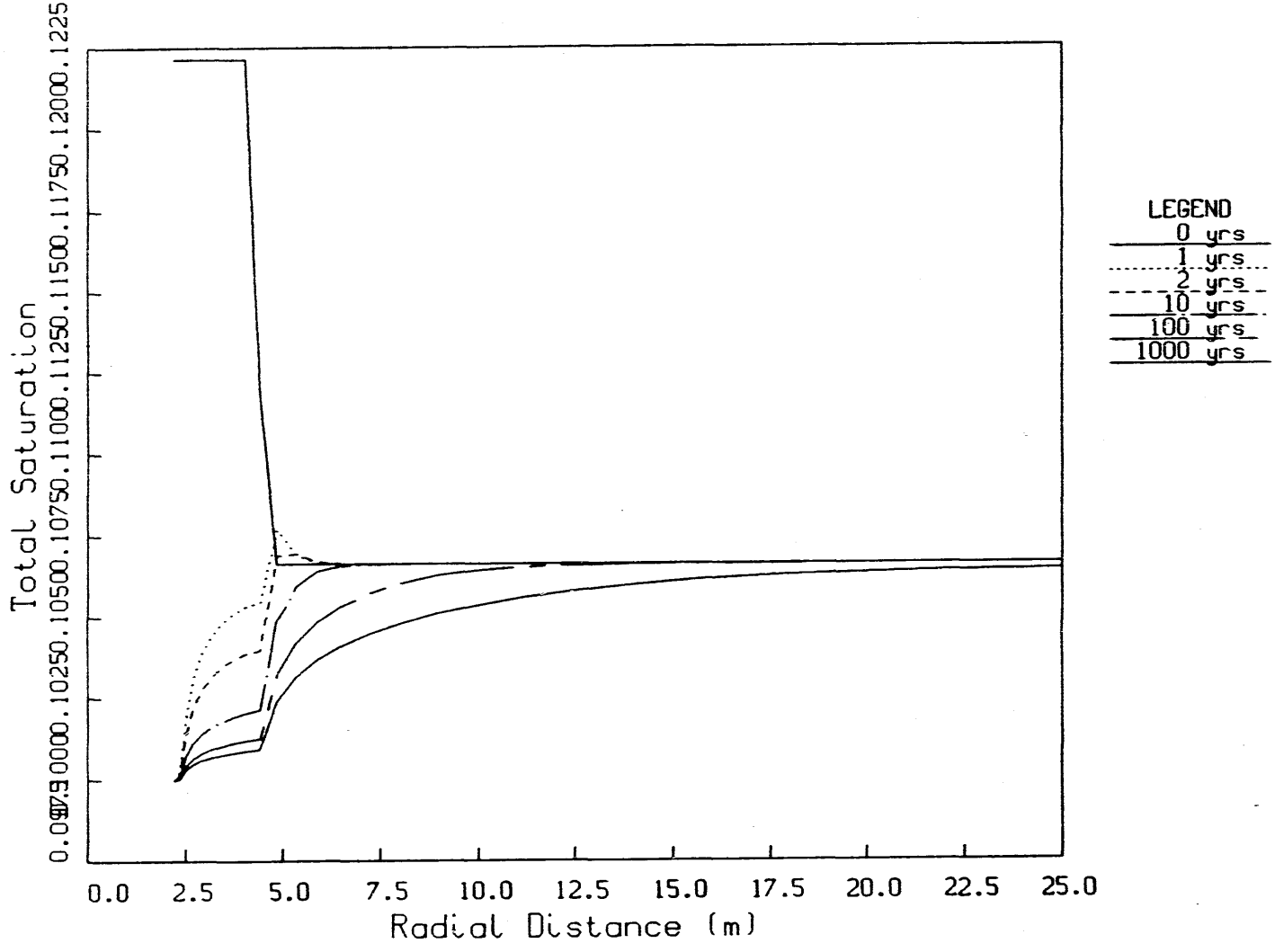

Figure 17: Dispersion of Shaft Drilling Water in Paintbrush Tuff: Retention Factor = 10%, With Ventilation

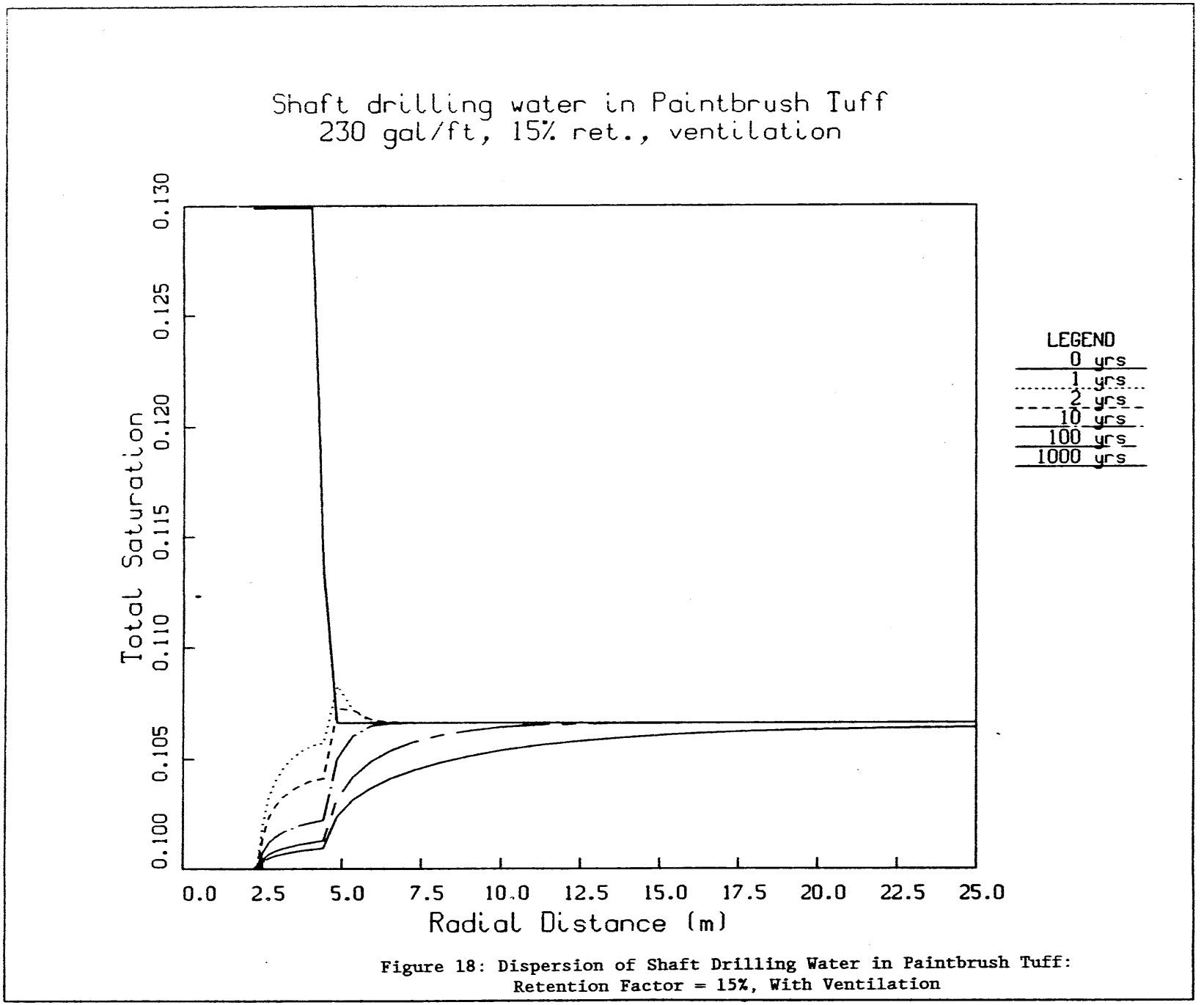

Figure 18: Dispersion of Shaft Drilling Water in Paintbrush Tuff: Retention Factor = 15%, With Ventilation

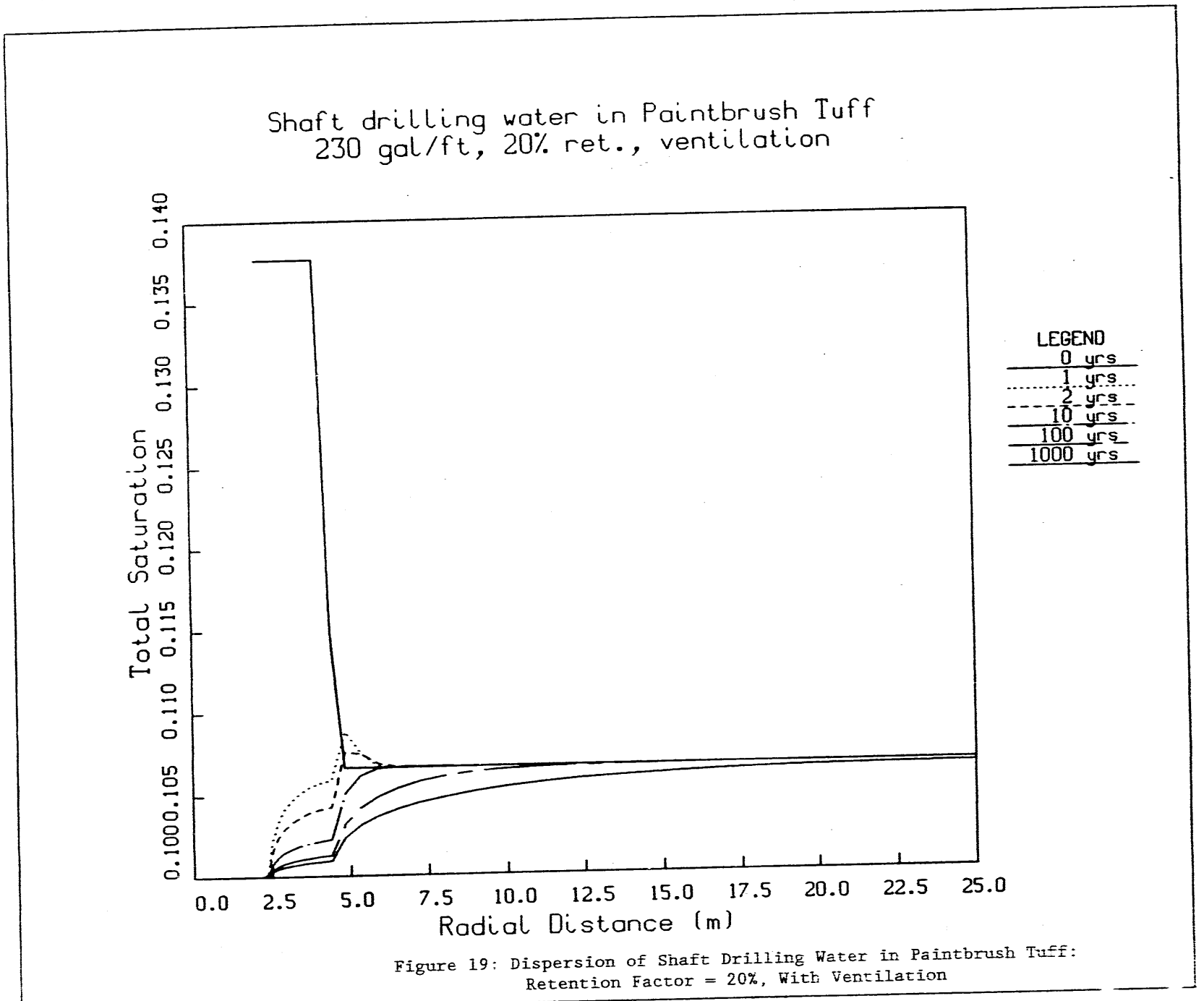

Figure 19: Dispersion of Shaft Drilling Water in Paintbrush Tuff: Retention Factor = 20%, With Ventilation

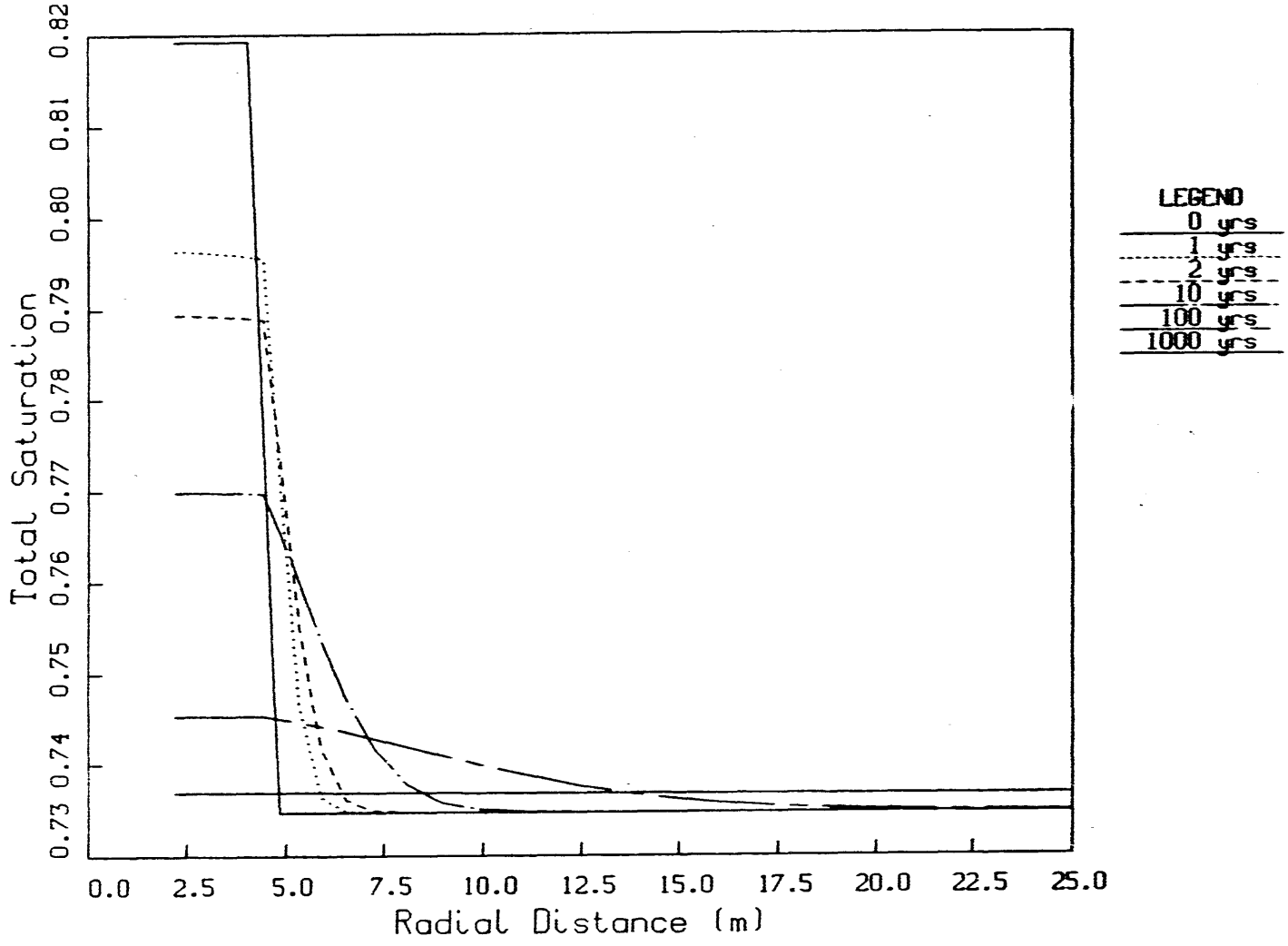

Figure 20: Dispersion of Shaft Drilling Water in Topopah Springs: Retention Factor = 15%, No Ventilation

Figures 21-24: Dispersion History of Shaft Water in Topopah Springs: Retention Factor = 15%, No Ventilation

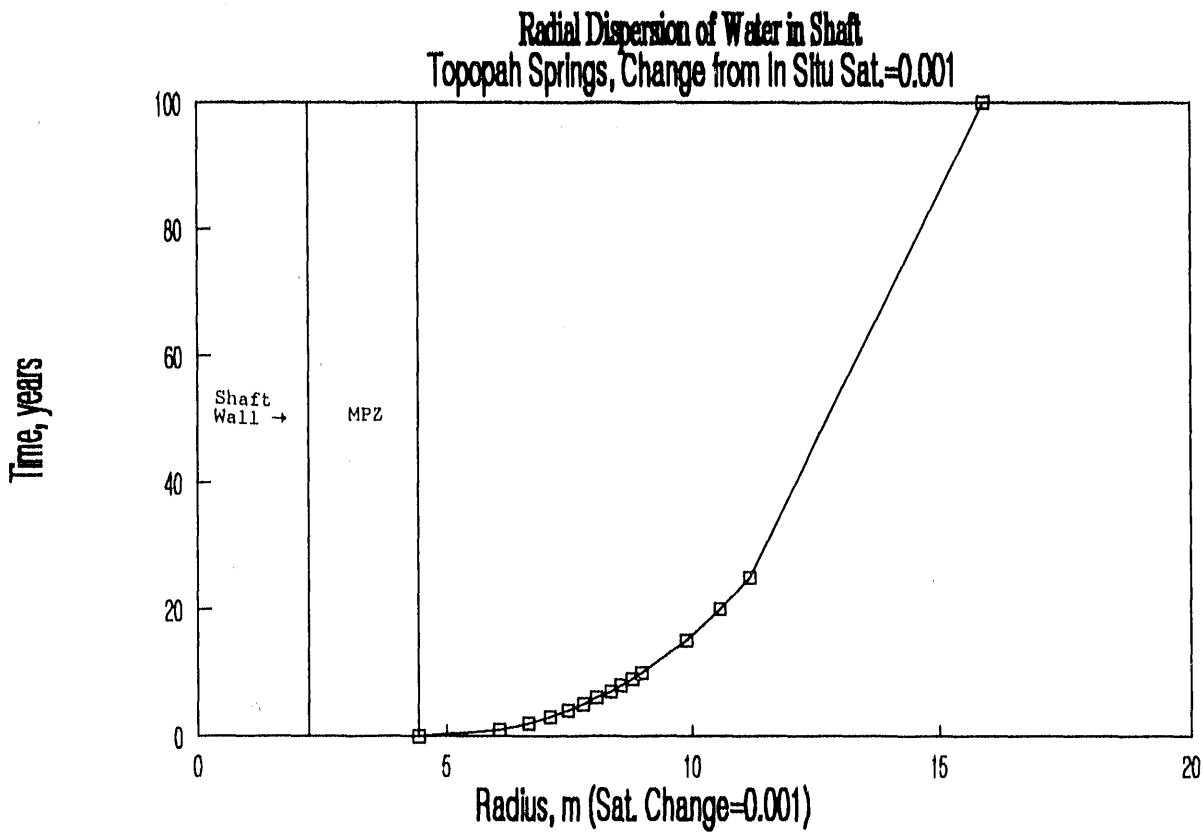

Figure 21: Topopah Springs, Change from In Situ Saturation=0.001

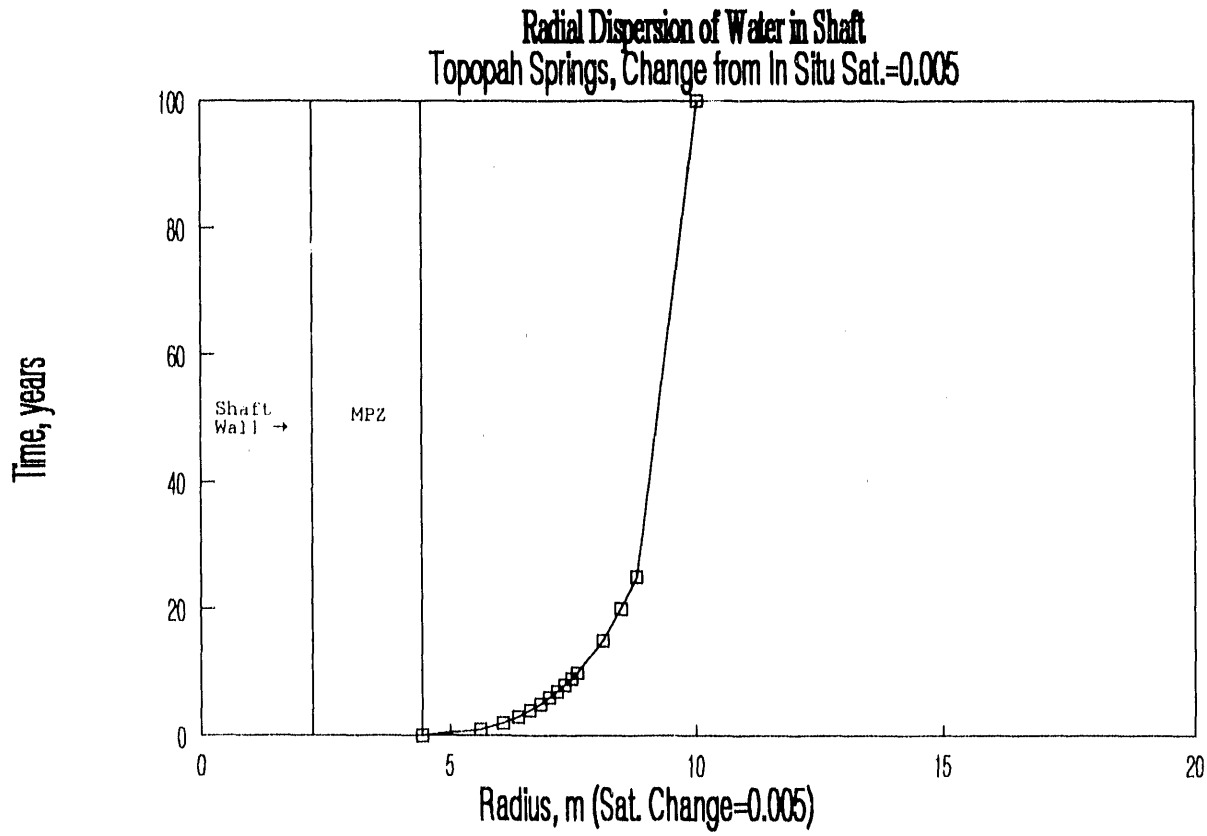

Figure 22: Topopah Springs, Change from In Situ Saturation=0.005

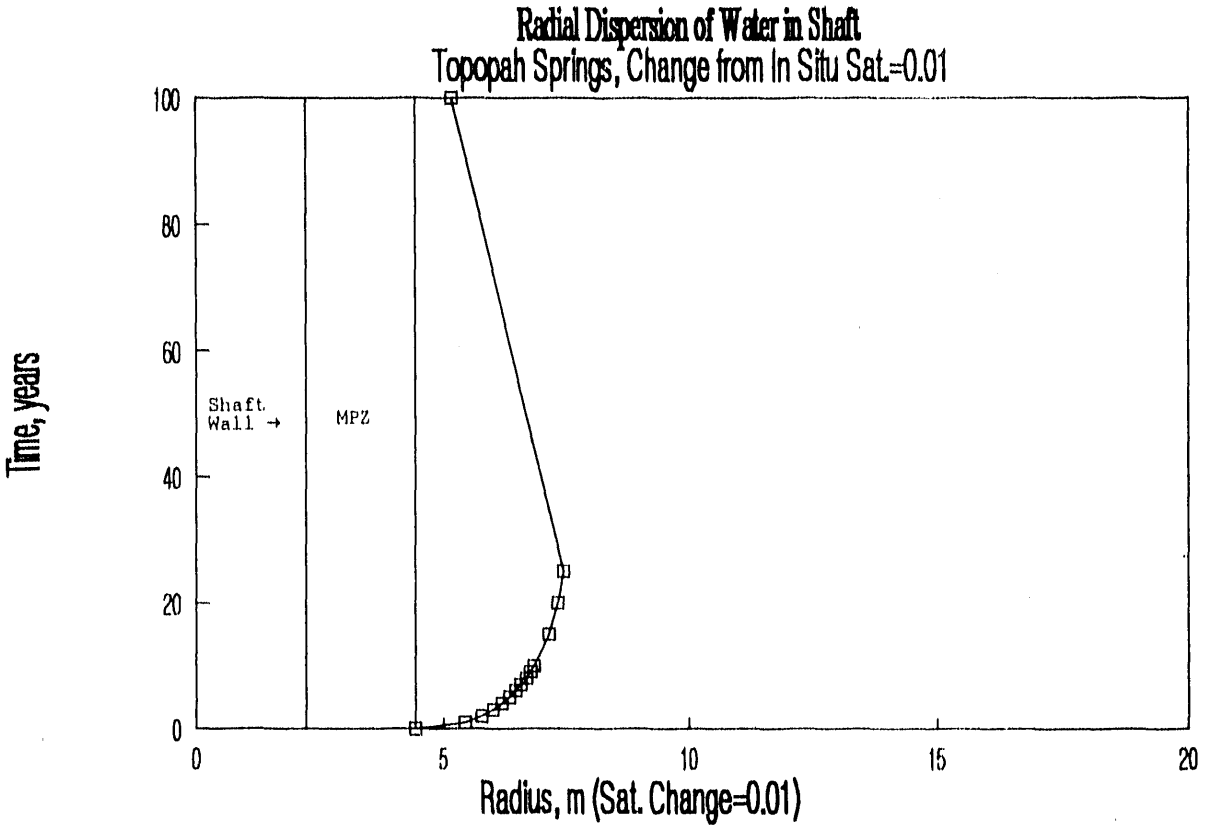

Figure 23: Topopah Springs, Change from In Situ Saturation=0.01

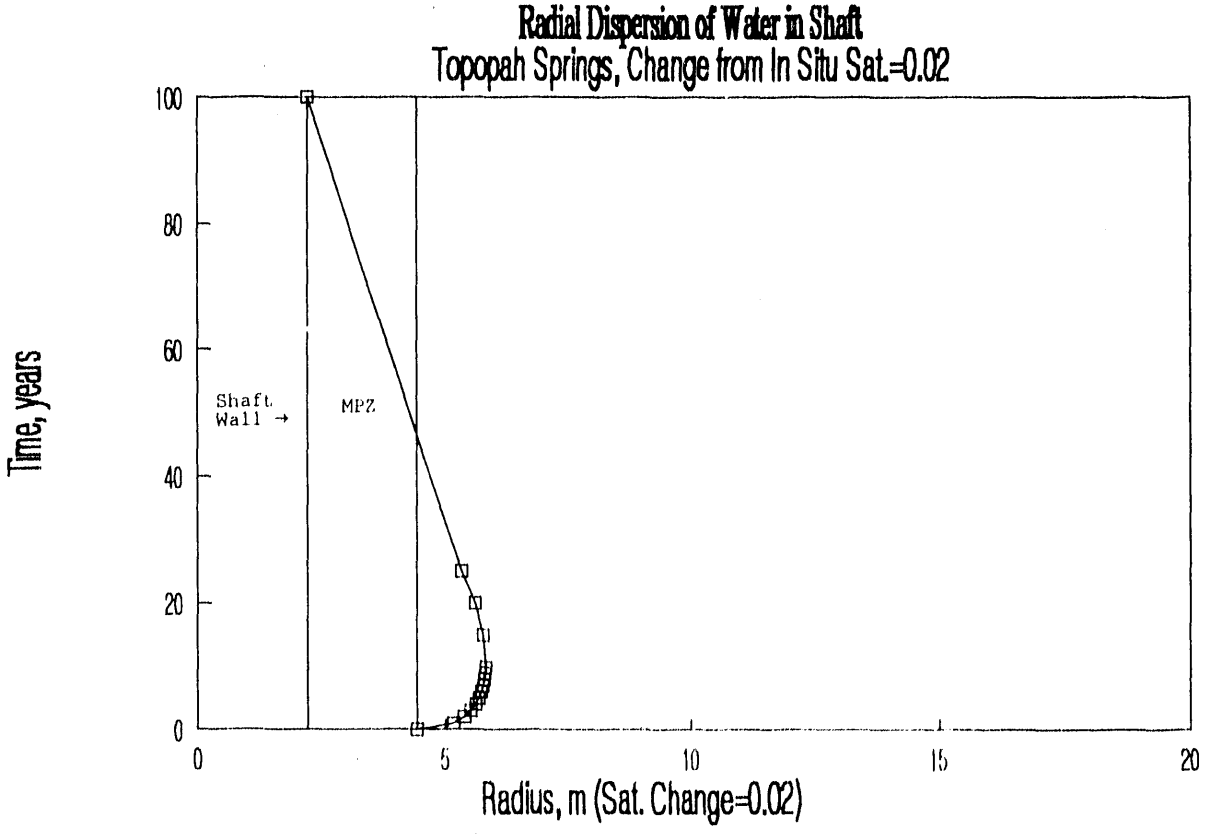

Figure 24: Topopah Springs, Change from In Situ Saturation=0.02

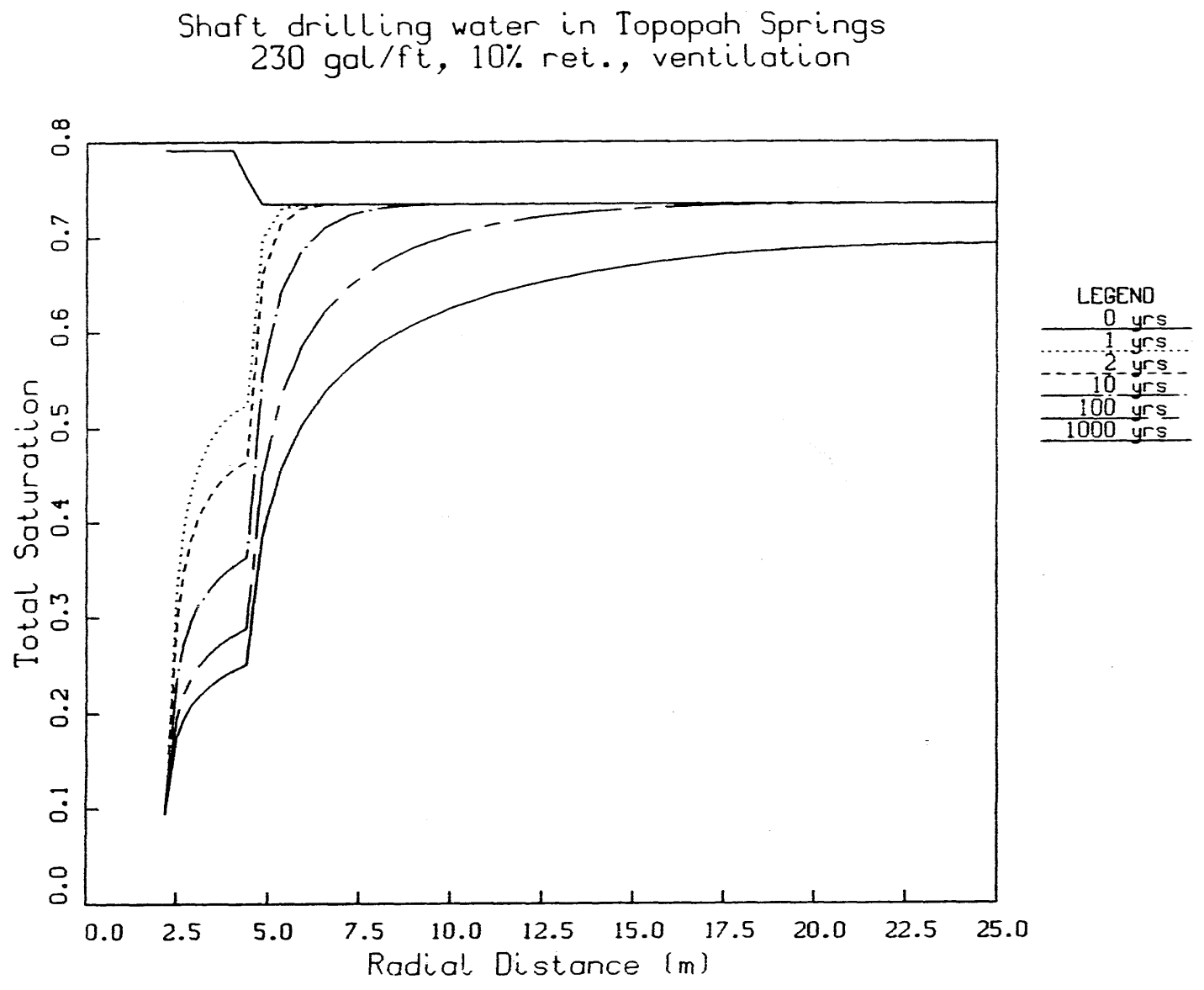

Figure 25: Dispersion of Shaft Drilling Water in Topopah Springs.
Retention Factor = 10%, With Ventilation

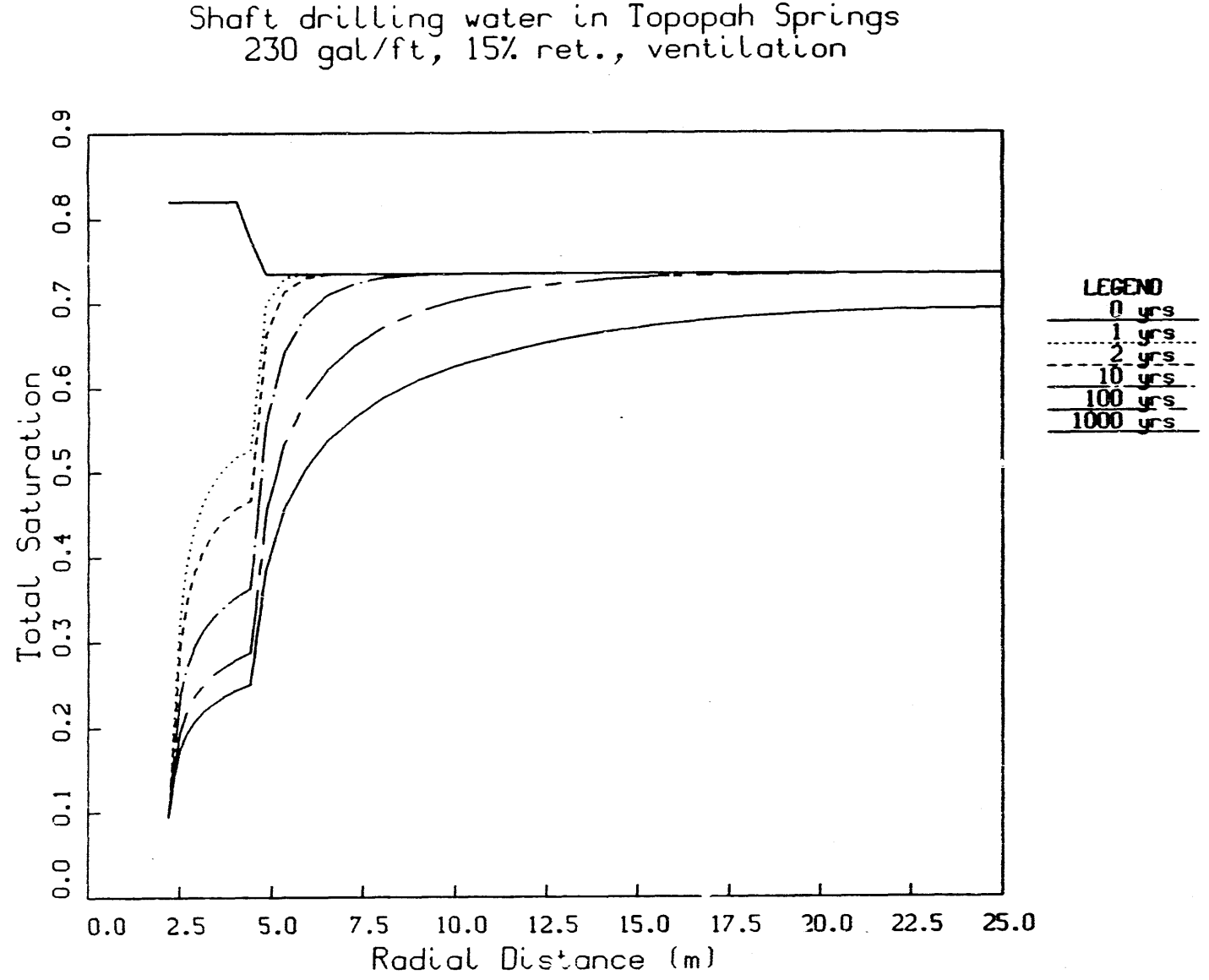

Figure 26: Dispersion of Shaft Drilling Water in Topopah Springs: Retention Factor = 15%, With Ventilation

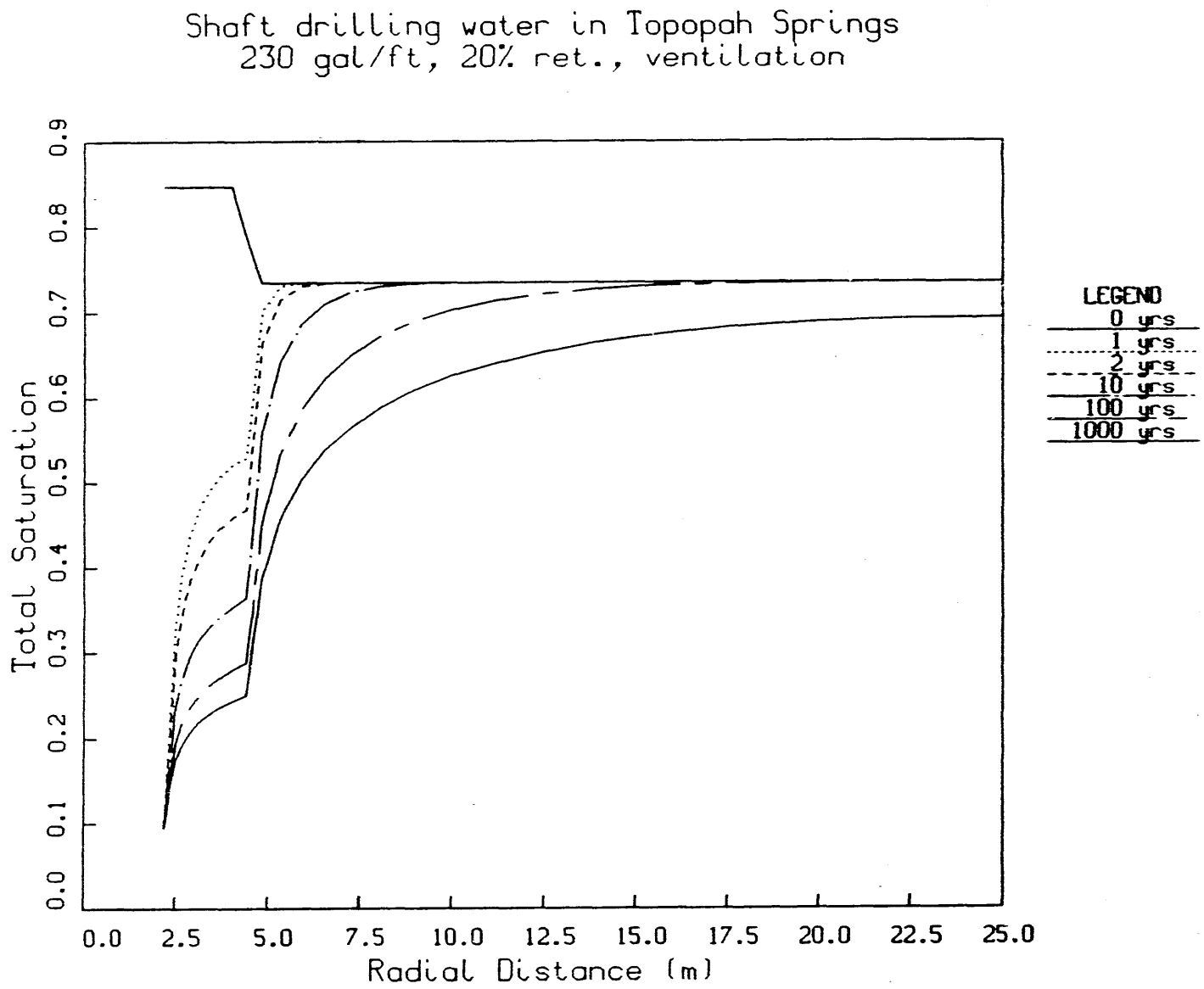

Figure 27: Dispersion of Shaft Drilling Water in Topopah Springs: Retention Factor = 20%, With Ventilation

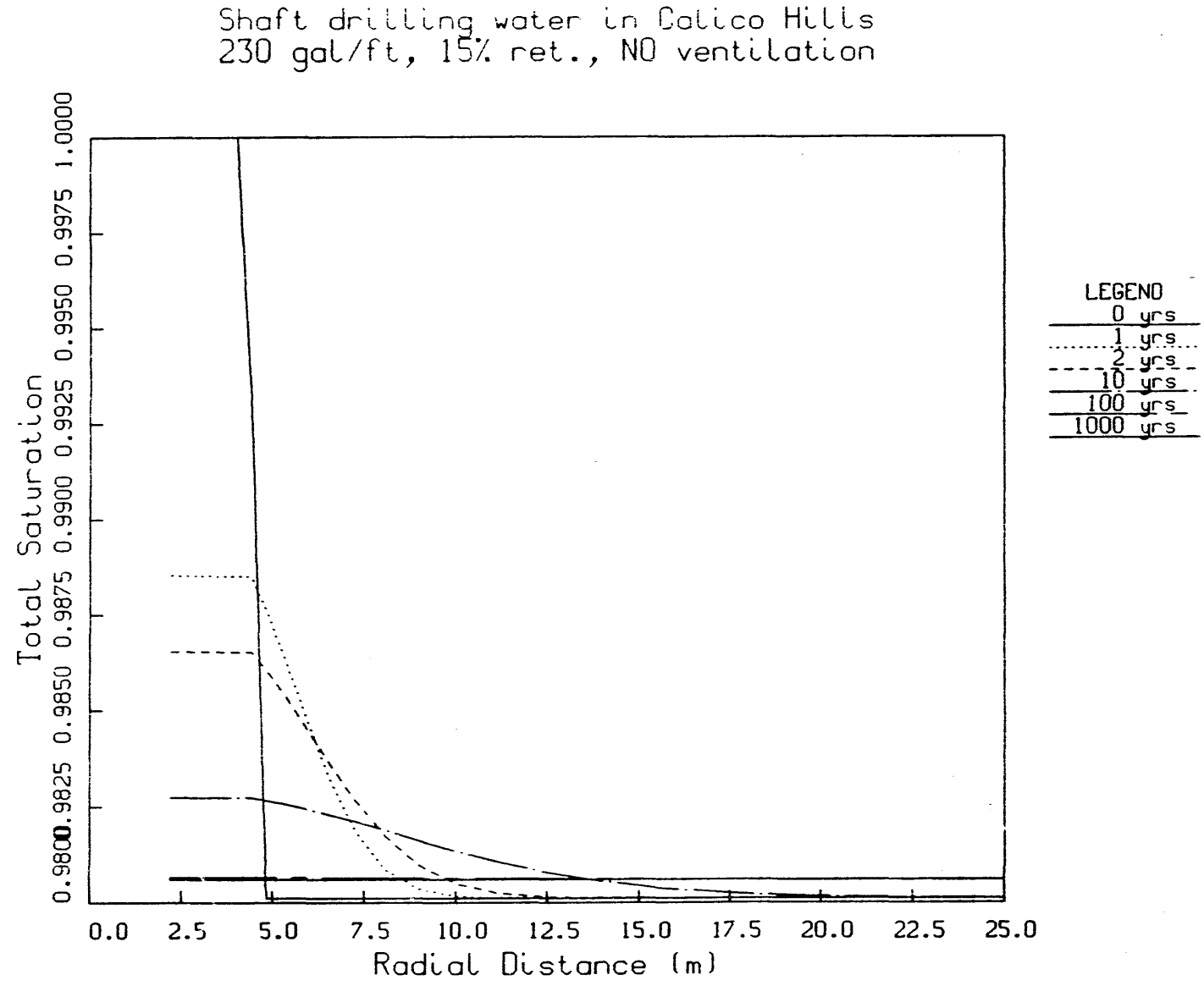

Figure 28: Dispersion of Shaft Drilling Water in Calico Hills: Retention Factor = 15%, No Ventilation

Figures 29-30: Dispersion History of Shaft Water in Calico Hills: Retention Factor = 15%, No Ventilation

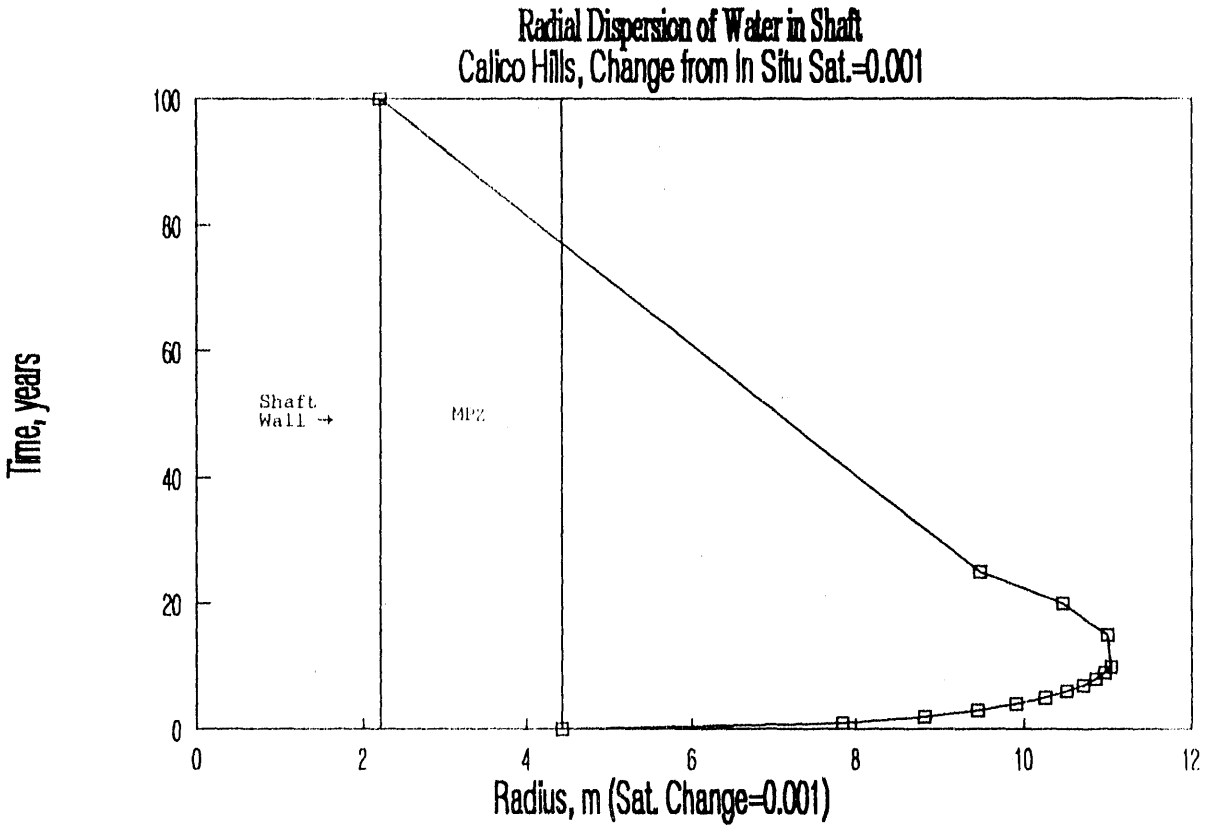

Figure 29: Calico Hills, Change from In Situ Saturation=0.001

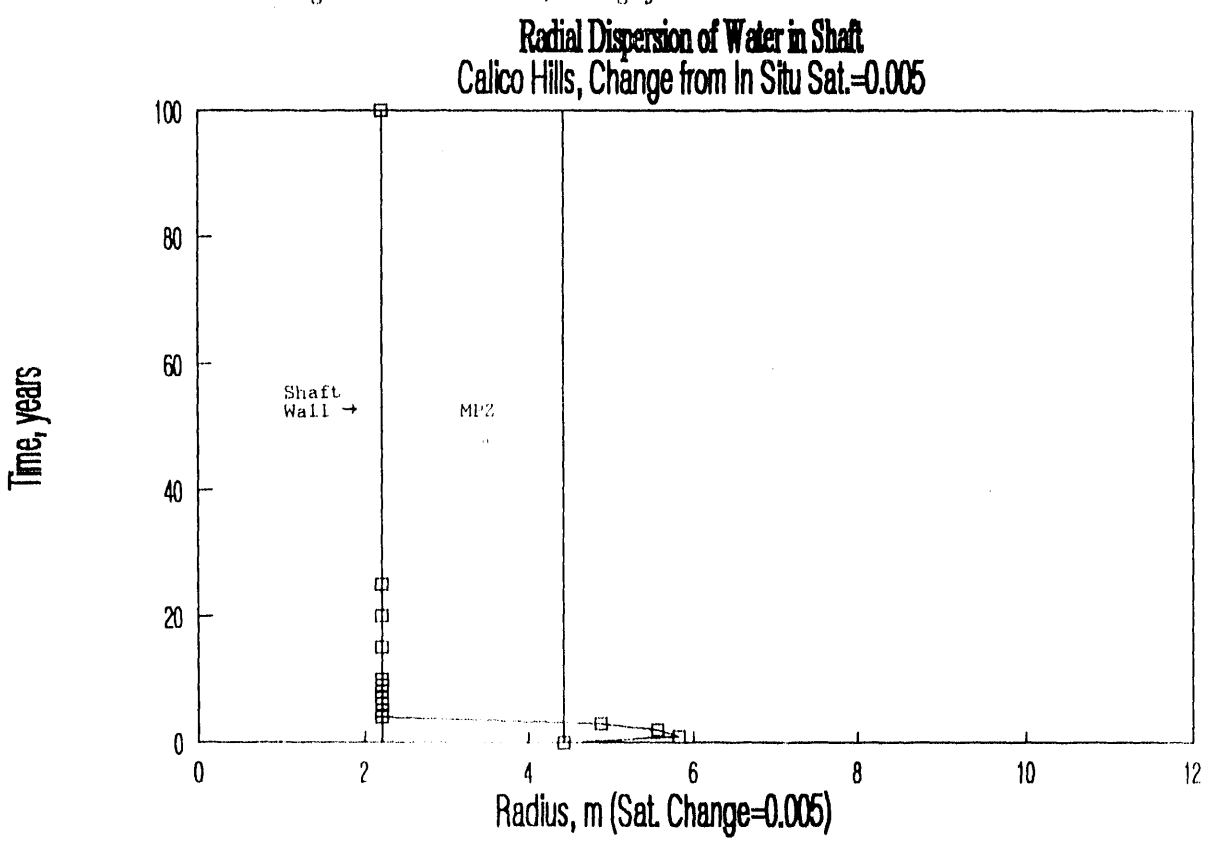

Figure 30: Calico Hills, Change from In Situ Saturation=0.005

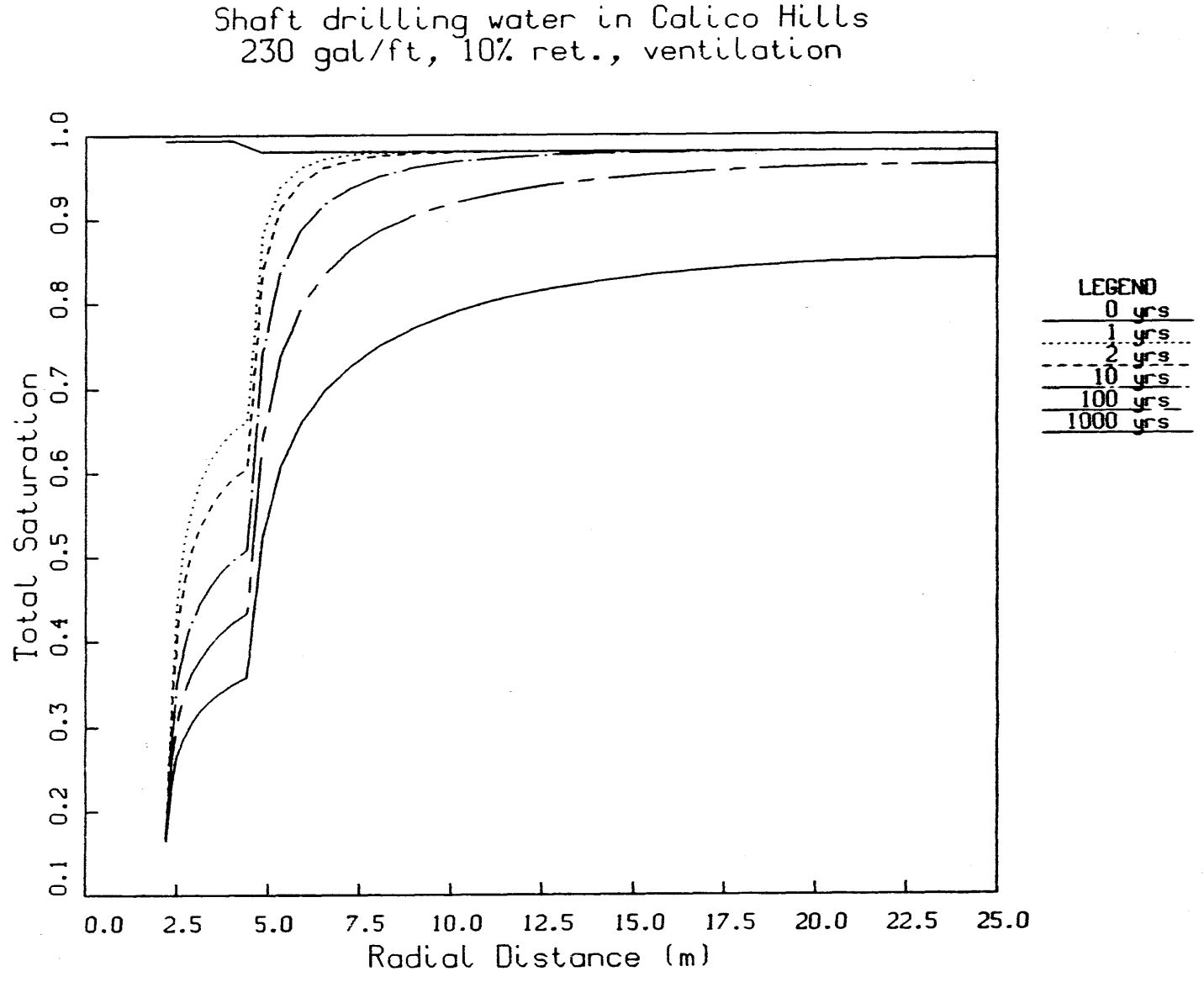

Figure 31: Dispersion of Shaft Drilling Water in Calico Hills: Retention Factor = 10%. With Ventilation

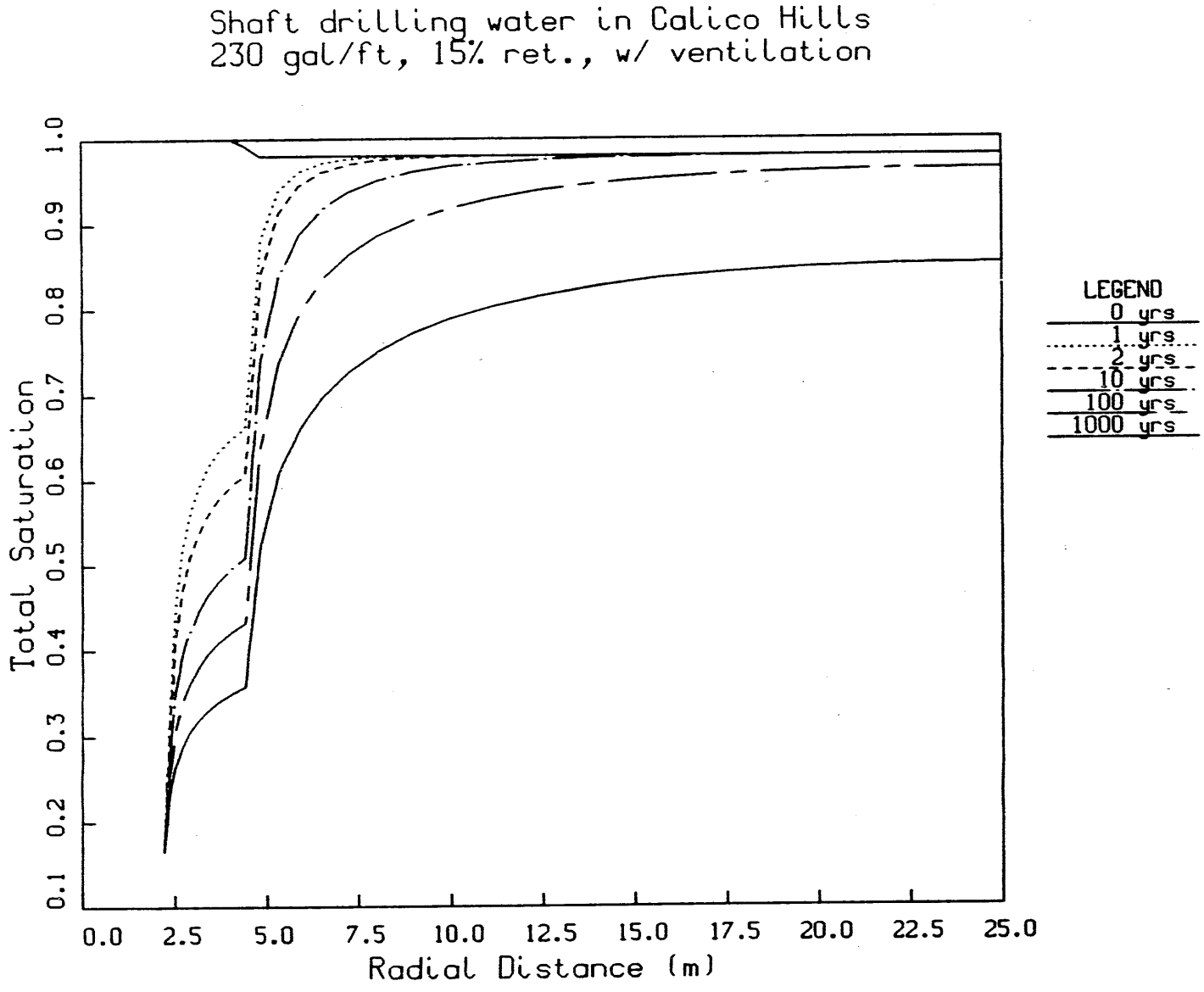

Figure 32: Dispersion of Shaft Drilling Water in Calico Hills: Retention Factor = 15%, With Ventilation

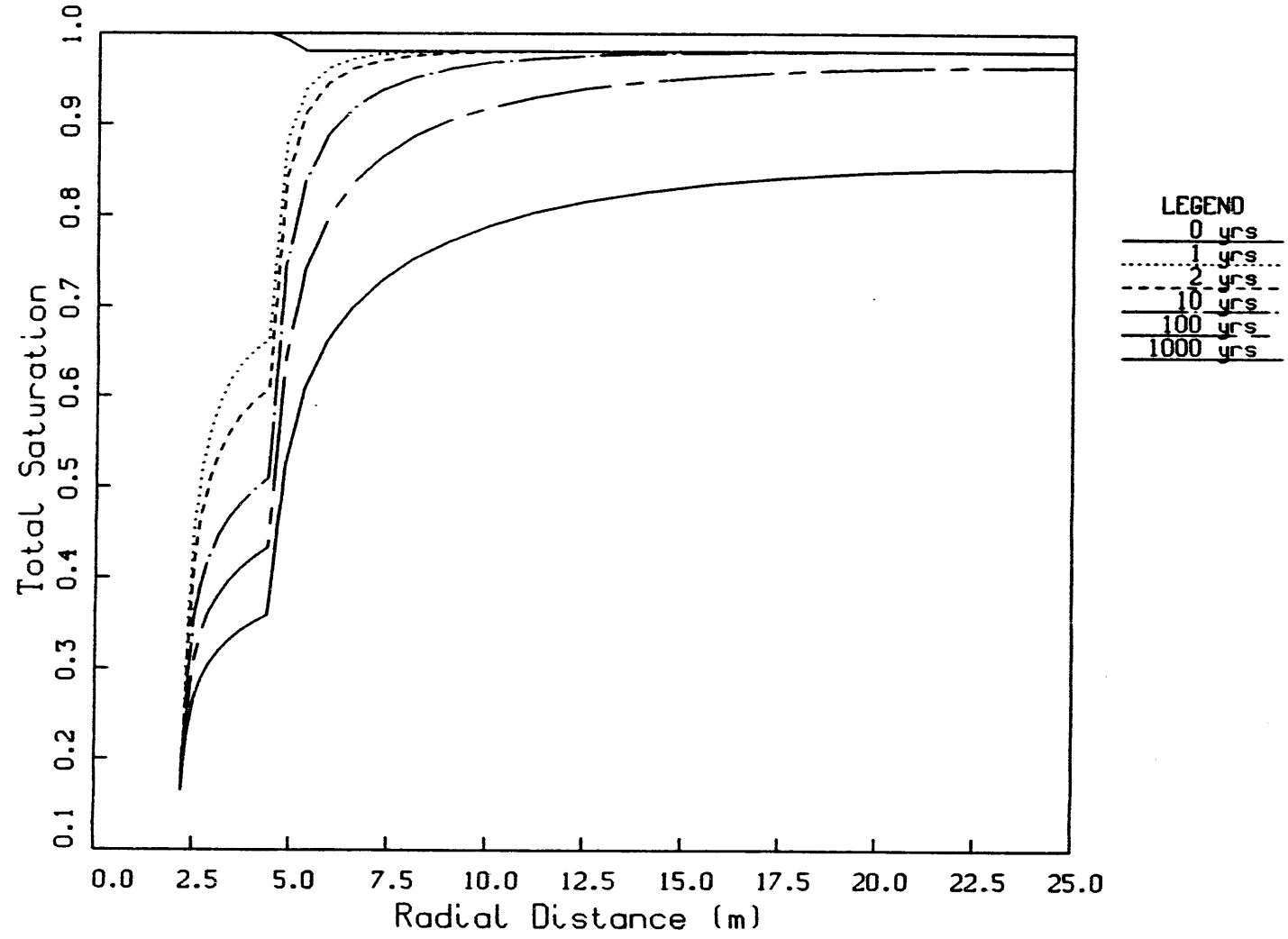

Figure 33: Dispersion of Shaft Drilling Water in Calico Hills: Retention Factor = 20%, With Ventilation

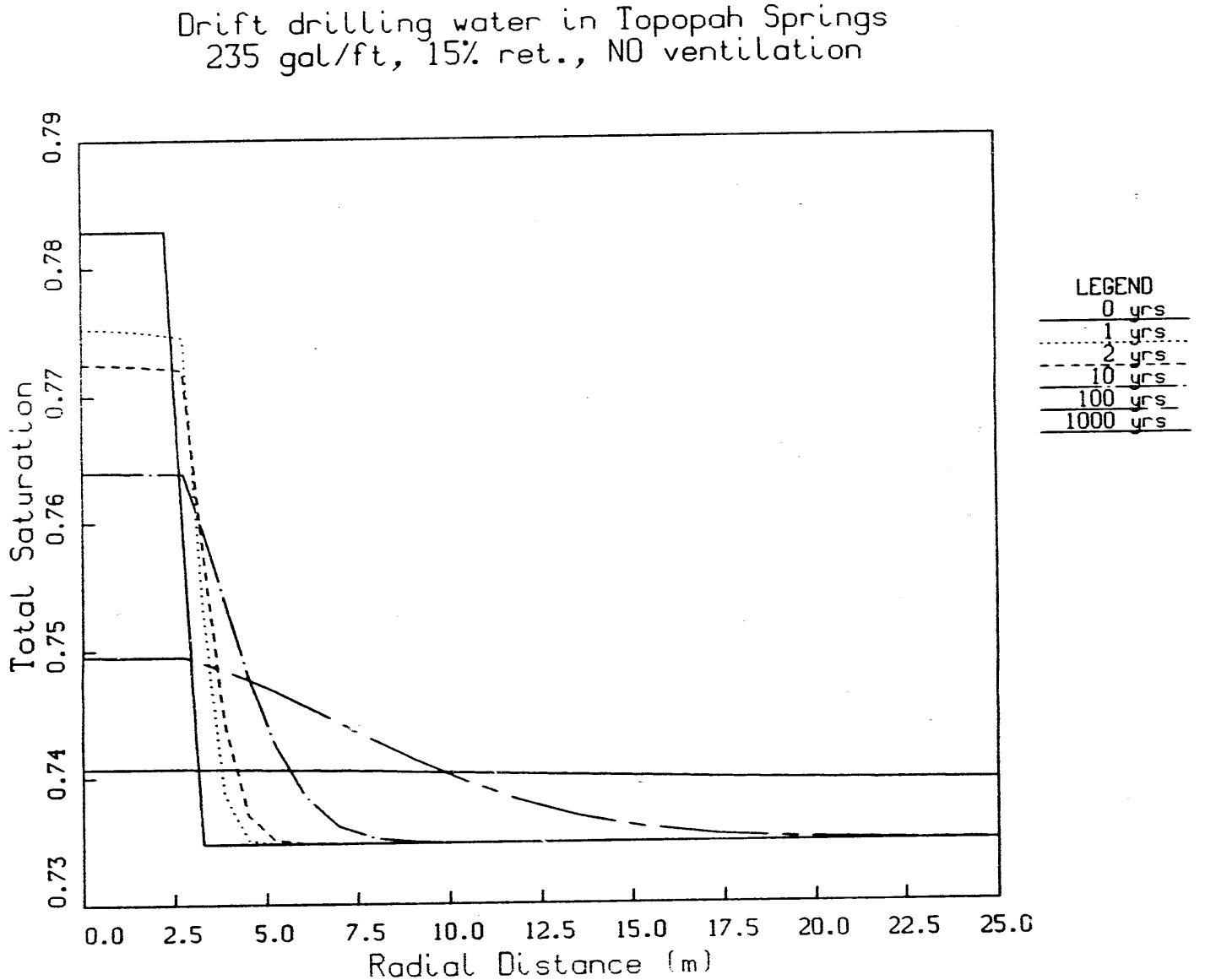

Figure 34: Dispersion of Drift Drilling Water in Topopah Springs: Retention Factor = 15%, No Ventilation

Figures 35-38: Dispersion History of Drift Water in Topopah Springs: Retention Factor = 15%, No Ventilation

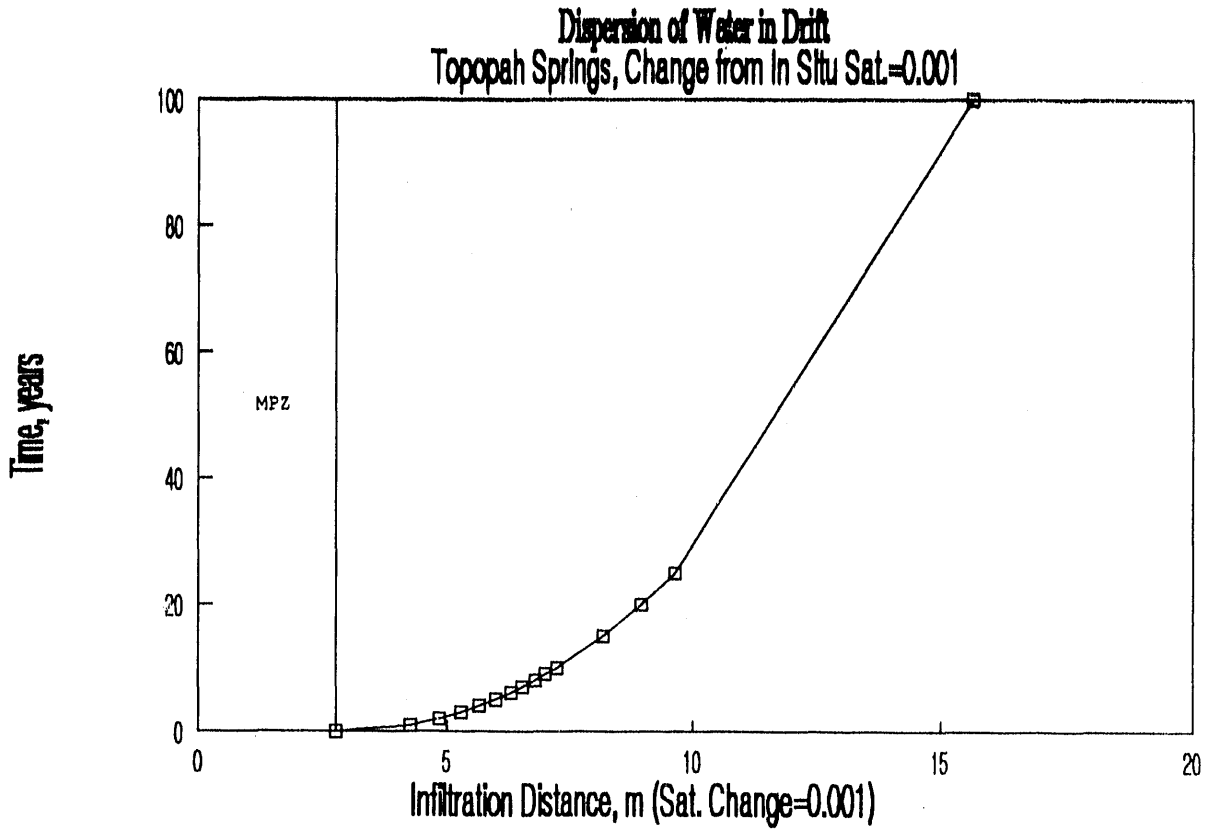

Figure 35: Topopah Springs, Change from In Situ Saturation=0.001

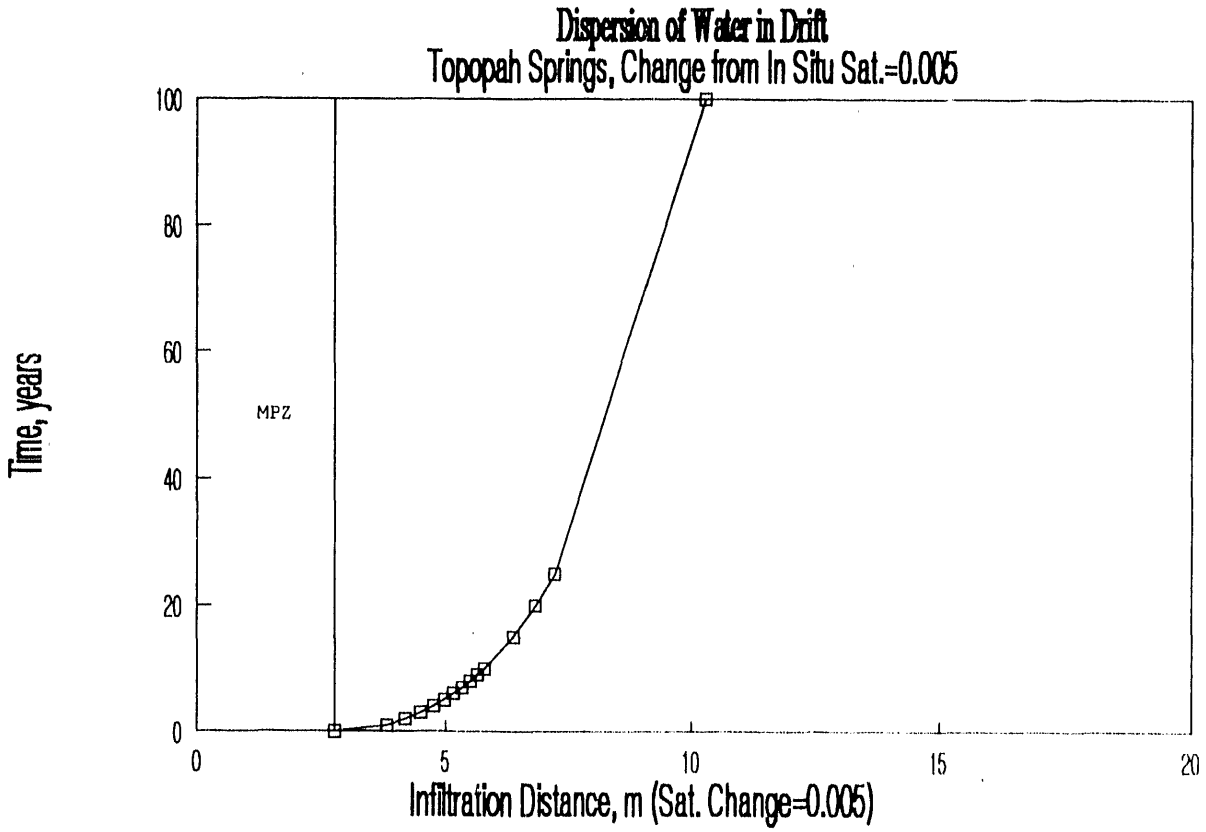

Figure 36: Topopah Springs, Change from In Situ Saturation=0.005

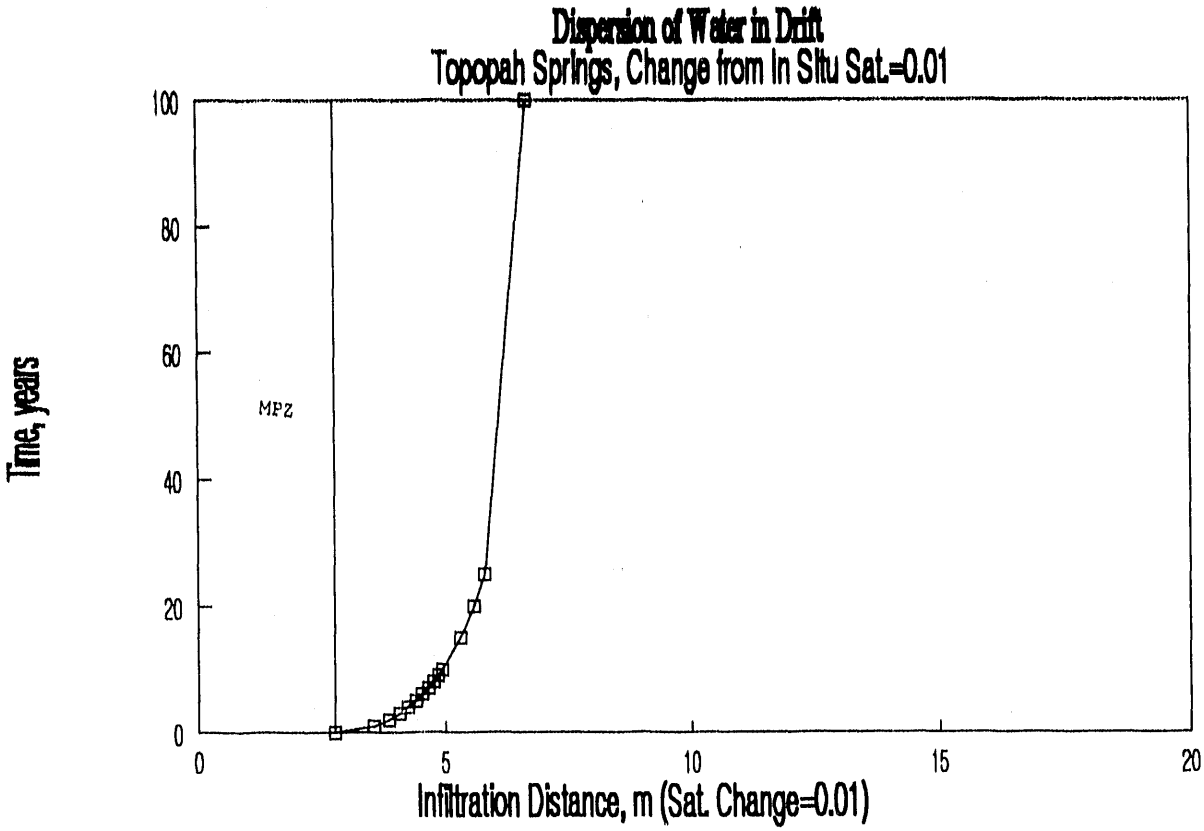

Figure 37: Topopah Springs, Change from In Situ Saturation = 0.01

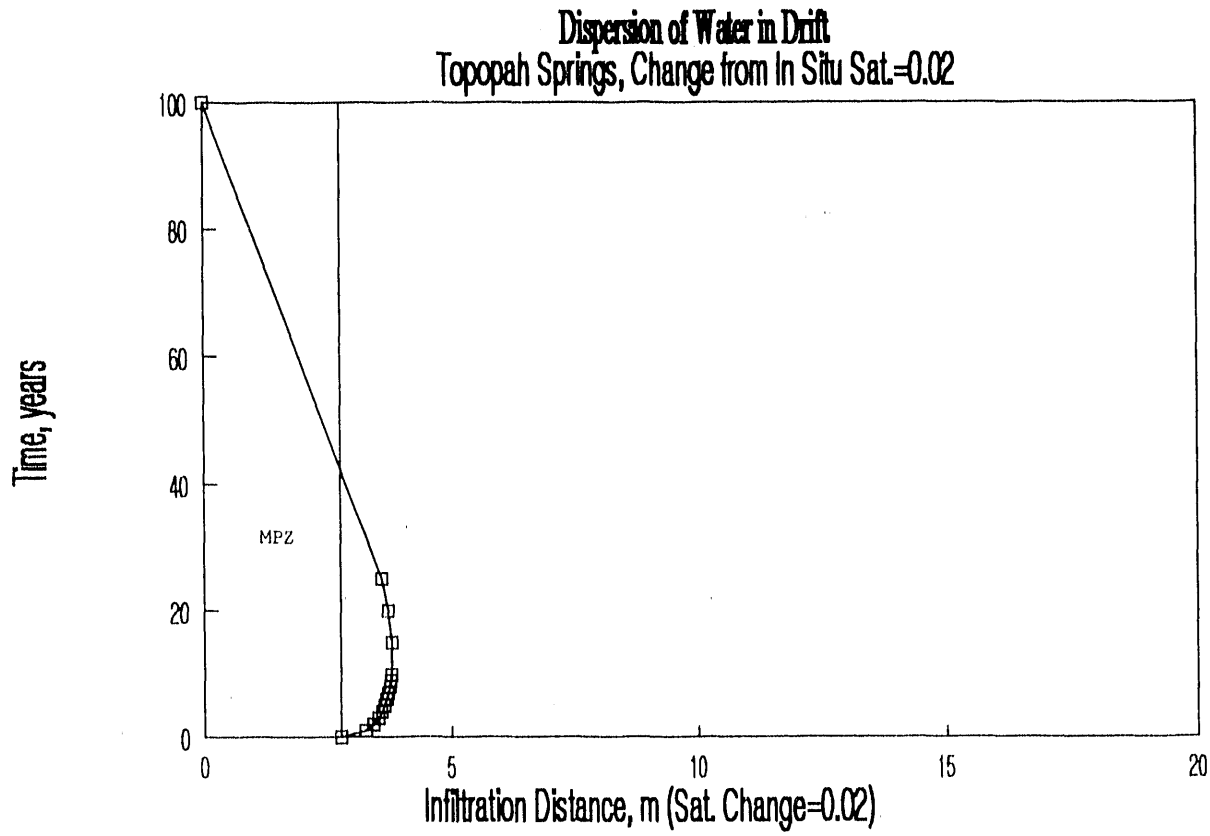

Figure 38: Topopah Springs, Change from In Situ Saturation = 0.02
Retention Factor = 15%, No Ventilation

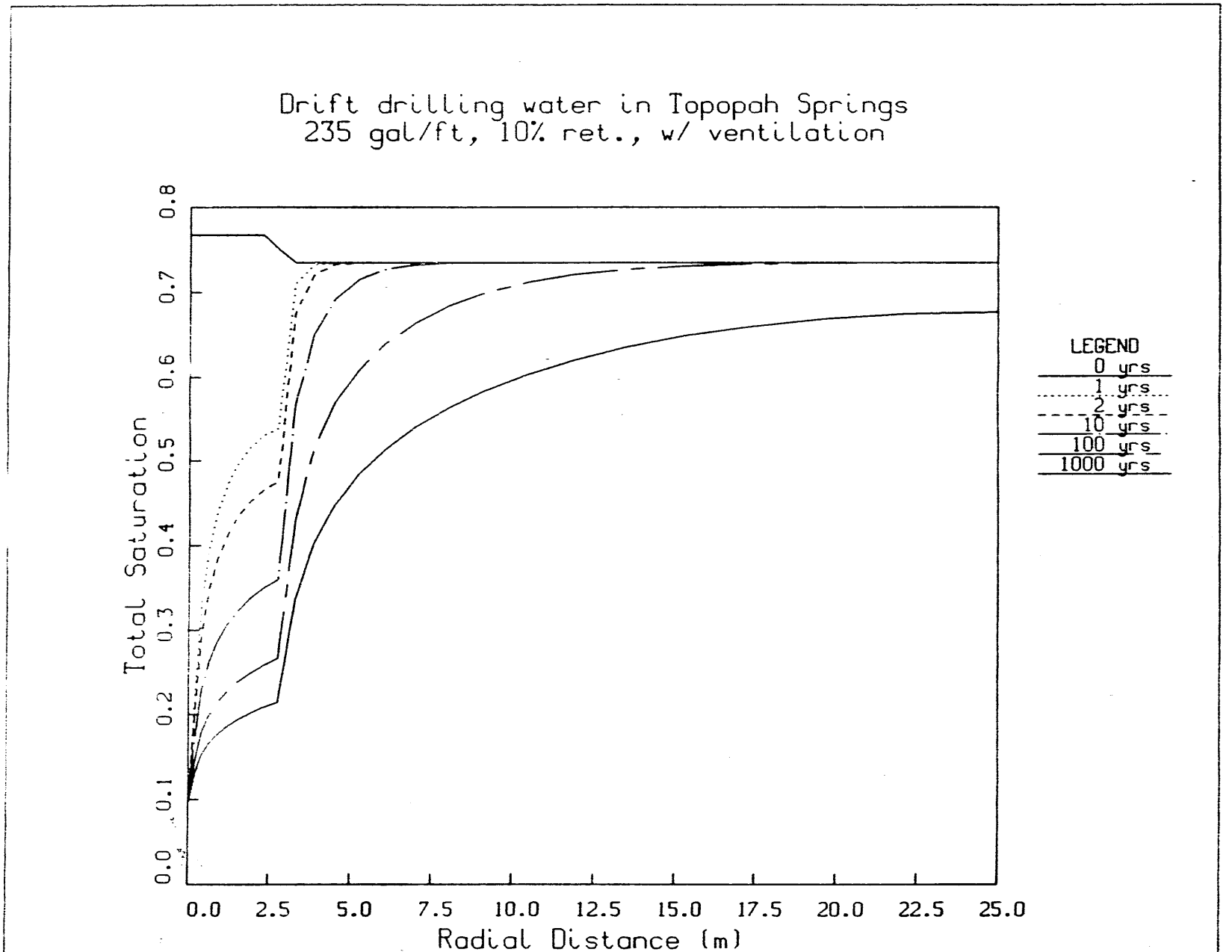

Figure 39: Dispersion of Drift Drilling Water in Topopah Springs: Retention Factor = 10%, With Ventilation

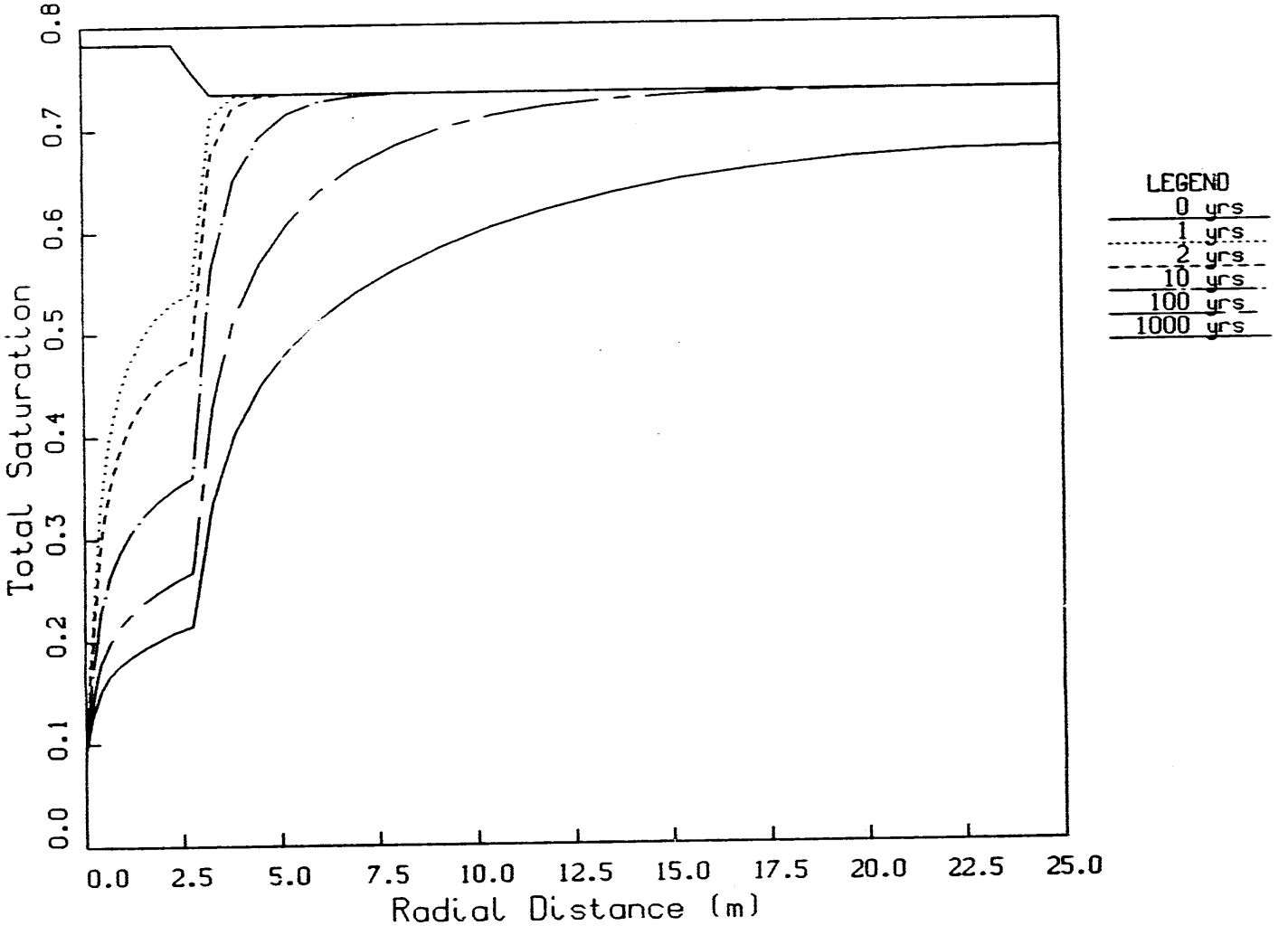

Figure 40: Dispersion of Drift Drilling Water in Topopah Springs: Retention Factor = 15%, With Ventilation

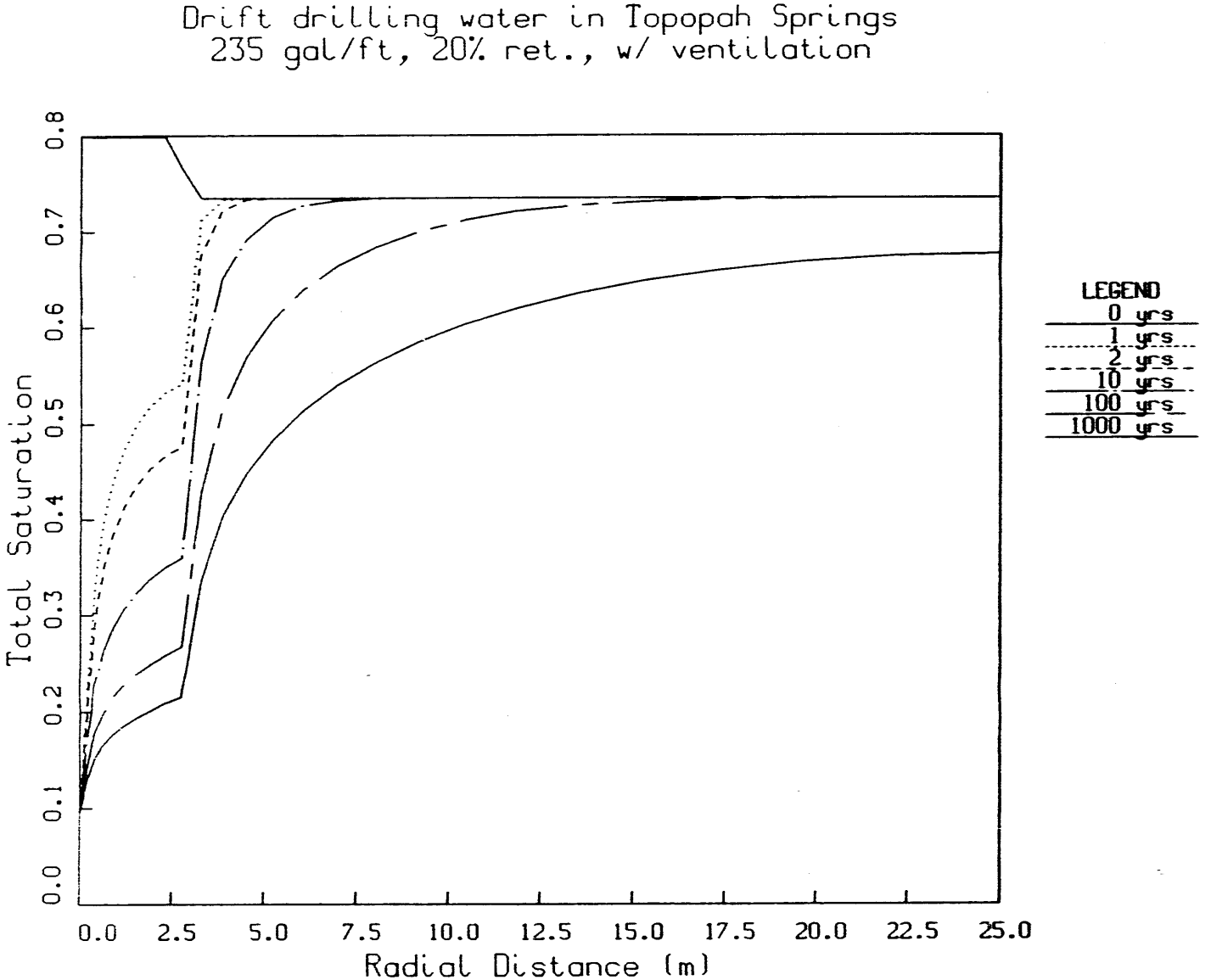

Figure 41: Dispersion of Drift Drilling Water in Topopah Springs: Retention Factor = 20%, With Ventilation

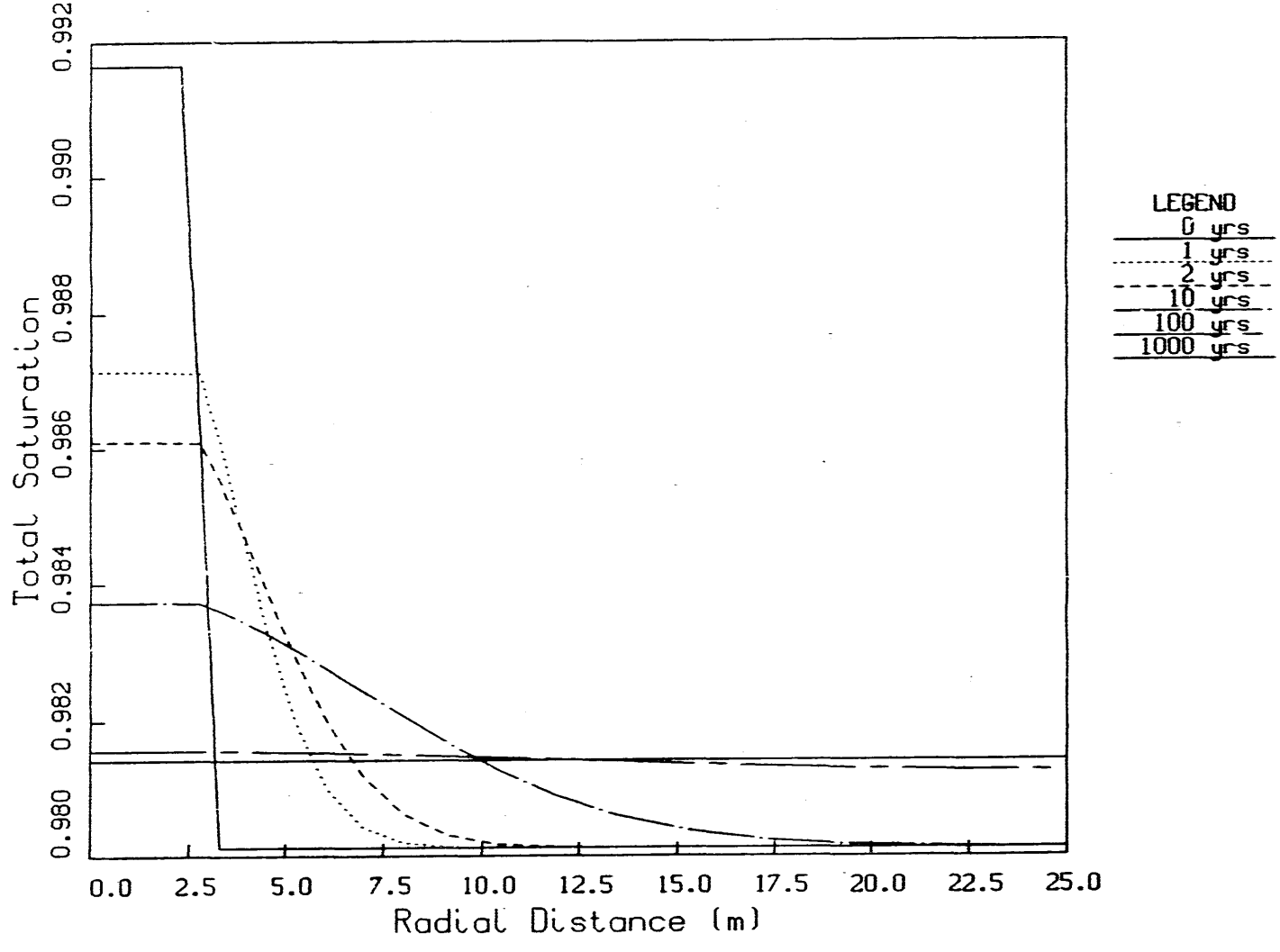

Figure 42: Dispersion of Drift Drilling Water in Calico Hills: Retention Factor = 15%, No Ventilation

Figures 43-44: Dispersion History of Drift Water in Calico Hills: Retention Factor = 15%, No Ventilation

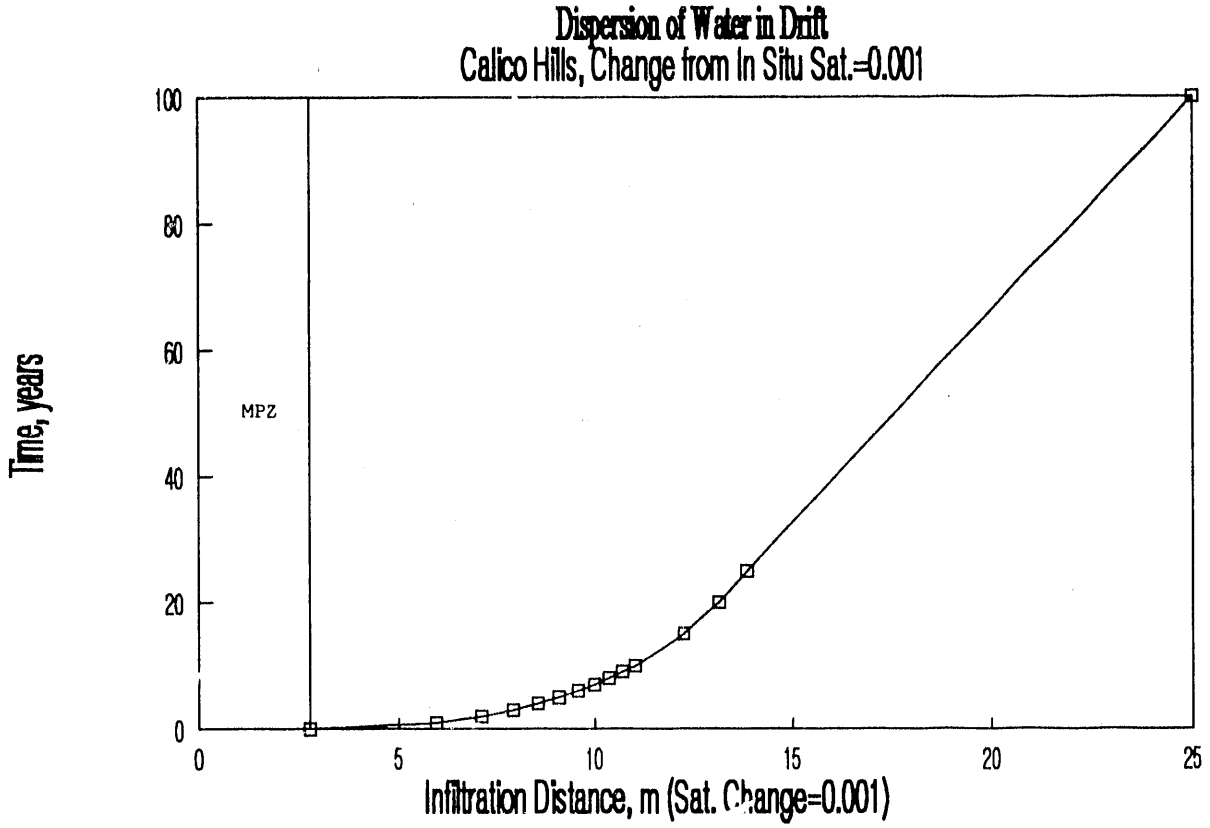

Figure 43: Calico Hills, Change from In Situ Saturation=0.001

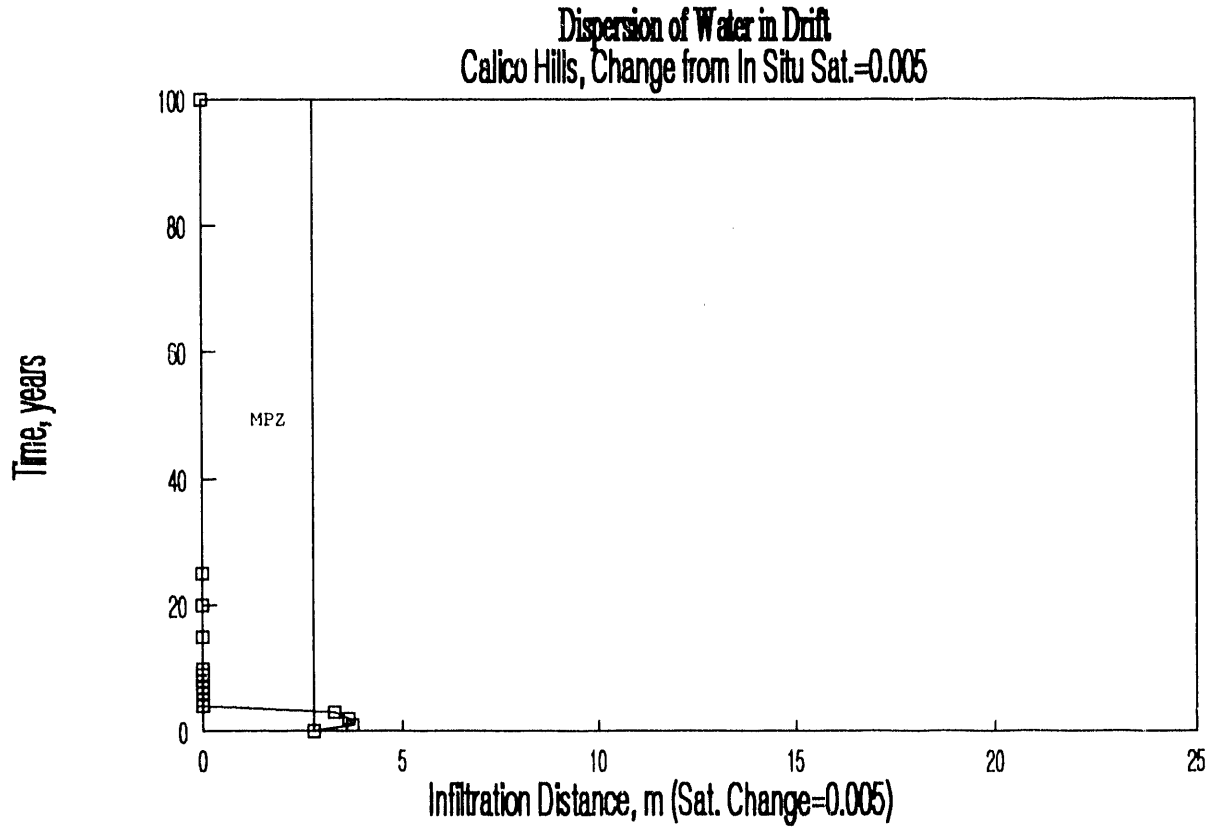

Figure 44: Calico Hills, Change from In Situ Saturation=0.005

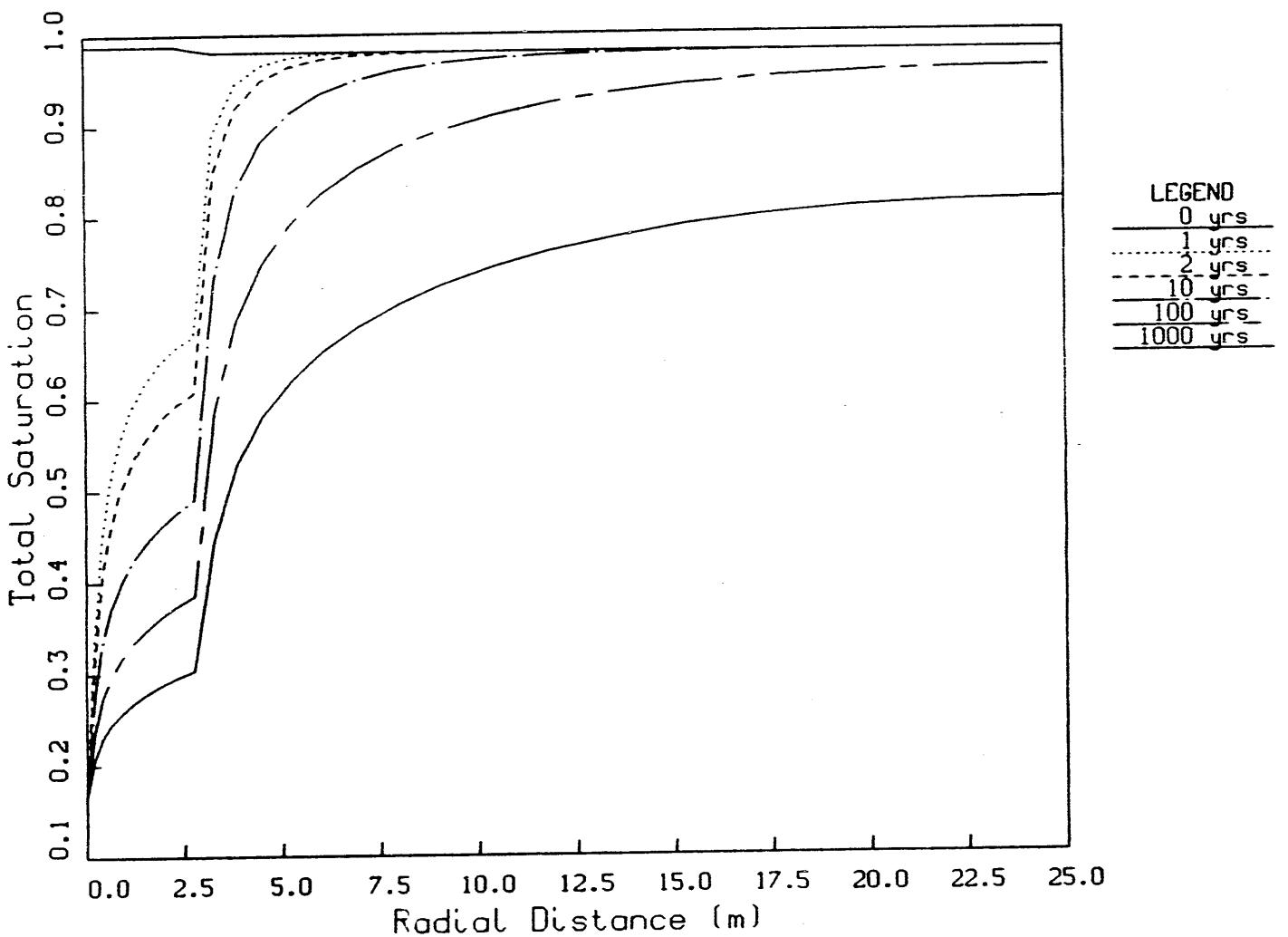

Figure 45: Dispersion of Drift Drilling Water in Calico Hills: Retention Factor = 10%, With Ventilation

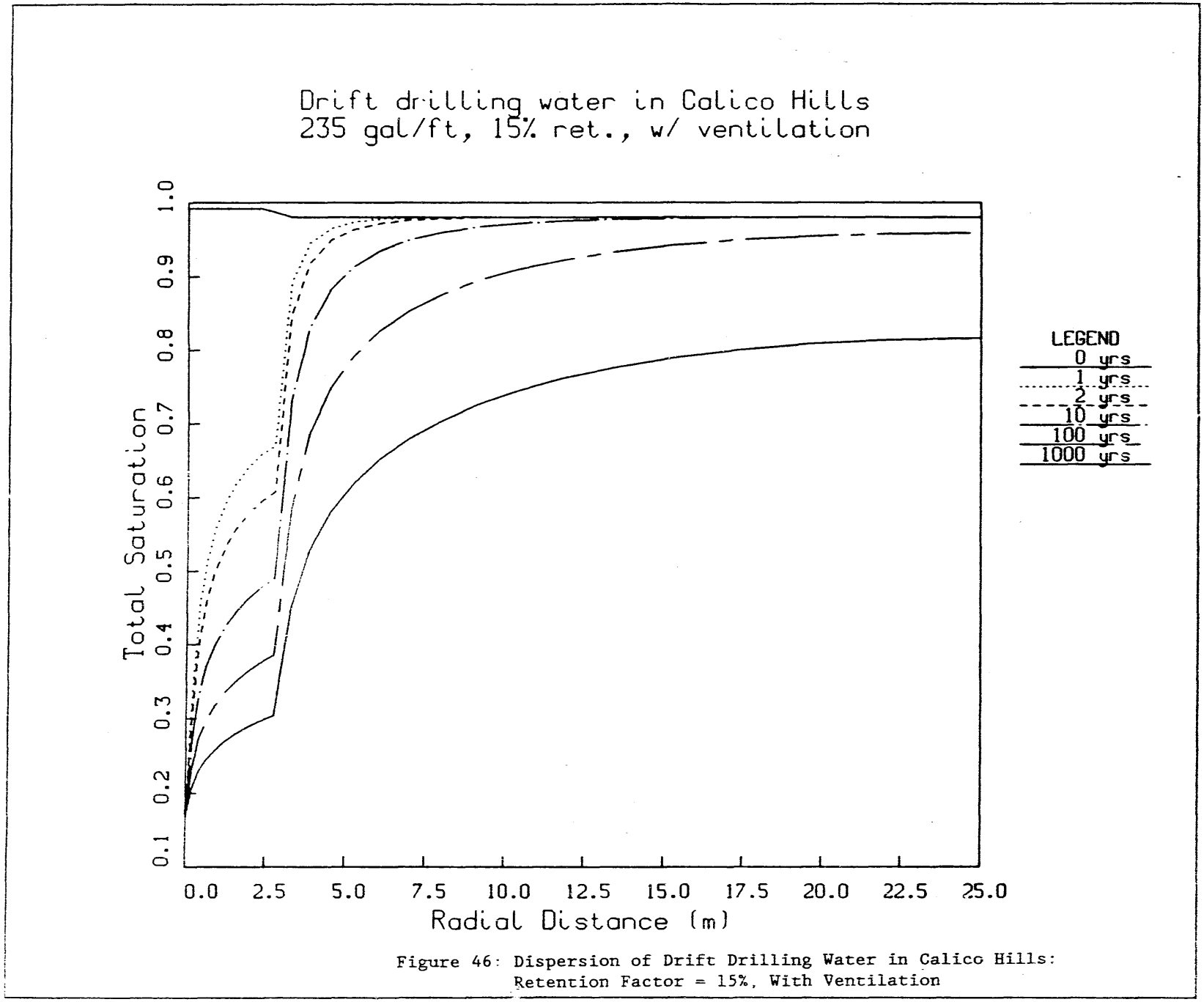

Figure 46: Dispersion of Drift Drilling Water in Calico Hills: Retention Factor = 15%, With Ventilation

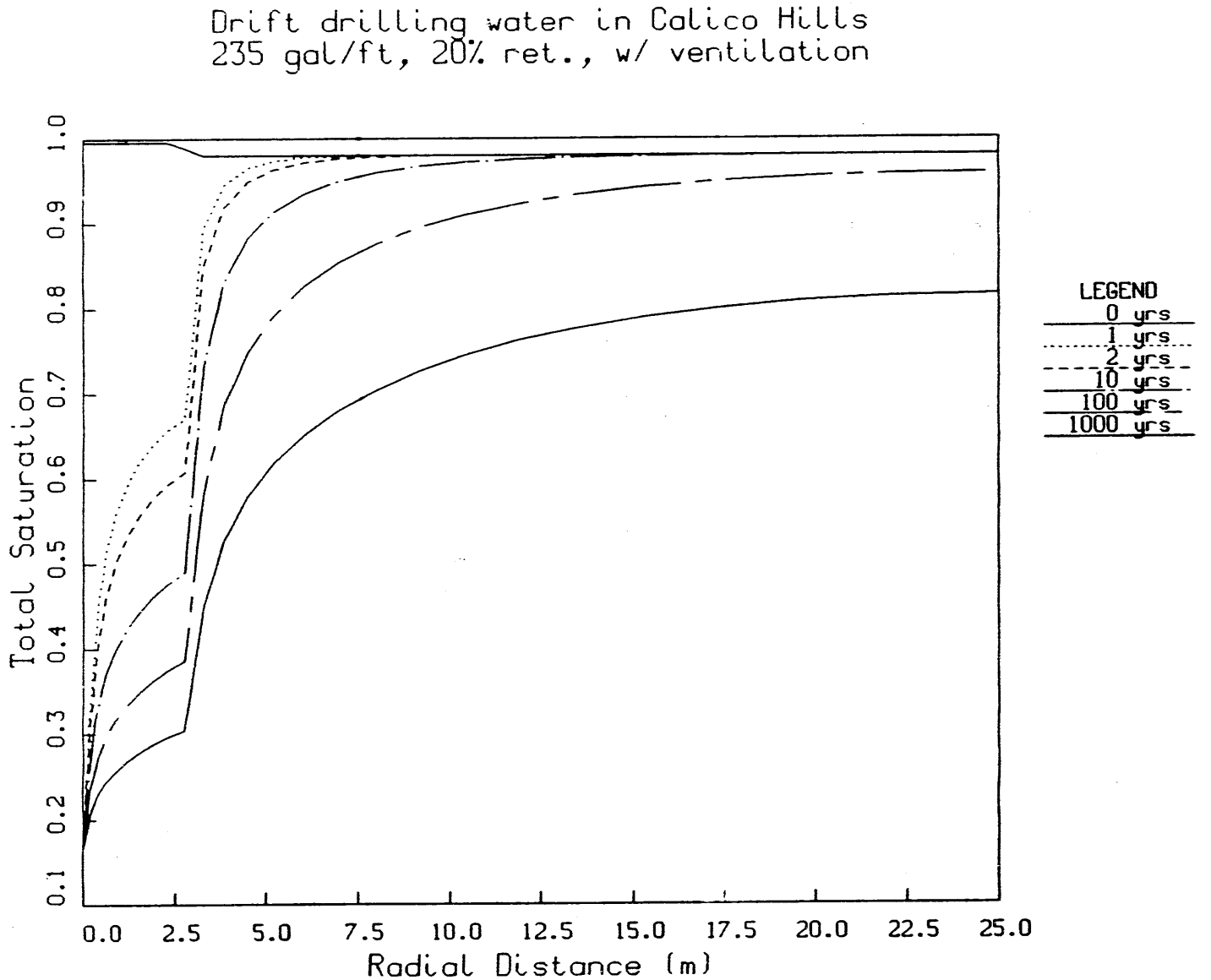

Figure 47: Dispersion of Drift Drilling Water in Calico Hills: Retention Factor = 20%, With Ventilation

APPENDIX D

REFERENCE INFORMATION BASE AND SITE ENGINEERING PROPERTIES DATA BASE

This report uses information from the Reference Information Base; see Appendix B for a listing of the values used.

This report contains no candidate information for inclusion in the Reference Information Base.

This report contains no candidate information for inclusion in the Site and Engineering Properties Data Base.

DISTRIBUTION LIST

1 J. W. Bartlett, Director (RW-1)
Office of Civilian Radioactive
Waste Management
U.S. Department of Energy
1000 Independence Avenue, S.W.
Washington, D.C. 20585

1 F. G. Peters, Deputy Director (RW-2)
Office of Civilian Radioactive
Waste Management
U.S. Department of Energy
1000 Independence Avenue, S.W.
Washington, D.C. 20585

1 T. H. Isaacs (RW-4)
Office of Strategic Planning
and International Programs
Office of Civilian Radioactive
Waste Management
U.S. Department of Energy
1000 Independence Avenue, S.W.
Washington, D.C. 20585

1 J. D. Saltzman (RW-5)
Office of External Relations
Office of Civilian Radioactive
Waste Management
U.S. Department of Energy
1000 Independence Avenue, S.W.
Washington, D.C. 20585

1 Samuel Rousso (RW-10)
Office of Program and Resources
Management
Office of Civilian Radioactive
Waste Management
U.S. Department of Energy
1000 Independence Avenue, S.W.
Washington, D.C. 20585

1 J. C. Bresee (RW-10)
Office of Civilian Radioactive
Waste Management
U.S. Department of Energy
1000 Independence Avenue, S.W.
Washington, D.C. 20585

1 C. P. Gertz (RW-20)
Office of Geologic Disposal
Office of Civilian Radioactive
Waste Management
U.S. Department of Energy
1000 Independence Avenue, S.W.
Washington, D.C. 20585

1 S. J. Brocoum (RW-22)
Analysis and Verification Division
Office of Civilian Radioactive
Waste Management
U.S. Department of Energy
1000 Independence Avenue, S.W.
Washington, D.C. 20585

1 D. D. Shelor (RW-30)
Office of Systems and Compliance
Office of Civilian Radioactive
Waste Management
U.S. Department of Energy
1000 Independence Avenue, S.W.
Washington, D.C. 20585

1 J. Roberts (RW-33)
Office of Civilian Radioactive
Waste Management
U.S. Department of Energy
1000 Independence Avenue, S.W.
Washington, D.C. 20585

1 G. J. Parker (RW-332)
Office of Civilian Radioactive
Waste Management
U.S. Department of Energy
1000 Independence Avenue, S.W.
Washington, D.C. 20585

1 Associate Director (RW-40)
Office of Storage and Transportation
Office of Civilian Radioactive
Waste Management
U.S. Department of Energy
1000 Independence Avenue, S.W.
Washington, D.C. 20585

1 Associate Director (RW-50)
Office of Contract Business
Management
Office of Civilian Radioactive
Waste Management
U.S. Department of Energy
1000 Independence Avenue, S.W.
Washington, D.C. 20585

1 C. G. Russomanno (RW-52)
Office of Civilian Radioactive
Waste Management
U.S. Department of Energy
1000 Independence Avenue, S.W.
Washington, D.C. 20585

1 D. U. Deere, Chairman
Nuclear Waste Technical
Review Board
1100 Wilson Blvd. #910
Arlington, VA 22209-2297

1 Dr. Clarence R. Allen
Nuclear Waste Technical Review Board
1000 E. California Blvd.
Pasadena, CA 91106

1 Dr. John E. Cantlon
Nuclear Waste Technical Review Board
1795 Bramble Dr.
East Lansing, MI 48823

1 Dr. Melvin W. Carter
Nuclear Waste Technical Review Board
4621 Ellisbury Dr., N.E.
Atlanta, GA 30332

1 Dr. Donald Langmuir
Nuclear Waste Technical Review Board
109 So. Lookout Mountain Cr.
Golden, CO 80401

1 Dr. D. Warner North
Nuclear Waste Technical Review Board
Decision Focus, Inc.
4984 El Camino Real
Los Altos, CA 94062

1 Dr. Dennis L. Price
Nuclear Wast Technical Review Board
1011 Evergreen Way
Blacksburg, VA 24060

1 Dr. Ellis D. Verink
Nuclear Waste Technical Review Board
4401 N.W. 18th Place
Gainesville, FL 32605

5 C. P. Gertz, Project Manager
Yucca Mountain Project Office
U.S. Department of Energy
P.O. Box 98608--MS 523
Las Vegas, NV 89193-8608

1 C. L. West, Director
Office of External Affairs
DOE Field Office, Nevada
U.S. Department of Energy
P.O. Box 98518
Las Vegas, NV 89193-85180

12 Technical Information Officer
DOE Field Office, Nevada
U.S. Department of Energy
P.O. Box 98518
Las Vegas, NV 89193-8518

1 P. K. Fitzsimmons, Director
Health Physics & Environmental
Division
DOE Field Office, Nevada
U.S. Department of Energy
P.O. Box 98518
Las Vegas, NV 89193-8518

1 D. R. Elle, Director
Environmental Protection Division
DOE Field Office, Nevada
U.S. Department of Energy
P.O. Box 98518
Las Vegas, Nv 89193-8518

1 Repository Licensing & Quality
Assurance Project Directorate
Division of Waste Management
U.S. Nuclear Regulatory Commission
Washington, D.C. 20555

1 Senior Project Manager for Yucca
Mountain Repository Project Branch
Division of Waste Management
U.S. Nuclear Regulatory Commission
Washington, D.C. 20555

1 NRC Document Control Desk
Division of Waste Management
U.S. Nuclear Regulatory Commission
Washington, D.C. 20555

1 P. T. Prestholt
NRC Site Representative
301 E. Stewart Ave.
Las Vegas, NV 89101

1 E. P. Binnall
Field Systems Group Leader
Building 50B/4235
Lawrence Berkeley Laboratory
Berkeley, CA 94720

1 Center for Nuclear Waste
Regulatory Analyses
6220 Culebra Road
Drawer 28510
San Antonio, TX 78284

3 L. J. Jardine
Technical Project Officer for YMP
Mail Stop L-204
Lawrence Livermore National
Laboratory
P.O. Box 808
Livermore, CA 94550

4 R. J. Herbst
Technical Project Officer for YMP
N-5, Mail Stop J521
Los Alamos National Laboratory
P.O. Box 1663
Los Alamos, NM 87545

1 H. N. Kalia
Exploratory Shaft Test Manager
Los Alamos National Laboratory
Mail Stop 527
101 Convention Center Dr.
Suite 820
Las Vegas, NV 89109

1 J. F. Divine
Assistant Director for
Engineering Geology
U.S. Geological Survey
106 National Center
12201 Sunrise Valley Dr.
Reston, VA 22092

6 L. R. Hayes
Technical Project Officer
Yucca Mountain Project Branch--MS 425
U.S. Geological Survey
P.O. Box 25046
Denver, CO 80225

1 V. R. Schneider
Asst. Chief Hydrologist--MS 414
Office of Program Coordination
& Technical Support
U.S. Geological Survey
12201 Sunrise Valley Drive
Reston, VA 22092

1 R. B. Raup, Jr.
Geological Division Coordinator
MS 913
Yucca Mountain Project
U.S. Geological Survey
P.O. Box 25046
Denver, CO 80225

1 D. H. Appel, Chief
Hydrologic Investigations Program
MS 421
U.S. Geological Survey
P.O. Box 25046
Denver, CO 80225

1 E. J. Helley
Branch of Western Regional Geology
MS 427
U.S. Geological Survey
345 Middlefield Road
Menlo Park, CA 94025

1 Chief
Nevada Operations Office
U.S. Geological Survey
101 Convention Center Drive
Suite 860, MS 509
Las Vegas, NV 89109

1 D. Zesiger
U.S. Geological Survey
101 Convention Center Dr.
Suite 860 - MS509
Las Vegas, NV 89109

1 R. V. Watkins, Chief
Project Planning and Management
U.S. Geological Survey
P.O. Box 25046
421 Federal Center
Denver, CO 80225

1 A. L. Flint
U.S. Geological Survey
MS 721
P.O. Box 327
Mercury, NV 89023

1 D. A. Beck
U.S. Geological Survey
1500 E. Tropicana, Suite 201
Las Vegas, NV 89119

1 P. A. Glancy
U.S. Geological Survey
Federal Building, Room 224
Carson City, NV 89701

1 Sherman S. C. Wu
Branch of Astrogeology
U.S. Geological Survey
2255 N. Gemini Dr.
Flagstaff, AZ 86001

1 J. H. Sass
Branch of Tectonophysics
U.S. Geological Survey
2255 N. Gemini Dr.
Flagstaff, AZ 86001

1 DeWayne A. Campbell
Technical Project Officer for YMP
Bureau of Reclamation
Code D-3790
P.O. Box 25007
Denver, CO 80225

1 S. M. Dash
Science Applications International Corp.
14062 Denver West Parkway, Suite 255
Golden, CO 80401

1 K. W. Causseaux
NHP Reports Chief
U.S. Geological Survey
421 Federal Center
P.O. Box 25046
Denver, CO 80225

1 V. M. Glanzman
U.S. Geological Survey
913 Federal Center
P.O. Box 25046
Denver, CO 80225

1 J. H. Nelson
Technical Project Officer for YMP
Science Applications International Corp.
101 Convention Center Dr.
Suite 407
Las Vegas, NV 89109

2 SAIC-T&MSS Library
Science Applications International Corp.
101 Convention Center Dr.
Suite 407
Las Vegas, NV 89109

1 Elaine Ezra
YMP GIS Project Manager
EG&G Energy Measurements, Inc.
Mail Stop D-12
P.O. Box 1912
Las Vegas, NV 89125

1 R. E. Jackson, Program Manager
Roy F. Weston, Inc.
955 L'Enfant Plaza, Southwest
Washington, D.C. 20024

1 Technical Information Center
Roy F. Weston, Inc.
955 L'Enfant Plaza, Southwest
Washington, D.C. 20024

1 D. Hedges, Vice President,
Quality Assurance
Roy F. Weston, Inc.
4425 Spring Mountain Road, Suite 300
Las Vegas, Nevada 89102

1 D. L. Fraser, General Manager
Reynolds Electrical & Engineering Co.
Mail Stop 555
P.O. Box 98521
Las Vegas, NV 89193-8521

1 R. F. Pritchett
Technical Project Officer for YMP
Reynolds Electrical & Engineering Co.
MS 408
P.O. Box 98521
Las Vegas, NV 89193-8521

1 B. W. Colston
General Manager & President
Las Vegas Branch
Raytheon Services Nevada
Mail Stop 416
P.O. Box 95487
Las Vegas, NV 89193-5487

1 R. L. Bullock
Technical Project Officer for YMP
Raytheon Services Nevada
Suite P250, MS 403
101 Convention Center Dr.
Las Vegas, NV 89109

1 R. E. Lowder
Technical Project Officer for YMP
MAC Technical Services
101 Convention Center Drive
Suite 1100
Las Vegas, NV 89109

1 C. K. Hastings, Manager
PASS Program
Pacific Northwest Laboratories
P.O. Box 999
Richland, WA 99352

1 A. T. Tamura
Science and Technology Division
Office of Scientific and Technical Information
U.S. Department of Energy
P.O. Box 62
Oak Ridge, TN 37831

1 Carlos G. Bell, Jr.
Professor of Civil Engineering
Civil and Mechanical Engineering Department
University of Nevada, Las Vegas
4505 South Maryland Parkway
Las Vegas, NV 89154

1 C. F. Costa, Director
Nuclear Radiation Assessment Division
U.S. Environmental Protection Agency
Environmental Monitoring Systems Laboratory
P.O. Box 93478
Las Vegas, NV 89193-3478

1 ONWI Library
Battelle Columbus Laboratory
Office of Nuclear Waste Isolation
505 King Avenue
Columbus, OH 43201

1 T. Hay, Executive Assistant
Office of the Governor
State of Nevada
Capitol Complex
Carson City, NV 89710

3 R. R. Loux, Jr.
Executive Director
Nuclear Waste Project Office
State of Nevada
Evergreen Center, Suite 252
1802 North Carson Street
Carson City, NV 89710

1 C. H. Johnson
Technical Program Manager
Nuclear Waste Project Office
State of Nevada
Evergreen Center, Suite 252
1802 North Carson Street
Carson City, NV 89710

1 John Fordham
Water Resources Center
Desert Research Institute
P.O. Box 60220
Reno, NV 89506

1 Dr. Martin Mifflin
Water Resources Center
Desert Research Institute
2505 Chandler Avenue
Suite 1
Las Vegas, NV 89120

1 Eric Anderson
Mountain West Research-Southwest Inc.
2901 N. Central Ave. #1000
Phoenix, AZ 85012-2730

1 Department of Comprehensive Planning
Clark County
225 Bridger Avenue, 7th Floor
Las Vegas, NV 89155

1 Planning Department
Nye County
P.O. Box 153
Tonopah, NV 89049

1 Lincoln County Commission
Lincoln County
P.O. Box 90
Pioche, NV 89043

5 Judy Foremaster
City of Caliente
P.O. Box 158
Caliente, NV 89008

1 Economic Development Department
City of Las Vegas
400 East Stewart Avenue
Las Vegas, NV 89101

1 Community Planning & Development
City of North Las Vegas
P.O. Box 4086
North Las Vegas, NV 89030

1 Director of Community Planning
City of Boulder City
P.O. Box 367
Boulder City, NV 89005

1 Commission of the European Communities
200 Rue de la Loi
B-1049 Brussels
BELGIUM

2 M. J. Dorsey, Librarian
YMP Research and Study Center
Reynolds Electrical & Engineering Co., Inc.
MS 407
P.O. Box 98521
Las Vegas, NV 89193-8521

1 Amy Anderson
Argonne National Laboratory
Building 362
9700 So. Cass Ave.
Argonne, IL 60439

1 Deirdre M. Boak
Science Applications International Corp.
101 Convention Center Drive
Suite 407
Las Vegas, NV 89109

1	6300	T. O. Hunter
1	6310	T. E. Blejwas, Actg.
1	6310A	L. E. Shephard
1	6312	F. W. Bingham
1	6312	W. F. Chambers
1	6312	E. Dunn
1	6312	J. H. Gauthier
1	6312	P. G. Kaplan
1	6312	F. C. Lauffer
1	6312	S. A. Shannon
1	6312	M. L. Wilson
1	6313	L. S. Costin
5	6313	M. E. Fewell
5	6313	S. R. Sobolik
1	6313	A. H. Treadway
1	6315	F. B. Nimick, Actg.
1	6315	J. A. Fernandez
1	6316	R. P. Sandoval
2	6318	R. J. Macer for 100/12147/SAND91-0791/QA
1	6319	R. R. Richards
1	1510	J. C. Cummings
1	1511	J. S. Rottler
3	1511	R. R. Eaton
1	1511	P. L. Hopkins
1	1511	M. J. Martinez
1	1512	A. C. Ratzel
1	1513	R. D Skocypec
1	1514	H. S. Morgan
1	6257	T. E. Hinkebein
5	3141	S. A. Landenberger
8	3145	Document Processing for DOE/OSTI
3	3151	G. C. Claycomb
1	6310	70/12147/72-30/1.3/QA
20	6341	WMT Library
1	6410	D. J. McCloskey, Actg.
1	8523-2	Central Technical Files

The number in the lower right-hand corner is an accession number used for Office of Civilian Radioactive Waste Management purposes only. It should not be used when ordering this publication.

END

DATE FILMED

3/10/92